ABSTRACT

| | |
|---|---|
| Title of Dissertation: | INITIATION AND PROGRESSION OF BRAF/NRAS WILDTYPE MELANOMA IN UV-INDUCED MOUSE MODELS OF CUTANEOUS MELANOMA |
| | Helen Thompson Michael, Doctor of Philosophy 2018 |
| Dissertation directed by: | Professor Siba Samal<br>Department of Veterinary Medicine |

Melanoma is the deadliest skin cancer and is responsible for nearly 60,000 deaths worldwide each year. At least some melanomas are believed to arise from stepwise progression from normal melanocytes through a benign nevus stage to malignant melanoma and finally metastatic disease. Approximately 20-50% of melanomas have evidence of a pre-existing nevus, indicating that progression is an important route of melanomagenesis. Ultraviolet radiation exposure is believed to play an important role in nevus and melanoma formation, although the mechanisms of this remain unclear. Childhood sunburn and intermittent sun exposure are epidemiologically linked to increased melanoma risk. While most melanomas have activation of the mitogen activated protein kinase pathway, often due to mutations in *BRAF* or *RAS* genes, nearly 15% of cutaneous melanomas do not have an identified strong driver. Despite targeted therapies and immunotherapy, the death rate from melanoma has remained

nearly static for several decades, so there is a need to identify additional genes and pathways to provide novel therapeutic targets. We hypothesized that progression of melanocytic lesions from benign to malignant is associated with the acquisition of additional genomic mutations. Unlike wildtype mice, hepatocyte growth factor (HGF) transgenic mice have "humanized" distribution of melanocytes along the dermal-epidermal junction. Following a single dose of UV at 3 days of age, HGF mice develop melanocytic nevi and melanomas. In this project, two HGF models were used to generate melanocytic lesions. The first model, on an albino FVB background had a tumor incidence of only 10% and used melanocyte-specific green fluorescent protein expression to identify early nevi and melanomas. The second model, on a C57BL/6 had a high tumor incidence (80%), and 60% of tumor-bearing mice have metastatic lesions. Sequencing of melanocytic lesions at different stages revealed a variety of driver mutations, including *Nf1*, *Gnaq*, and *Gna11*, as well as genes and pathways with less established roles in melanoma development. Our data provide a broad overview of genes and pathways involved in progression of non-BRAF, non-NRAS melanoma. Additionally, we present the first potential germline variants that may increase metastatic susceptibility for melanoma patients. These genes suggest potential biomarkers for progression of melanocytic lesions.

# INITIATION AND PROGRESSION OF BRAF/NRAS WILDTYPE MELANOMA IN UV-INDUCED MOUSE MODELS OF CUTANEOUS MELANOMA

by

Helen Thompson Michael

Dissertation submitted to the Faculty of the Graduate School of the
University of Maryland, College Park, in partial fulfillment
of the requirements for the degree of
Doctor of Philosophy
2018

Advisory Committee:
Professor Siba Samal, Chair
Dr. Glenn Merlino
Professor Xiaoping Zhu
Professor David Mosser
Dr. R. Mark Simpson

# Acknowledgements

Numerous people have assisted in the completion of this work in both large and small ways and have my gratitude whether they are mentioned here or not. In particular, I greatly appreciate the dedication, hard work, and mouse knowledge of two amazing women, Cari Graff-Cherry and Sung Chin. My fellow lab mates, both current and past, have all helped me learn and kept the laboratory a fun and creative place. Special thanks are due to Chi-Ping Day, Antonella Sassano, and the summer students and post-baccalaureate fellows I've had the honor to mentor, Patricia Bunda, Alia Al Homsi, Tunde Smith, and Amelework Habtemichael. Many thanks to Glenn Merlino for letting me join his lab and hope someday to be as good of a mentor to others as he has been for me. Thanks to the CBSTP program, Mark Simpson, Shelley Hoover, Jennifer Dwyer, Hibret Amare Adissu, and the fellows for their support. Last, but not least, thank you to my parents, and my two- and four-legged family members Jim, Kai, Sasha, Arthur, Hugo and Charlie who have provided me with much needed support and patience.

# Table of Contents

This Table of Contents is automatically generated by MS Word, linked to the Heading formats used within the Chapter text.

# List of Tables

# List of Figures

# List of Abbreviations

| | |
|---|---|
| GFP | Green Fluorescent Protein |
| HGF | Hepatocyte Growth Factor |
| UV | Ultraviolet light |
| GS | FVB/N $HGF^{Tg/+}$; $DCTrtTA^{Tg/+}$; $Tre\text{-}H2BGFP^{Tg/+}$; $p16^{KO/+}$ model |
| BT | C57BL/6J $HGF^{Tg/+}$; $Tyr\text{-}CreERTA2^{Tg/+}$; $Cdkn2a^{Ca/+}$ model |
| NAM | Nevus-associated melanoma |
| DNM | De novo melanoma |
| SNV | Single nucleotide variant |
| nSNV | Nonsynonymous single nucleotide variant |
| INDELS | Insertion and deletions |
| RGP | Radial growth phase |
| VGP | Vertical growth phase |
| Met | Metastatic lesion |
| NCI | National Cancer Institute |
| CCR | Center for Cancer Research |

# Chapter 1: Introduction

Portions of this chapter were published in (Day, Marchalik et al. 2017)

Melanocytes are pigment cells that originate from the neural crest and occur primarily in the skin but are also found in the eyes, inner ears, lymph nodes, and other sites throughout the body. The major roles of melanocytes depend on their location and is not always understood. In the skin, melanocytes primary function to produce melanin pigment to protect epidermal keratinocytes from ultraviolet (UV) damage. On the other hand, in the inner ear, melanocytes are involved in maintaining the tissue-fluid barrier (Zhang, Dai et al. 2012). Individuals with a lack of melanocytes can have phenotypic effects from albinism to deafness and microphthalmia (Spritz and Hearing 1994, Tassabehji, Newton et al. 1994, Nakayama, Nguyen et al. 1998). Melanoma is the deadliest of the skin cancer. Worldwide incidence was over 350,000 diagnoses and 59,782 deaths in 2015 (Karimkhani, Green et al. 2017). The highest incidence occurs in the Australia, New Zealand, Europe, Canada, and the United States (Garbe and Leiter 2009, Karimkhani, Green et al. 2017). In the United States in 2018, there were approximately 91,000 invasive melanoma diagnoses and 9,000 deaths (Tsao, Bevona et al. 2003). Overall incidence of melanoma has been increasing over the past 30 years, although the death rate has remained relatively static (Garbe and Leiter 2009). Diagnoses of thinner and less invasive melanomas are rising in some studies, suggesting that some of the increase in incidence may be due to increased diagnosis of early tumors (van der Spek-Keijser, van der Rhee et al.

1997, Garbe, McLeod et al. 2000, Crocetti and Carli 2003, Demierre, Chung et al. 2005, Cubitt, Khan et al. 2013). Survival of patients with melanoma is strongly linked to stage at diagnosis. For patients who are diagnoses with only localized disease, have a >98% 5-year survival rate, while patients diagnosed with distant metastases have only a 22% 5-year survival rate (Tsao, Bevona et al. 2003).

***Classification of melanocytic lesions***

Melanocytic lesions range from benign lentigos and nevi (moles) to metastatic melanoma. Lentigo simplex are macular lesions with proliferations of nevi along the junction without formation of nests of nevus cells within the epidermis. Nevi can be either congenital or acquired and can range from macular to popular (Barnhill 2014). Congenital nevi are uncommon but can cover extensive portions of the skin and have a higher risk of malignant transformation than acquired nevi (Shah, Feintisch et al. 2016). Acquired nevi, on the other hand, are nearly universal and generally develop during childhood and adolescence (Rivers, MacLennan et al. 1995, Valiukeviciene, Miseviciene et al. 2005, Schafer, Merkl et al. 2006, Aalborg, Morelli et al. 2009, Crane, Mokrohisky et al. 2009). Nevus counts are highest in fair-skinned individuals (Crane, Mokrohisky et al. 2009). Acquired nevi are usually 2-4 mm in diameter and can be junctional, compound (epidermal and dermal), or dermal (Clark, Elder et al. 1984, MacKie, English et al. 1985, Aalborg, Morelli et al. 2009). Atypical or dysplastic nevi are often >5mm and show clinical (increased size, variable pigmentation) or histopathologic atypia (including cellular and nuclear variability) (Silva, Sa et al. 2011, Perkins and Duffy 2015). *In situ* melanomas are confined entirely within the epidermis and are considered a pre-cancerous lesion. Cutaneous

melanoma is the most common form but uveal, mucosal and acral (palms, soles, and nailbed) melanomas also occur. While cutaneous tumors are most common in pale-skinned populations, non-cutaneous melanomas do not have skin type predilections (Bradford, Goldstein et al. 2009). Cutaneous melanomas can be superficial spreading melanomas which have a radial growth phase (RGP) laterally along the epidermal-dermal junction followed by a vertical growth phase (VGP) with invasion through the basement and into the dermis and subcutaneous tissue. Nodular melanomas grow vertically into the dermis and subcutaneous tissue without much lateral spreading through the skin. Nodular melanomas are less commonly diagnosed but have a worse prognosis than superficial spreading melanomas.

Progression of nevi to melanoma is a rare but important route of melanoma formation. An individual nevus is believed to have a 1:3,000-1:11,000 chance of malignant transformation over an individual's lifetime (Tsao, Bevona et al. 2003). However, approximately 30% of melanomas have evidence of arising from a pre-existing nevus (Troxel 2003, Tsao, Bevona et al. 2003, Pampena, Kyrgidis et al. 2017). While nevi typically develop during childhood through early adulthood, most melanomas are diagnosed in people over the age of 55 (Garbe and Leiter 2009). Patients with high numbers of nevi and especially atypical nevi have a higher risk of progression (Goldstein and Tucker 2013)and can be clinically and histopathologically indistinguishable from early melanoma, leading to diagnostic and clinical challenges (Troxel 2003, Reddy, Farber et al. 2013). These diagnostic challenges mean that melanoma diagnosis is the single most-important source of malpractice suits for physician pathologists (Troxel 2003). Since there is no clear clinical guidance for

diagnosis or treatment of atypical melanocytic lesions (Reddy, Farber et al. 2013), there is an opportunity and need for further information to identify lesions at risk for or that have already undergone malignant transformation.

UV exposure is believed to play a role in development of melanocytic lesions (Whiteman, Whiteman et al. 2001, Valiukeviciene, Miseviciene et al. 2005, Oliveria, Saraiya et al. 2006, Dennis, Vanbeek et al. 2008, Aalborg, Morelli et al. 2009, Kulichova, Danova et al. 2014, Ghiasvand, Weiderpass et al. 2016, Madigan and Lim 2016), although the mechanisms of the relationship remain unclear. People with pale, non-tanning skin and red hair have the highest risk of melanoma (Mitra, Luo et al. 2012), as well as other forms of skin cancer (Mitra, Luo et al. 2012). Epidemiological studies have linked childhood sunburn, intermittent sunburn, tanning behavior, and living in areas with higher UV indices with higher melanoma risk (Whiteman, Whiteman et al. 2001, Dennis, Vanbeek et al. 2008, Kulichova, Danova et al. 2014, Ghiasvand, Weiderpass et al. 2016, Madigan and Lim 2016).

***Effects of UV on skin and melanocytes***

Sunlight is overwhelmingly the largest source of UV exposure reaching the earth and is composed of 95% UVA (320-340nm) and 5% UVB (290-320nm). UVC rays are blocked by stratospheric ozone (Douki, Reynaud-Angelin et al. 2003, El Ghissassi, Baan et al. 2009). UVA penetrates more deeply into the skin and extends into the dermis, while only a small amount of UVB reaches the junctional melanocytes (Herrling, Jung et al. 2006, Meinhardt, Krebs et al. 2008) (Fig. 1). Many indoor tanning beds use high dose UVA with little to no UVB (Wang, Setlow et al. 2001). Both UVA and UVB can cause DNA damage and alter the microenvironment

within the skin (Kligman, Akin et al. 1985, Pearse, Gaskell et al. 1987, Labat-Robert, Fourtanier et al. 2000). Epidemiologic data suggest potential roles for both UVA and UVB in melanoma development, but the comparative importance of UVA and UVB on human melanoma development remains controversial.

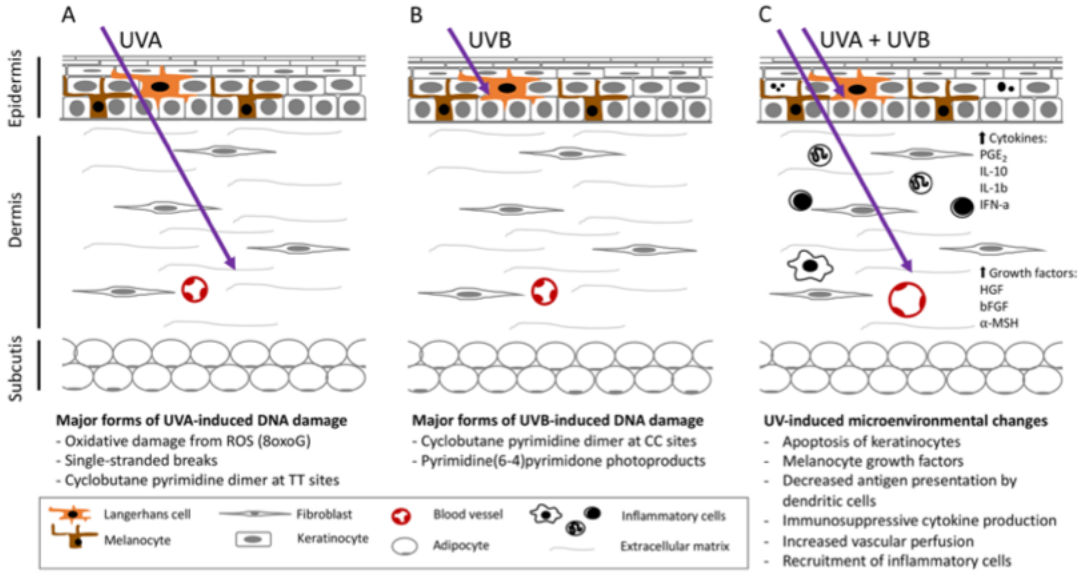


**Figure 1. Major effects of UV irradiation on the skin.** UVA (A) and UVB (B) penetrate into the skin to different depths (purple arrows) and cause different types of DNA damage. UVA/UVB exposure additionally causes a variety of changes in the skin microenvironment. Figure published previously in Day et al 2017.

Much of the attention on UV and melanoma has focused on the mutagenic role of UV. *In vitro* studies show that UVB causes the formation of 6-4 photoproducts and signature CC > TT mutations at dipyrimidine sites through the formation of cyclobutane pyrimidine dimers (CPDs), although other patterns including C > T transitions at dipyrimidine sites are also seen *in vitro* (Fig 1B) (Brash 2015). UVA is a less potent DNA damaging agent and can damage DNA indirectly through oxidative damage from reactive oxygen species and through formation of CPDs at TT sites (Fig 1A), which usually do not lead to C > T transitions (Tyrrell 1973, Tyrrell, Ley et al.

1974, Noonan, Zaidi et al. 2012). Human cutaneous melanomas are highly mutated with a predominance of C > T transitions at dipyrimidine sites but fewer CC > TT transitions, which is consistent with UV mutagenesis(Brash, Rudolph et al. 1991). Melanocytes play a substantial role in protection of hairless skin from UV irradiation. Melanin is produced both constitutively, providing baseline skin pigmentation and in direct response to UV exposure. Keratinocytes with UV-induced DNA damage signal to melanocytes to increase both production and transfer of melanin to surrounding keratinocytes (D'Orazio, Nobuhisa et al. 2006, Brenner and Hearing 2008, Wicks, Chan et al. 2011). An individual cutaneous melanocyte may contact up to 30-40 keratinocytes with dendritic processes (Brenner and Hearing 2008, Wang, Fukunaga-Kalabis et al. 2016). Keratinocytes accept melanosomes from the melanocytes and then arrange the melanin into caps over their nuclei (Montagna and Carlisle 1991, Kobayashi, Nakagawa et al. 1998). These melanin caps can function both to scatter and absorb energy from UV irradiation (Kaidbey, Agin et al. 1979). Melanin is produced both constitutively and in response to UV exposure.

In addition to mutagenesis, effects of UV on the skin microenvironment likely also play a role in the initiation and progression of melanoma (Fig 1C). Keratinocytes and dermal fibroblasts produce many melanocyte growth factors, including basic fibroblast growth factor, hepatocyte growth factor (HGF), and endothelin 1 and 3 (Haass and Herlyn 2005). Crosstalk between keratinocytes and melanocytes, and other cells within the skin microenvironment, allows adaption to external stimuli. Following UV, surviving keratinocytes secrete melanocyte growth factors (including α-MSH, EDN1), which increase cytokine and melanin production (Natarajan, Ganju

et al. 2014, Wang, Fukunaga-Kalabis et al. 2016). In addition, direct and indirect interactions between melanoma cells and keratinocytes and fibroblasts can influence the behavior and metastatic potential of melanoma cells (Hsueh, Gupta et al. 2000, Li, Satyamoorthy et al. 2001, Li, Satyamoorthy et al. 2003, Golan, Messer et al. 2015). There is increasing evidence that UV-induced microenvironmental changes may be important during initiation and progression of melanocytic lesions.

***Major mutations in human melanoma***

Cutaneous melanoma has the highest number of mutations of any tumor type (Hodis, Watson et al. 2012, Lawrence, Stojanov et al. 2013). Activation of the mitogen-activated protein kinase (MAPK) pathway is common, and driver mutations are common in this pathway. Hotspot mutations in *BRAF* are particularly common, and approximately 50% of cutaneous melanomas have V600E mutations (Hodis, Watson et al. 2012, Lawrence, Stojanov et al. 2013). BRAF V600E mutations are also present in 30-90% of benign acquired nevi (Pollock, Harper et al. 2003, Uribe, Wistuba et al. 2003, Yazdi, Palmedo et al. 2003, Poynter, Elder et al. 2006, Karram, Novy et al. 2013, Tschandl, Berghoff et al. 2013, Yeh, von Deimling et al. 2013, Shitara, Tell-Marti et al. 2015). *NRAS* mutations in codons 12/13 and 61 are mutually exclusive with *BRAF* mutations and are seen in approximately 20% of melanomas and 25-95% of congenital nevi (Bauer, Curtin et al. 2007, Kinsler, Thomas et al. 2013, Charbel, Fontaine et al. 2014, Roh, Eliades et al. 2015). *NRAS* mutations are more common in giant congenital nevi than in small or medium ones (Aalborg, Morelli et al. 2009, Roh, Eliades et al. 2015). Loss-of-function mutations in *NF1*, a MAPK repressor, occur in approximately 13% of melanomas (Hodis, Watson et al.

2012, Nissan, Pratilas et al. 2014, Krauthammer, Kong et al. 2015), and at higher rates in desmoplastic melanomas (Wiesner, Kiuru et al. 2015). Approximately 17% of melanomas do not contain mutations in *BRAF*, *NRAS* or *NF1* and are classified as "triple wildtype" tumors. Interestingly, none of the major driver mutations in cutaneous melanoma are typical C > T transitions. These non-canonical mutations may or may not be related to UV; *in vitro* studies have found that up to 10% of UV-induced mutations can be T > A transversions (Brash 2015). Regardless, *BRAF* mutations are most common in sun-exposed nevi and melanoma, suggesting a link to UV (Dong, Phelps et al. 2003, Bauer, Curtin et al. 2007, Karram, Novy et al. 2013). Non-cutaneous melanomas generally do not have BRAF or NRAS mutations and may exhibit other site-specific drivers. Uveal melanomas frequently contain hotspot mutations in *GNAQ* (44%) or *GNA11* (40%) (Van Raamsdonk, Bezrookove et al. 2009, Van Raamsdonk, Griewank et al. 2010). *GNAQ* are also commonly mutated in cutaneous "blue nevi" and melanomas that arise from blue nevi (Van Raamsdonk, Bezrookove et al. 2009, Huang, Urtatiz et al. 2015). Mutations in *BAP1*, *SF3B1*, *CYSLTR2*, and *EIF1AX* are also found as drivers in uveal melanoma (Harbour, Roberson et al. 2013, Field, Decatur et al. 2016, Moore, Ceraudo et al. 2016). Mucosal melanoma does not have a dominant driver, and studies of different populations find different frequencies of various drivers including *KIT* exon 11, *NRAS*, *NF1*, *GNAQ/11*, and *SF3B1* (Sheng, Kong et al. 2016, Cosgarea, Ugurel et al. 2017, Hayward, Wilmott et al. 2017, Hintzsche, Gorden et al. 2017). Acral melanomas are reported to contain *BRAF*, *KIT*, *GNAQ* and *NRAS* (Furney, Turajlic et al. 2014, Moon, Choi et al. 2018). UV-type mutations are less commonly seen in

uveal, mucosal and acral melanomas and structural rearrangements are more common in these lesion types (Hayward, Wilmott et al. 2017).

Melanoma susceptibility and progression is also associated with mutation of cell cycle-associated tumor suppressor genes. *CDKN2A*, which codes the cell cycle checkpoint genes p16/INK4A and p14/ARF, is frequently mutated or lost in melanoma. Germline *CDKN2A* mutation is associated with familial melanoma and with atypical mole syndrome (Monzon, Liu et al. 1998, Ciotti, Struewing et al. 2000, Chaudru, Laud et al. 2005, Harland, Taylor et al. 2005, Laud, Marian et al. 2006). Alterations in *CDKN2A* appear to be associated with melanoma progression (Cachia, Indsto et al. 2000, Shain, Joseph et al. 2018, Zeng, Jorapur et al. 2018). *CDKN2A* is deleted in approximately 50% of melanomas (Plummer, Middleton et al. 2005) and is hypermethylated or mutated in an additional 15-20% (Cachia, Indsto et al. 2000, Hodis, Watson et al. 2012). Somatic *CDKN2A* mutations are uncommon in melanocytic nevi, suggesting that acquired alterations are associated with progression (Papp, Pemsel et al. 1999, Kumar, Angelini et al. 2004, Wang, Presland et al. 2005, Shain, Yeh et al. 2015). Amplification and activating mutations in the CDKN2A binding partner, CDK4, are also associated with both familial and sporadic melanoma (Mantelli, Barile et al. 2002, Helsing, Nymoen et al. 2008, Puntervoll, Yang et al. 2013). Mutations in the tumor suppressor *TP53* are also seen in approximately 20% of melanomas and are associated with UV exposure (Zerp, van Elsas et al. 1999, Hodis, Watson et al. 2012). Unlike most other major driver and tumor suppressor mutations, *TP53* mutations are often UV-type C > T transitions (Brash, Rudolph et al. 1991, Stahl, Stranneheim et al. 2011, Viros, Sanchez-Laorden et al. 2014).

Additional non-cell cycle associated tumor suppressors are also commonly involved. Reduced expression of PTEN is seen in approximately half of melanomas, whether or not mutations in *PTEN* are identified (Zhou, Gimm et al. 2000, Mikhail, Velazquez et al. 2005, Goel, Lazar et al. 2006). Mutations are associated with thicker tumors and are found in approximately 10% of primary melanomas with higher frequencies in metastatic melanomas and cell lines (Guldberg, thor Straten et al. 1997, Birck, Ahrenkiel et al. 2000, Celebi, Shendrik et al. 2000, Reifenberger, Wolter et al. 2000, Goel, Lazar et al. 2006, Aguissa-Toure and Li 2012). *PTEN* mutations significantly co-occur with *BRAF* mutation, but trend towards mutual exclusivity with *NRAS* and *GNAQ* mutations (Tsao, Zhang et al. 2000, Cerami, Gao et al. 2012, Gao, Aksoy et al. 2013). *TERT* promoter mutations, germline and somatic, are seen in approximately 20-33% of primary cutaneous melanomas, especially on chronically sun-exposed skin, and up to 85% of metastatic melanomas and are associated with thicker cutaneous lesions and worse survival, especially in conjunction with BRAF mutation (Horn, Figl et al. 2013, Huang, Hodis et al. 2013, Gessi, van de Nes et al. 2014, Populo, Boaventura et al. 2014, Ekedahl, Lauss et al. 2016, Bao, Prescott et al. 2017, Seynnaeve, Lee et al. 2017). The common acquired mutations noted in *TERT* promoters are UV-type mutations (Horn, Figl et al. 2013, Fredriksson, Elliott et al. 2017). Fittingly, acral, mucosal and uveal tumors on non-sun exposed sites have much lower rates of *TERT* promotor mutations (Griewank, Murali et al. 2013, Koopmans, Ober et al. 2014, Miao, Wang et al. 2015, Vazquez Vde, Vicente et al. 2016, Liang, Chen et al. 2017). Alterations in *BAP1*, either as germline variants or somatic mutations are associated with uveal melanomas and cutaneous melanoma

(especially Spitz nevi and associated melanomas) (Harbour, Onken et al. 2010, Njauw, Kim et al. 2012, Murali, Wiesner et al. 2013, Gupta, Lane et al. 2015). *BAP1* alterations are associated with an increased risk of metastasis in uveal melanoma (Njauw, Kim et al. 2012, Kalirai, Dodson et al. 2014, Koopmans, Verdijk et al. 2014, Gupta, Lane et al. 2015).

Despite having identified some of the major drivers and tumor suppressors, much remains unknown about the initiation and progression of melanoma. The prevalence of strong drivers like *BRAF* and *NRAS* in both benign and malignant melanocytic lesions indicates that these mutations are not sufficient to cause tumorigenesis. There is still a need to understand how UV exposure contributes to lesion initiation and transformation.

***UV-induced mouse models of melanoma***

The long latency between childhood and early adulthood sun exposure and melanoma formation makes it especially challenging to prospectively study the role of UV on melanoma development. Since UV can function in multiple capacities as tumor initiator, tumor promotor and inducer of microenvironmental changes, the most significant roles for UV can be difficult to identify by studying human melanoma patients alone.

Animal models, on the other hand, provide a platform for prospective studies to investigate specific questions and address causative associations. Although several species have been involved in the modeling of UV-induced cutaneous melanoma, including opossum (*Monodelphis domestica)*, platyfish (*Xiphophorus spp.*) and zebrafish (*Danio rerio)*, in this review we will focus exclusively on genetically

engineered mouse (GEM) models (Robinson, VandeBerg et al. 1994, Leyvraz, Spataro et al. 1997, Chan, Robinson et al. 2001, Nairn, Kazianis et al. 2001, Lee, Sharma et al. 2006). The development of mouse models for melanoma was initially difficult due to the resistance of wildtype mice to melanomagenesis, even after repeated exposure to chemical carcinogen, UV, or both (Romerdahl, Donawho et al. 1988, Jiang, Ananthaswamy et al. 1999). However, use of hairless (Skh-hr2) mice treated with DMBA followed by repeated UV was able to induce nevi and melanomas in treated animals (Epstein, Epstein et al. 1967, Husain, Pathak et al. 1991, Pathak 1991). Interestingly, some of the melanomas and nevi in these mice had *Nras* mutations near the 61$^{st}$ codon, which is a hotspot for human congenital nevi and melanomas (Husain, Pathak et al. 1991). In the last decade, technological advances have generated GEM models that harbor oncogenic mutations associated with human melanoma to prospectively investigate clinically relevant questions about the role of UV in cutaneous melanoma.

Differences in mouse and human skin need to be considered when assessing mouse melanoma studies that have investigated the role of UV in melanoma biology. These studies use a variety of strains of mice, doses, timing and types of UV administration. Studies focus primarily on the ability of UV to induce melanoma with or without a pre-existing melanocytic lesion, and on how UV-induced microenvironmental changes can alter the progression of melanoma. Although the variability in the studies makes it difficult to directly compare results, it also highlights a wide variety of possible roles of UV, depending on the dose, waveband, and context, in the development and progression of cutaneous melanoma.

### Similarities and differences between human and mouse skin

Human and mouse skin have some distinct features. Both mouse and human skins are composed of dermis and epidermis, contain hair follicles, and have a similar distribution of blood vessels and nerves. Human skin is thicker (1.5–6 mm), has epidermal layers (5-8) and rete ridges, and is adherent to underlying tissues. In contrast, mouse skin is thinner (0.7-0.8mm) with fewer epidermal keratinocyte layers (2-3), has no rete ridges, does not adhere to underlying tissue, and has a panniculus muscle layer. Mice also have a heavy hair coat that protects their skin from UV. In human skin, melanocytes are located along the dermal-epidermal junction as well as in hair follicles. In mouse skin, the vast majority of melanocytes are restricted to the hair follicles. During embryonic development in both species, melanoblasts migrate out of the neural tube, through the dermis to the dermal-epidermal junction. As hair follicles develop, some of these junctional melanocytes move into the developing follicles. In wildtype mice, junctional melanocytes do not persist after the neonatal stage in haired areas. Since junctional melanocytes are not present in wildtype mice, melanomas derived from mouse models may arise from cells of origin that differ from human melanomas. Additionally, these differences in anatomic location mean that in wildtype mice melanocytes are not interacting directly with keratinocytes and are receiving very different microenvironmental signals compared to melanocytes in the human epidermis.

Although melanocytes in both species produce both eumelanin and pheomelanin, these are produced in different frequencies (Thody, Higgins et al. 1991, Liu, Kempf et al. 2003). UV increases the quantity of melanin produced and can alter

the type produced (Hennessy, Oh et al. 2005). In humans, the frequency of each type of melanin varies widely with skin and hair coloration: people with darker skin produce higher quantities of eumelanin, while fair-skinned red heads produce a higher proportion of pheomelanin. Mice generally produce both types of melanin as well, but in many cases mouse strains produce either primarily eumelanin or pheomelanin (Liu, Kempf et al. 2003).

Human and mouse skin microenvironments also have some notable differences. Because of the dense hair coat, mouse skin undergoes frequent hair cycles. In each cycle the hair follicles grow and degenerate, leading to turnover of mature melanocytes and cycling of melanocyte stem cells in the bulge of the hair follicle. Hair follicle involution also involves activation of immune cells, including macrophages and T cells in the skin (Eichmuller, van der Veen et al. 1998). In contrast, human skin does not exhibit obvious hair cycles. Finally, the skin microbiome and resident immune cells are different between the two species (Pasparakis, Haase et al. 2014). These microenvironmental changes may have implications both in the development of cutaneous melanoma and in the immunological responses in human and mouse skin.

In summary, mouse and human skin have some anatomic and functional differences that influence their response to UV and the development of melanoma. The contrasting melanocyte distribution and resultant differences in melanocyte microenvironment in human and mouse skin may be a major factor in the different susceptibility to melanoma in these species. These differences should be considered when choosing mouse models of UV-induced melanoma and in translating findings to

human melanoma patients. Careful choice of the appropriate model and experimental planning will provide the most valuable information for translational studies.

### Neonatal UV can induce melanoma in hepatocyte growth factor transgenic mice

A number of GEM models have been recruited to explore the role of UV melanomagenesis, including those overexpressing HGF, the ligand for the receptor tyrosine kinase MET. HGF/MET signaling plays a significant role in embryonic cell migration and has been associated with increased metastasis and drug resistance in human melanomas (Halaban, Rubin et al. 1992, Hartmann, Prospero et al. 1998, Gaggioli, Deckert et al. 2005, Straussman, Morikawa et al. 2012). Studies have shown that HGF promotes the survival of melanoblasts derived from neural crest and melanocytes in mouse skin (Kos, Aronzon et al. 1999). Human keratinocytes and skin fibroblasts secrete increased amounts of HGF following UV exposure (Yamaguchi and Hearing 2009). Mouse skin expresses HGF in small amounts (Yang and Park 1995). Mice broadly expressing an HGF transgene gain constitutive activation of pathways downstream of MET, resulting in increased skin pigmentation due to survival of melanocytes at the epidermal-dermal junction, which persists into adulthood(Noonan, Otsuka et al. 2000, Imokawa 2004, Aoki, Yamada et al. 2009). Therefore, HGF-tg mice are regarded to exhibit a “humanized” melanocyte distribution in the skin.

HGF is not a strong driver in cutaneous melanoma. Without carcinogenic treatment (UV or DMBA), melanomas occur rarely in the skin of HGF-tg mice within 1-2 years (Noonan, Otsuka et al. 2000, Noonan, Recio et al. 2001). Adult UV, even at

prolonged repetitive dosing, does not induce melanomas in HGF mice but can induce other skin tumors (Noonan, Otsuka et al. 2000). In contrast, a single burning UV dose at 3.5 days can induce nevi and melanoma in HGF-tg mice (Noonan, Recio et al. 2001). This is relevant because childhood sunburn is recognized as an important risk factor for melanoma formation (Dennis, Vanbeek et al. 2008). Melanocytic nevi and melanomas arising in the HGF-tg model are histologically heterogeneous and recapitulate the variety seen in human cutaneous melanocytic lesions. Disruptions of the *CDKN2A* locus or activation of CDK4 accelerate melanoma development following neonatal UV in the HGF model (Thomas, Liu et al. 2007, Gaffal, Landsberg et al. 2011). Targeted expression of surviving (BIRC5) can also enhance UV-induced melanogenesis by preventing apoptosis of UV-exposed melanocytes, suggesting that the dysregulation of senescence or apoptosis can play critical roles in the transformation of melanocytes following neonatal UV (Thomas, Liu et al. 2007). Melanocytic cells undergo significant changes associated with differentiation between the end of gestation and by one week after birth (Hirobe 1984). Therefore, neonatal UV exposure is likely to affect a distinct population of melanocytic cells compared to adult UV – namely, progenitor melanoblasts vs. mature melanocytes, respectively. This may help account for the increased risk of melanoma seen with childhood sunburn vs. adult sunburn in human patients. The UV-treated HGF-tg mouse represents a good model for human melanomas that does not possess either a *BRAF* or *NRAS* mutation (approximately 30% of cutaneous melanomas). Since there is no pre-existent dominant driver oncogene, UV may serve as both tumor initiator and promoter for "*de novo*" melanomagenesis in the HGF-tg model. This feature makes

the HGF-tg mouse especially suitable in evaluating etiological factors, environmental risks, and prevention of UV-induced nevi and melanoma following childhood sun exposure.

### UV can enhance melanomagenesis following activation of dominant driver mutations

In contrast to the use of neonatal UV in the HGF-tg mouse models, studies examining the role of UV in melanocytic nevi and melanomas with a dominant oncogenic driver mutation have primarily focused on adult UV exposure. Mice with mutations in the RAS/RAF pathways (HRAS, NRAS or BRAF) show melanocytic hyperplasia and increased numbers of extrafollicular melanocytes within the dermis compared with wildtype mice. These models are consistent with the theory that RAS/RAF mutations are founding mutations in melanocytic nevi and melanomas (Yeh, von Deimling et al. 2013, Shain and Bastian 2016). According to this theory, subsequent UV may lead to contributory mutations and/or microenvironmental changes that can promote melanomagenesis.

The first model to investigate the role of UV in melanoma development expressed a powerful viral oncogene SV40 T antigen (TAg-tg) using a mouse tyrosinase promotor (Kelsall and Mintz 1998). TAg-tg mouse pups were exposed to daily UV for 3-10 days (Kelsall and Mintz 1998), leading to melanomas. Following transplantation, some of the UV melanomas became metastatic. This study demonstrated that UV could promote tumor development in the context of a powerful driver oncogene. Based on this model, researchers then tried to build melanoma

models by adding different combinations of altered alleles that are more relevant to human melanoma.

RAS mutations (primarily NRAS but occasionally HRAS) are common in human congenital nevi and cutaneous melanoma. Chin and colleagues observed that mice expressing a mutant HRAS transgene by virtue of the mouse tyrosinase promotor (TPras) and loss of $p16^{Ink4a}$ developed melanoma without additional carcinogens (Chin, Pomerantz et al. 1997). TPras mutant mice with wildtype $p16^{Ink4a}$ were used to compare the effects of single exposure to the chemical carcinogen (DMBA) with twice weekly UV and a known tumor promotor (TPA) (Broome Powell, Gause et al. 1999). DMBA was very efficient and induced melanocytic lesions with a high penetrance (86-88%). UVB exposure alone induced melanocytic lesions only in 20% of mice and most of these lesions were nevi. Combined treatment with UVB and TPA increased the lesion penetrance to 78%. Interestingly, the melanomas that arose in the UV-exposed groups occurred only in albino TPras mice, suggesting a protective role for melanin in this model.

Other studies using TPras mice have investigated the role of neonatal UV and cell cycle checkpoints on development of RAS mutant melanomas. Kannan et al. (2002) found that UV exposure accelerated melanomagenesis in $p19^{Arf}$ knockout mice, but not in $p16^{Ink4a}$ knockout albino mice (Kannan, Sharpless et al. 2003). In $p19^{Arf}$ knockout mice, UV-induced melanomas demonstrated increased cdk6 expression, leading to disruption of the RB pathway. Hacker et al. (2006) reported that neonatal UV exposure also increased the frequency and accelerated the development of melanomas in TPras mice carrying a $CDK4^{R24C}$ mutation (Hacker,

Muller et al. 2006). It is not clear whether these findings are specific to neonatal UV or would also be found following adult UV in these strains. These studies indicate that functional disruption of the $p16^{Ink4a}$/CDK4/CDK6/RB pathway can facilitate mutant RAS-driven melanomagenesis in UV-associated and non-UV-associated pathways.

$BRAF^{V600E}$ mutations are the most common driver mutations in human cutaneous melanoma. Epidemiologic and genomic data suggest that $BRAF^{V600E}$ mutations may be the initiating lesion in melanocytic nevi, with subsequent UV acting as a tumor promotor. To test this hypothesis, Viros et al. induced $BRAF^{V600E}$ mutations using tyrosinase-driven Cre-Lox recombination in 2-month old mice followed by weekly broad-spectrum UV starting at 3 months (Viros, Sanchez-Laorden et al. 2014). This UV regimen both accelerated melanoma formation in the BRAF model and increased the number of tumors per mouse. UV-exposed tumors also had significantly higher numbers of somatic single nucleotide variants and a higher percentage of C > T transitions than non-UV exposed tumors, consistent with human melanomas and UV mutagenesis. Exclusively in the UV-exposed tumors, *Trp53* mutations were additionally identified. *Trp53* is known to be a mutational target of UV, and the $p19^{Arf}$/p53 pathway facilitates $BRAF^{V600E}$ mutant mouse melanoma (Luo, Sheng et al. 2013, Viros, Sanchez-Laorden et al. 2014). These data also suggest that UV following BRAF mutation can enhance the likelihood of malignant transformation of nevi.

### Sunscreen provides partial protection against UV-induced DNA damage and melanoma

Melanoma incidence has been rising over the last few decades and there is a need for evidence-based advice for protecting against melanoma and other skin cancers. Sunscreen use appears both epidemiologically and experimentally to protect against melanoma, which further highlights the importance of UV in melanomagenesis. Prospective mouse studies have shown that sunscreen use reduces, but does not eliminate, the risk of melanoma following neonatal or adult UV (Wolf, Donawho et al. 1994, Klug, Tooze et al. 2010, Viros, Sanchez-Laorden et al. 2014). Sunscreen reduced clinical and histologic evidence of UV damage in the skin, including inflammation, skin darkening and evidence of UV damage to keratinocytes (Wolf, Donawho et al. 1994, Viros, Sanchez-Laorden et al. 2014). DNA damage to melanocytes was also reduced, with reduced numbers of TT dimers and reduced numbers of C > T transitions in mice treated with sunscreen before UV exposure compared with controls (Klug, Tooze et al. 2010, Viros, Sanchez-Laorden et al. 2014). Although melanoma formation was reduced in sunscreen-protected mice, it was still higher than in non-UV exposed mice. Sun protective fabrics were superior in preventing UV-melanoma than sunscreens (Viros, Sanchez-Laorden et al. 2014). These studies all found that sunscreen use prevented melanoma despite using a variety of UV doses, sunscreens and mouse strains (Wolf, Donawho et al. 1994, Klug, Tooze et al. 2010, Viros, Sanchez-Laorden et al. 2014). These data provide strong, prospective support for the use of sunscreens to reduce melanomagenesis. However, sunscreen use does not entirely eliminate UV-induced melanoma formation and

prevention of sunburn alone does not remove the risk of melanoma. Mouse models of UV-induced melanoma provide a powerful tool to test the efficacy of sunscreens and other preventive strategies in preventing melanoma and other UV-induced skin damage.

**UV-induced microenvironmental changes impact melanoma development**

In addition to direct mutagenic effects, UV can influence the microenvironment in ways that can enhance melanomagenesis. UV has long been known to cause immunosuppression within the skin. UV leads to locally decreased antigen presentation, expansion of regulatory T cells, and lower numbers of effector T cell in the exposed skin (Loser and Beissert 2009). In fact, the immunosuppressive effect of UV is used to treat psoriasis, and can suppress contact hypersensitivity (Byrne, Spinks et al. 2002). Therefore, several models have been developed to study how UV-induced changes in the skin microenvironment influence melanoma development and progression.

Bald et al. used the HGF-tg/Cdk4$^{R24C}$ mouse to model the effects of UV on cutaneous melanomas (Bald, Quast et al. 2014). Twice weekly exposure to UV following melanoma initiation did not result in increased tumor formation but did enhance angiotropism and metastasis in some of the UV exposed tumors. Sequencing of tumors was not performed, so it is not known if there were genomic differences between the UV- and non-UV-exposed tumors that may have affected metastasis. However, UV-induced keratinocyte damage led to an increase in Myd88 TLR4+ neutrophils in the UV-exposed mice. Myd88/TLR4 neutrophils enhanced angiotropism of both mouse and human melanoma cells *in vivo* and *in vitro*. This

study demonstrates that UV can alter the microenvironment in ways that contribute to tumor progression and metastasis and suggests that UV on pre-existing nevi or early melanomas may contribute to progression.

Using a model of neonatal UV, Zaidi et al. showed that UV can recruit interferon-gamma-expressing macrophages that create an environment favorable for melanoma growth and survival (Zaidi, Davis et al. 2011). These interferon-gamma-expressing macrophages were also found in a majority of human melanomas. The role of these macrophages in the development and persistence of melanocytic nevi has yet to be investigated but may be clinically relevant. This response was neonatal-specific in the mice tested and may help to explain the significance of childhood sunburn as a risk factor for melanoma.

**Purpose and hypothesis**

Although a variety of drivers have been identified in nevi and melanoma, the alterations associated with initiation and progression remain unclear, particularly for triple wildtype lesions. Additionally, targeted therapies to treat BRAF mutant melanoma initially show a dramatic response, but tumors invariably develop resistance leading to minimal improvements in lifespan (Villanueva, Vultur et al. 2011). Recent developments in immunotherapy have dramatically improved lifespan for responders, but only 30-60% of patients have a therapeutic response, depending on the immunotherapeutic target (Hodi, O'Day et al. 2010, Wolchok, Chiarion-Sileni et al. 2017). There is a need to identify genes and pathways that could be useful for diagnostics or novel therapies.

Our laboratory had developed two new HGF models: the GS model on an FVB background with melanocyte-specific GFP expression and the BT model on a C57BL/6 background with inducible CDKN2A loss. These two new models allowed exploration of progression of very early UV-induced melanocytic lesions (GS model) and of the effect of UV followed by heterozygous *Cdkn2a* alteration. We hypothesized that melanocytic lesion progression from nevus to melanoma to metastatic melanoma is associated with acquisition of genomic alterations at each stage. To investigate this hypothesis, we established three aims: 1) Characterize early melanocytic lesion development and progression in the GS model; 2) Characterize melanocytic lesion progression in the BT model; 3) Characterize genomic alterations associated with lesion progression in the GS and BT models.

# Chapter 2: Melanocytic lesion development and progression in an FVB mouse model of cutaneous melanoma


***Summary***

Approximately 30% of melanomas have evidence of association with a pre-existing nevus. Mechanisms underlying the progression of nevi to melanoma remain incompletely characterized. We hypothesized that nevus progression would be associated with the accumulation of additional genomic mutations at each stage of progression. To further investigate the early stages of nevus transformation, we designed the GS model on an HGF background with melanocyte-specific GFP expression and heterozygous loss of p16/INK4A for slow tumor development. Following a single UV exposure, GS mice develop melanocytic nevi, and approximately 10% of mice had progression to melanoma starting at an average of 251 days. Melanocytic lesions were histologically variable and both junctional and dermal nevi and melanomas were seen. Progression generally proceeded through a radial growth phase followed by vertical growth and nodule formation. Following transplantation into GFP-tolerized syngeneic mice, vertical growth phase melanomas rapidly established and reached exponential growth, while radial growth phase tumors grew slowly or regressed. Through this project, we were able to generate nevi, radial growth phase and vertical growth phase lesions for further genomic analysis as well as transplantable tumors and cell lines for future studies.

## ***Introduction***

In 1984, Clark first suggested that some melanomas undergo a stepwise progression from a normal melanocyte through a benign nevus to malignant melanoma (Clark, Elder et al. 1984) (Fig 2). Approximately 30% of melanomas have evidence of a nevus precursor at diagnosis, while the remaining 70% appear to have arisen de novo (Pampena et al 2017). These nevus-associated melanomas (NAMs) differ from de novo melanomas (DNM) in many ways. NAMs occur in younger patients, are on average thinner than de novo melanoma and have better survival outcomes (Rhodes and Melski 1982, Friedman, Rigel et al. 1983, Kaddu, Smolle et al. 2002, Lin, Luo et al. 2015, Cymerman, Shao et al. 2016, Pampena, Kyrgidis et al. 2017, Pandeya, Kvaskoff et al. 2018). Patients with NAMs also tend to have a higher total nevus

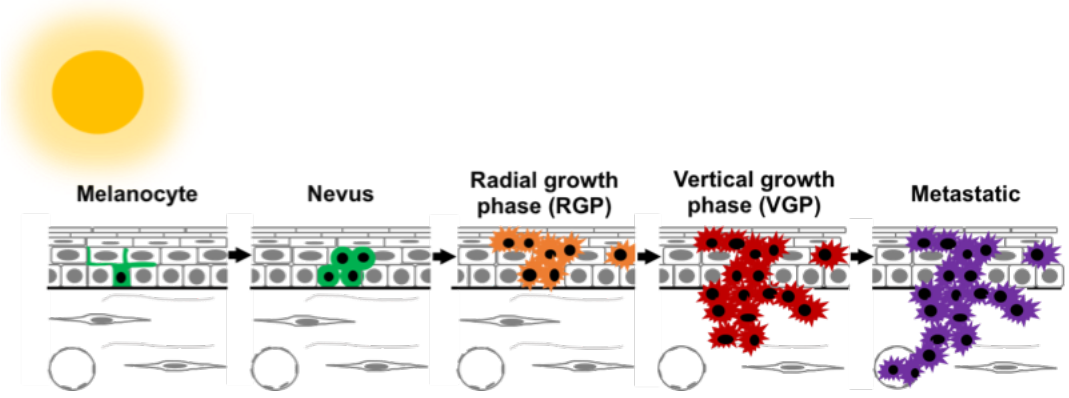


**Figure 2: Proposed stepwise progression of melanocytic lesions.** Accumulation of additional genomic changes in a Vogelsteinian-like manner is presumed to occur to allow progression to different steps.

count (Pandeya, Kvaskoff et al. 2018). Interestingly, skin surrounding NAMs generally shows less evidence of sun damage than that around DNMs and NAMs are epidemiologically associated with intermittent sun exposure (Purdue, From et al. 2005, Newton-Bishop, Chang et al. 2010, Pandeya, Kvaskoff et al. 2018). These

features suggest that there may be alternate pathways leading to melanoma for NAMs and DNMs.

Previous observations of melanoma development in FVB HGF models suggested a stepwise progression of melanocytic lesions (Recio, Noonan et al. 2002, Noonan, Dudek et al. 2003). However, in the albino FVB mice, it is not possible to identify lesions at very early stages, since they are flat and non-pigmented. By combining the albino HGF mouse model with a newly generated model with inducible melanocyte-specific GFP expression, we hypothesized that GFP-containing melanocytic lesions would be similar to previously HGF melanocytic nevi and melanomas and the GFP expression would allow us to identify and track stepwise progression of lesions from melanocytic nevi to malignant melanoma. To facilitate evaluation of progression, we chose a model with only a heterozygous p16/INK4A alteration which should lead to slow progression and lower tumor incidence than is seen in models with p19/ARF alterations (Recio, Noonan et al. 2002, Ha, Ichikawa et al. 2007). Samples for further histologic and genomic evaluation could be collected from lesions at difference clinical stages, allowing us to identify changes that occur during progression of lesions.

## ***Methods***

### Mouse model

Mice for nevus development (GS) mice were developed on an FVB/N background from F1 cross of male Hepatocyte growth factor (HGF) mice and female Dct-rtTA2s-M2; Tre-H2BGFP; $p16^{KO}$ mice. Dct-rtTA2s-M2; Tre-H2BGFP mice have melanocyte-specific nuclear GFP expression (Zaidi, Hornyak et al. 2011). Mice were

maintained on doxycycline-fortified (200 mg/kg) feed (Bio-Serv, Flemington, NJ) throughout their lives. Only male mice were used for the GS study due to poor survival of females. UV exposure protocol has been previously described (Noonan, Recio et al. 2001, Noonan, Zaidi et al. 2012). Briefly, 3-day old mice were exposed to 9.58 kJ/$m^2$ of UV using a FS40 sunlamp lamp for with 60% UVB and 40% UVA. Starting at 2 months of age, mice were shaved and imaged monthly using a Maestro Fluorescent Imaging System (Caliper Lifesciences, Waltham, MA) for green fluorescent protein (GFP) expression. Nevus number and first evidence of lesion transformation were determined based on GFP images. Mice were followed until humane endpoints were met, including total tumor size > 2$cm^2$, respiratory distress, and tumor ulceration. Animal use was approved by the Animal Care and Use Committee at NCI-Frederick and NCI-Bethesda.

**Sample Collection**

Biopsy samples were taken with 2-3mm biopsy punches (Integra Miltex, Plainsboro, New Jersey) or removed following euthanasia. GFP was visualized for biopsy or resection using a Nightsea (Lexington, MA) BlueStar flashlight or swan neck lamp and yellow filter glasses. At euthanasia, the entire back skin was examined using a GFP lighting system to find lesions that may have been missed with imaging. If tumors were collected, spleen samples were flash frozen and internal organs were examined for GFP fluorescence and collected if there was evidence of GFP fluorescence. Lesions > 2mm were divided into portions for histology, nucleotide extraction and transplantation or viably frozen. Histology samples were fixed with 10% neutral buffered formalin for 24 hours and then shifted to 70% ethanol until

processing and embedding. Histology samples were sent to Histoserv, Inc. (Gaithersburg, MD) for paraffin embedding, sectioning and hematoxylin eosin staining. Samples for nucleotide extraction were flash frozen in liquid nitrogen and stored at -80$^{o}$C. Viably frozen samples were placed in FBS + 10% DMSO and slowly frozen to -80$^{o}$C and stored in liquid nitrogen.

**Tumor transplantation**

Fresh or viably frozen tissue was used for transplantation into GFP-tolerized FVB/N Glowing head mice(Day, Carter et al. 2014). 0.5-2mm tumor chunks were inserted into the subcutaneous flank tissue using a trocar. Tumor growth was measured every 3-7 days. When tumors reached >300 mm$^3$, they were resected with wide margins. Following resection, mice were examined for tumor regrowth at the primary site weekly until mice reached humane endpoints. Transplant recipients were injected with doxycycline (80 μg/g body weight) 24 hours before resection or euthanasia to induce GFP expression (Zaidi, Hornyak et al. 2011). Sample collection and necropsy were performed as described for primary mice.

**Immunohistochemistry**

Melanocytic origin was confirmed using immunohistochemistry. Antibodies used include Pep8h (gift of Vincent Hearing, NIH, Bethesda, MD), GFP (Cell Signaling, Danvers, MA), Pep1 (gift of Vincent Hearing), Sox10 (CellMarque, Rocklin, CA). Samples were deparaffinized with xylene, rehydrated through graded alcohols before heat induced epitope retrieval using target retrieval buffer (Dako/Agilent, Santa Clara, CA) for 10 minutes in an IHC-specific microwave or steamer and 10 minutes cooling

on the bench. Primary antibody concentrations and incubation periods are in Table 1. ImmPRESS anti-rabbit AP secondary polymer (Vector laboratories, Burlingame, CA) or goat anti-rabbit biotinylated secondary antibody (Dako E0432) and VECTASTAIN ABC HRP Kit (Vector laboratories, Burlingame, CA) followed by ImmPACT NovaRED substrate (Vector laboratories, Burlingame, CA) or ImmPACT Vector Red alkaline phosphatase substrate (Vector laboratories, Burlingame, CA). Slides were dehydrated and then cover-slipped using Permount mounting medium (Fisher Scientific, Waltham, MA).

**Table 1. Immunohistochemistry antibody concentrations and incubation conditions.**

| Antibody | Antibody species | Concentration | Incubation conditions |
|---|---|---|---|
| GFP | Rabbit | 1:100 | Overnight at 4$^{o}$C |
| Pep8h | Rabbit | 1:5000 | Overnight at 4$^{o}$C |
| Sox10 | Rabbit | 1:100 | 30 min on benchtop |
| Pep1 | Rabbit | 1:5000 | Overnight at 4$^{o}$C |

**Melanoma cell line development**

Tumor processing and media recipes (Table 2) were adapted from protocols from Meenhard Herlyn's laboratory (Wistar Institute, Philadelphia, PA). Tissue chunks were harvested during tumor resection or following euthanasia and placed in medium (DMEM + 10% FBS or Mel2% medium) and shipped on ice to Bethesda. Tumor pieces were received in 2-5 hours in Bethesda. Tumor chunks were washed in DMEM, 10% FBS, and 50μg/mL Gentamicin (wash medium) four times. Tissues were then transferred to 150mm tissue culture dishes and minced using two scalpel blades until tissue pieces were <1mm. 50 mL of Collagenase IV in DMEM

(STEMCELL Technologies, Vancouver, BC) with 100μM HEPES buffer, 5% FBS, and 20μg/mL Gentamicin. Tissue pieces were triturated in the digestion solution and then incubated overnight on a rocker plate at 4°C. The next day, tissue was triturated and then transferred to a 50 mL conical tube. Tissue pieces were allowed to settle to the bottom of the conical tube for 5 minutes, and then the supernatant was transferred to a fresh conical. Tissue chunks were either washed several times in wash medium to harvest additional cells or run through the GentleMACS tissue dissociator (Miltenyi Biotec, Auburn, CA) if tissue had not dissociated well. Collected dissociated cells were spun down (1200 rpm for 7 minutes) and washed with wash medium 3 times. Cells were then plated with Mel2% medium (Table 2) into 24 well plates coated in 1% gelatin. Plates were monitored for growth or bacterial contamination and medium was changed 2x weekly. Cells were passaged using 90% Versene (Fisher Scientific, Waltham, MA) and 10% 2.5% trypsin to dissociate cells. New cell lines were grown at least two passages on 1% gelatin in Mel2% medium and then were transferred to Tu2% medium and grown directly on tissue culture dishes (Table 2).

**Table 2. Recipes for Mel2% and Tu2% media.**

| | **Mel 2%** | **Tu2%** |
|---|---|---|
| Component | Final concentration | Final concentration |
| MCDB153 | 78% | 78% |
| Leibovitz's L-15 | 20% | 20% |
| FBS | 2% | 2% |
| Insulin (rhuman) | 5 μg/ml | 5 μg/ml |
| Bovine pituitary extract | 15 μg/ml | -- |
| Epidermal growth factor | 5 ng/ml | -- |
| $CaCl_2$ | 1.68 mM | 1.68 mM |

### Statistics

Statistics were performed using Prism 7 (GraphPad Software, Inc., La Jolla, CA). A Kolmogorov-Smirnov test was used to compare the number of nevi in groups with or without melanoma development. Two-sided Fisher's exact test was used to assess probability of progression in mice with different numbers of nevi. Kaplan-Meier survival curves was used to evaluate differences in survival and transplant growth. The Logrank test for trend was used to compare curves from rounds of serial transplantation.

## ***Results***

### Melanoma formation in GS mice primarily occurred through nevus progression

Consistent with our hypothesis, melanocytic lesions in the GS model progressed from nevi to melanoma over time. At two months of age, nevi were readily visible as well-circumscribed, bright GFP lesions on the dorsum of UV-exposed GS mice (Fig 3A, right panel and insets). GS mice, with or without UV had a reticular GFP pattern that was absent in wildtype littermates, and likely represented junctional melanocytes (Fig 3A left and middle panel). A total of 256 GS mice were followed from two months of age through euthanasia. Nevi were noted in 80% of the mice at the 2 months with a median of 2 nevi per mouse (range 0-20) (Fig 3B). The size and GFP intensity of most nevi remained unchanged over the lifetime of the mouse. Nevi were flat macules and did not form palpable lesions. Most of the nevi were only visible with GFP lighting or imaging and could not be detected by palpation or in normal lighting.

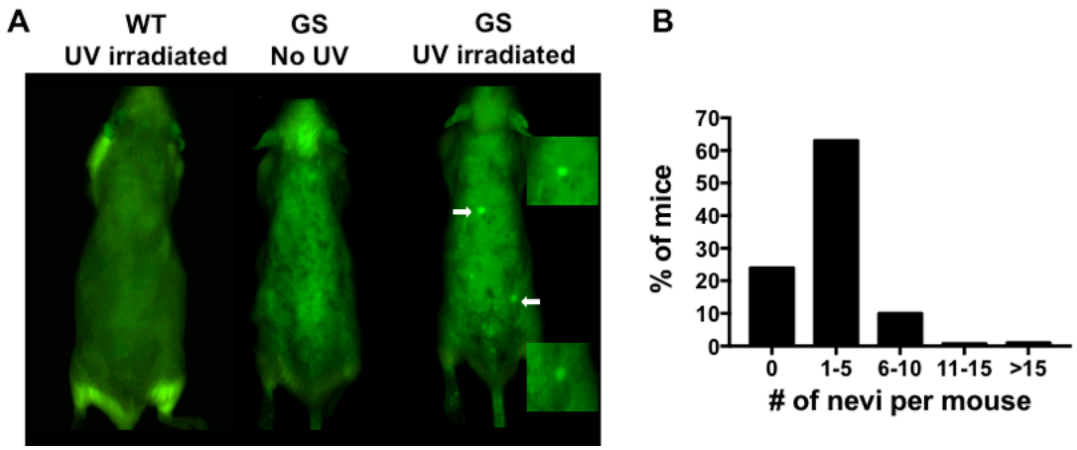


**Figure 3. Nevi developed in the majority of UV irradiated GS mice.** A) Junctional melanocytes were visible as a reticular green pattern on the backs of GS mice, but not on wildtype littermates. Well circumscribed, GFP positive macular lesions were visible on the backs of UV irradiated GS mice by 2 months of age. B) Dorsal nevi (>1mm) appeared in 75% UV irradiated GS mice with a median number of 2.67 nevi per mouse.

Melanocyte GFP expression was strong, so percutaneous imaging was sensitive so monthly percutaneous imaging allowed tracking of individual lesions over the lifespan of the mice. Increased lesion size and/or increased GFP intensity within areas of the lesion were interpreted as clinical evidence of resumption of growth and tumorigenesis (Fig 4A). Melanomas developed in approximately 10% (27/256) of the mice enrolled in the study (Fig 4B). The first evidence of tumor growth was noted at a median of 251 days of age (range 93-614 days). Average survival of all GS mice was 267 days. Melanoma-bearing mice had significantly longer survival than melanoma-free mice (397 vs 189, respectively, $p < 0.0001$) (Fig 4C). Due to effects of the HGF transgene in FVB mice, there was substantial mortality of HGF mice before 6 months of age (Takayama, La Rochelle et al. 1996), and 112/256 (44%) mice died before 6 months. Even after censoring of mice that died

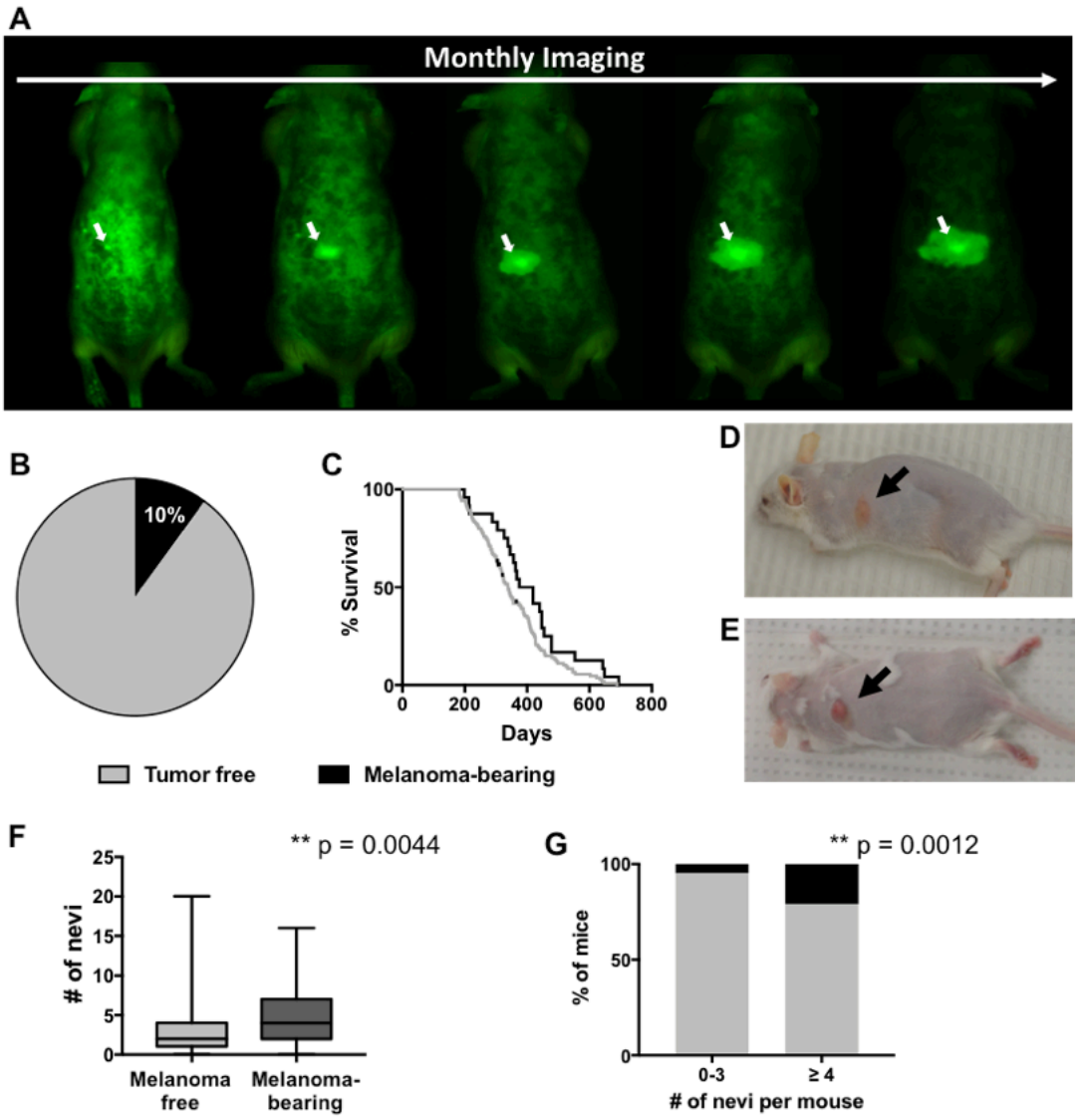


**Figure 4. GS nevi progressed to melanoma.** A) Monthly percutaneous GFP imaging showing growth of an RGP melanoma from a nevus (white arrow) over 4 months. Increases in both size and intensity of GFP (cell density) were detected. Irregular margins and variations in GFP intensity were consistent with clinical features of melanoma. B) Only 10% of GS mice developed melanomas over their lifespan. C) For mice that survived to 6 months of age, melanoma-bearing mice survived longer than tumor-free mice. GS RGP (D) and VGP (E) melanomas were visible as pink areas on the skin. F) Melanoma-bearing mice had a median of 7 nevi compared with 2 nevi in melanoma-free mice. G) A significantly higher proportion of mice with 4 or more nevi developed melanomas.

before 6 months, melanoma-bearing mice had significantly longer survival than

tumor-free mice (397 vs 339 days, respectively, p = 0.04). One third of melanomas started to grow within the first six months, but only 2% (2/112) of mice that died before 6 months of age had melanomas. In comparison, 17% (24/143) of mice that survived to 6 months developed melanomas.

Clinically, melanomas were generally flat, although 6 lesions developed raised areas either within a larger flat area or as a discrete nodular lesion. However, melanomas were often visible as discolored pink areas on the skin (Fig 4D), similar to what was previously described in FVB melanomas (Recio, Noonan et al. 2002). Ulceration occurred in both macular and nodular melanomas (Fig 4E). Gross metastatic lesions were found in the lung of 3 tumor-bearing primary mice.

Similar to findings in human patients with NAMs, GS mice who developed melanoma had a significantly higher median number of nevi at 2 months compared with mice whose lesions did not progress to melanoma (7 vs 2, p = 0.0044) (Fig 4F). Additionally, mice with 4 or more nevi had a significantly higher rate of melanoma development than mice with 3 or fewer (21% vs 5%, p = 0.0012) (Fig 4G).

**Melanocytic lesions are histologically variable**

HGF models have historically had histologically variable lesions, similar to the variety of human melanomas. We anticipated that the GS model would be similar and indeed there was substantial variability in the GS melanocytic lesions. The melanocytic nevi and RGP lesions were small and thin, which sometimes caused difficulty in acquiring diagnostic histology samples. Eighty-eight histology sections of melanocytic lesions were examined. Melanocytic origin was confirmed by expression in at least part of the lesion of at least one melanocytic marker. Nineteen

samples were non-diagnostic. Forty-eight samples nevi were histologically and clinically consistent with nevi and represented a variety of nevus types. Normal mouse skin contains 1-3 layers of epidermal keratinocytes with a thin overlaying layer of keratin, and a dermis with rare spindloid cells (Fig 5A). Unlike in human skin, in HGF mice, junctional melanocytes were either above the basement membrane in the epidermis or just below the basement membrane in the superficial dermis. The

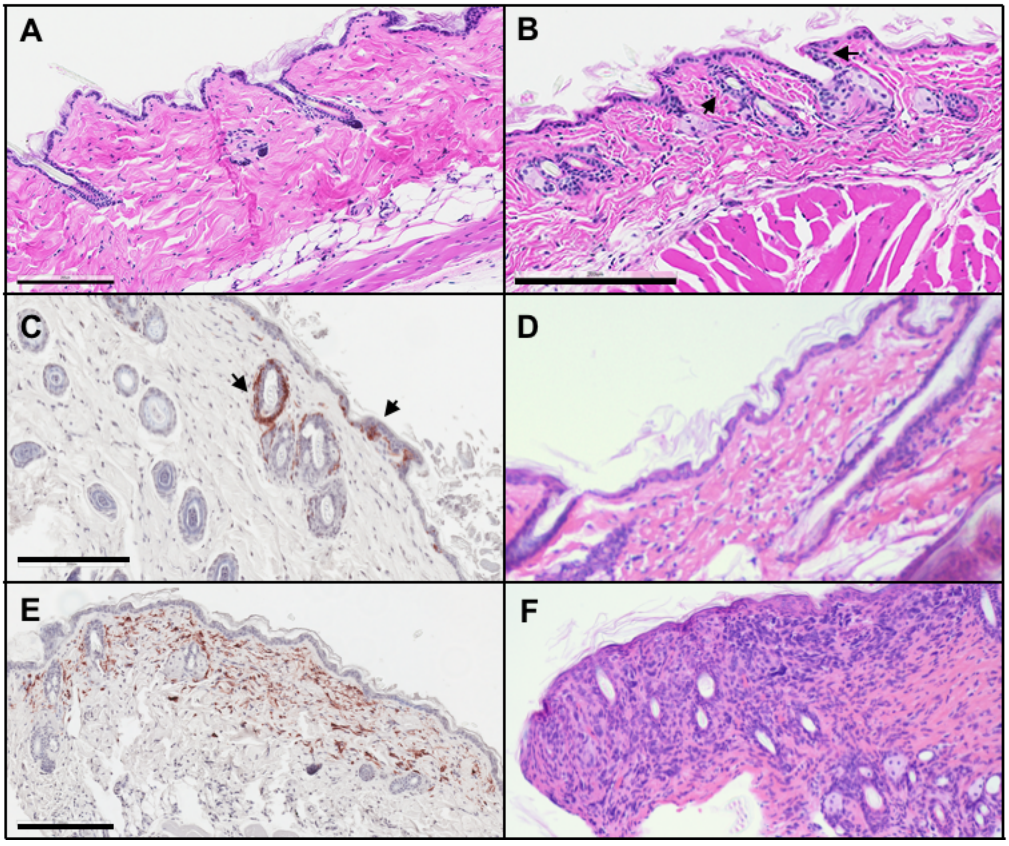


**Figure 5. Histologic appearance of GS nevi.** A) Normal FVB mouse skin has 1-2 layers of epidermis with low numbers of cells within the dermis. B and C) Junctional nevus with increased melanocytes along hair follicles (arrows). D and E) Increased numbers of melanocytes in the superficial dermis in some nevi were the most common form of melanocytic lesion. F) Compound nevi with both junctional dermal components. Melanocytes in C and E are immunolabeled with anti-DCT and visualized with Nova Red.

majority of the nevi (29/48) consisted of individual cells rather than nevus cell nests, consistent with lentigo simplex-type lesions (Fig 5A). Junctional-type nevi were the next most common nevus type (10/48) and had nests of nevus cells along the basement membrane and, in some cases, along the hair follicles (Fig 5B). Three compound nevi consisted of substantial populations of both junctional and dermal nevus cells (Fig 5C). Two nevi were dermal with nests of nevus cells primarily in the deep dermis (Fig 5D). Atypical nevi (4/48) were compound or dermal nevi with cellular atypia including anisocytosis, anisokaryosis, and prominent nucleoli with minimal mitotic figures (Fig 5E).

Melanomas were also histologically diverse and similar to other HGF models and human lesions. Most of the tumors had histologic evidence of extension laterally along the basement membrane in the epidermis or superficial dermis, consistent with a superficial spreading-type melanoma. Since mouse skin lacks rete ridges, tumors were considered to extend laterally if melanoma cells were found more than 3 hair follicles from the main tumor. Twenty-one lesions were histologically diagnosed as melanomas. Nine tumors were histologically diagnosed as RGP tumors. The majority of the tumor cells in the RGP tumors were found along the junction and hair follicles with only individual cells or small nests in the superficial dermis (Fig 6A). An additional 2 tumors appeared clinically and histologically consistent with either RGPs or atypical nevi. Both lesions were approximately 2 mm in diameter, one had grown rapidly over the previous month and was on the lateral flank and was therefore not visible in the imaging. Histology of both showed junctional nests and small numbers of dermal melanocytes with mildly increased atypia. Interestingly, this mouse had a

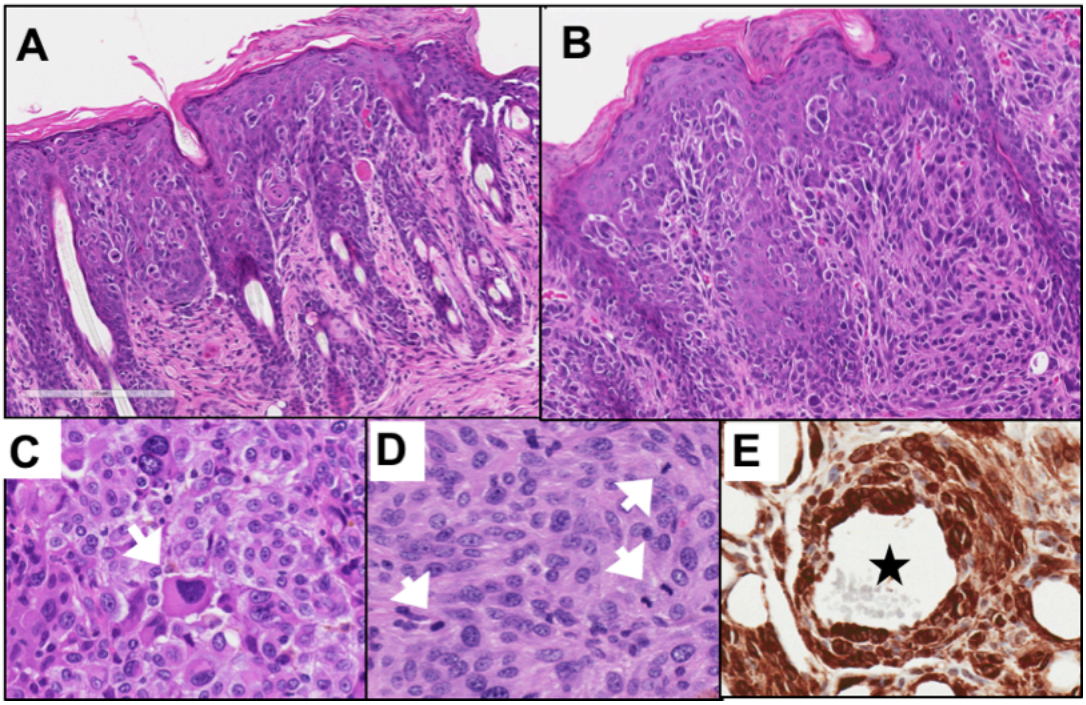


**Figure 6. Histologic appearance of GS melanomas.** A) Melanoma cells are focused along the junctional area, within the epithelium, and hair follicles in RGP mice. Melanoma cells in the dermis are in small nests or individual cells. B), in VGP lesions, melanoma cells are present both along the junction and in large numbers in the dermis. Epithelial hyperplasia and hyperkeratosis is common. C) Atypical giant cells (arrow) are seen in some VGP melanomas. D) Mitotic figures (arrows) are more frequent in VGP melanomas. E) Vascular tropism and pseudo-vessel (star) formation is seen in some VGP melanomas. Melanocytes are immunolabeled with anti-DCT antibody and developed using the Nova Red.

lung metastasis, suggesting at least one of the histologic samples wasn't representative. These tumors were grouped with the RGP tumors for analysis. Eleven tumors were histologically diagnosed as VGP tumors and all had a substantial dermal component, either in conjunction with junctional components (Fig 6B) or as an exclusively dermal melanoma. One was determined to be a metastasis following sequencing (see Chapter 4). Intraepidermal nests of melanoma cells were seen in 9 of the 11 tumors. The other two were dermal and extended in one case up to the junction. Epithelial hyperplasia and hyperkeratosis were seen in 6 of the VGP tumors

and epidermal ulceration was seen in 3 (Fig 6B). Cellular morphology ranged from epithelial cells to round or spindle cells and multiple morphologies were often seen in individual tumors. Giant atypical cells were seen in 2 tumors (Fig 6C). Increased mitotic figures, sometimes bizarre mitotic figures were also seen (Fig 6D). Vascular tropism and pseudovessel formation was a frequent characteristic of GS melanomas (Fig 6E).

**RGP and VGP tumors behave differently following transplantation**

To further investigate the capacity of GS lesions to progress, lesions that were clinically suggestive of melanoma were transplanted into GFP-tolerized syngeneic mice. Transplantation not only gives lesions more time to grow and progress but can also validate that tumors can grow outside of their original site. Since establishment of tumor areas in the dermis is differentiation between RGP and VGP tumors, we hypothesized that VGP tumors would grow more quickly and more reliably following syngeneic transplantation. Twenty-six lesions were transplanted, 17 were RGP lesions, 4 were VGP lesions, 2 were diagnosed histologically as nevi, and 3 were metastatic lung lesions. There were substantial differences in growth following transplantation of the RGP and VGP tumors (Fig 7A). All 4 of the transplanted VGP tumors reached exponential growth phase, while only 6/17 RGP lesions reached the exponential growth phase, and no nevi reached exponential growth phase. One RGP lesion rapidly reached an exponential growth phase and then regressed fully. Only one of the transplanted lung lesions reached an exponential growth phase. No transplanted nevus lesions grew.

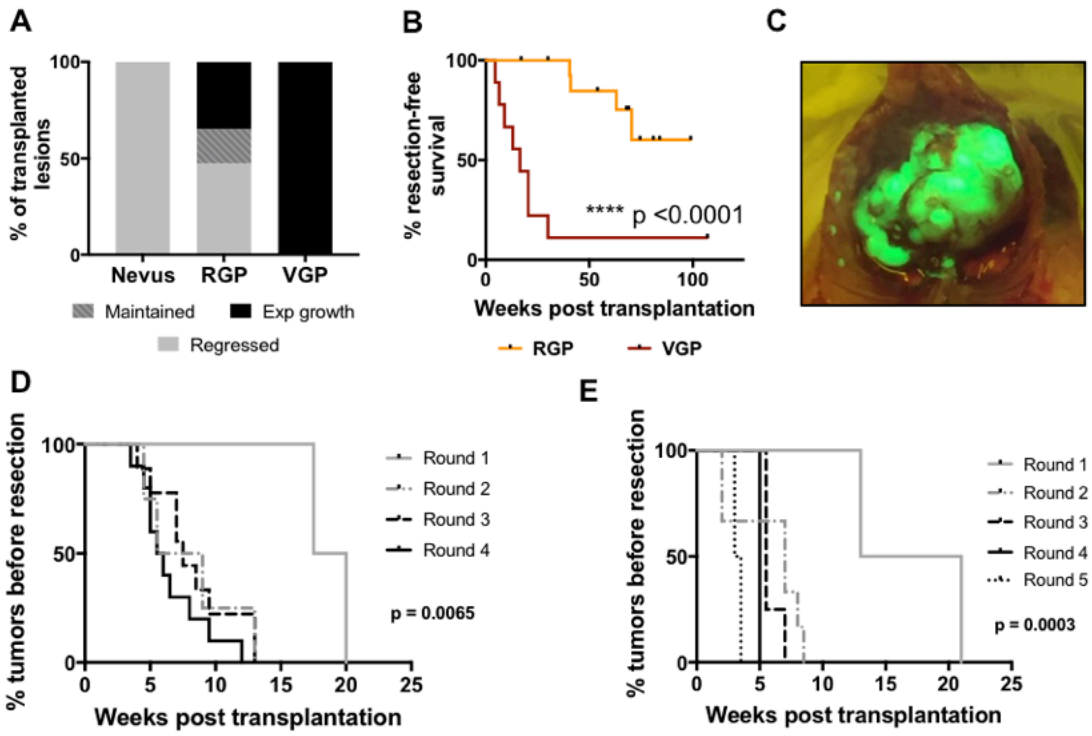


**Figure 7: Radial and vertical growth phase tumors behave differently following transplantation.** A) VGP tumors are more likely to reach exponential growth (3/3) following transplantation than RGP (6/17) or nevi (0/2). The majority of nevi and RGP lesions regress following an initial growth phase. B) Tumors transplanted after reaching VGP (red) reach resection size ($300mm^{3)}$ at an mean of 16.5 weeks, while only a few RGP tumors reached resection size. C) Diaphragm metastases following two rounds of transplantation showing retained GFP expression. D and E) Serial transplantation lead to tumors reaching the resection size (>300 $mm^3$) faster.

Additionally, VGP nodular tumors reached exponential growth phase more rapidly following transplantation than did RGP tumors (Fig 7B). Transplant regression was common in transplanted RGP and nevus lesions. GFP was usually maintained following transplantation and in metastatic lesions, although partial or complete loss occurred in some lesions (Fig 7C). Loss of GFP occurred more frequently in recipients maintained on constant dox treatment.

To build a transplantable tumor bank for future preclinical research, transplanted tumors that reached exponential growth were resected after the tumor

size exceeded 300-500 $mm^3$ and portions of the tumor were viably frozen and re-transplanted. Subsequent transplantation cycles grew more rapidly than the first cycle. Two non-metastatic tumor lines became metastatic following serial transplantation. Two cell lines, F4679HI and F5377HI, were developed from tissue from these serially transplanted lines.

***Conclusions***

The GS model was designed with the hypothesis that by building a model where it is difficult to develop tumors, important tumor pathways and genes involved in tumor development will be uncovered. Although the rate of nevus progression in the GS model is approximately 15-50x higher than in human populations but is still uncommon. Additionally, approximately half of tumors were still in radial growth phase when mice were euthanized. In both human patients and GS mice, higher numbers of nevi is associated with a higher risk for melanoma formation. (Pampena, Pellacani et al. 2018). Human and GS nevus-associated melanomas arise most frequently on the trunk (Bevona, Goggins et al. 2003, Pampena, Pellacani et al. 2018) and are most commonly diagnosed as superficial spreading melanomas (Pampena, Pellacani et al. 2018). Without the GFP expression in lesions, many of the macular nevi would not have been identified. GFP expression also enabled detection not only increased size but also increases in GFP intensity (i.e. melanocyte density) in flat lesions.

A pitfall of the study was the number of non-diagnostic histologic sample. Nevi and early melanomas were often hard to capture histologically due to their small size and subdivision of lesions to provide histologic, genomic, and transplantation

sections. Due to the thinness of mouse skin and the size of the biopsies it was difficult to embed the samples precisely and obtain sections through the best part of the sample, especially when multiple biopsies were embedded in the same block. Formalin fixation was selected for optimal tissue preservation but, following fixation and alcohol dehydration, the GFP is no longer visible to provide visible landmarks. As a result, histology samples were not always diagnostic, or did not match the clinical presentation. This unfortunately led to an inability to histologically classify some of the samples or a potential to misclassify early melanomas as nevi. For the purposes of this study, histologic and clinical (GFP intensity, growth, shape, and ulceration) information were used together to classify lesions where histology was inconclusive or histology and clinical findings were incongruous.

Transplantation results confirmed that there are real biological differences between lesions identified as RGP lesions and VGP lesions. Since GS mice develop tumors late in life, it is not always possible to follow lesions long enough to determine if macular lesions would have progressed to nodular lesions. Transplantation, therefore provided a way to extend tumor life and test whether all lesions were capable of progression. Although both RGP and VGP tumors were able to establish initially as subcutaneous lesions, VGP lesions were able to establish tumors with continued growth relatively rapidly, while RGP lesions in many cases completely regressed or maintained a small lesion size without measurable growth for long periods. Causes of regression are unknown and could be caused by immune-mediated attack an inability to sustain growth. However, progression of RGP primary tumors to exponential growth and from VGP to metastatic lesions occurred following

transplantation. Growth and survival after subcutaneous transplantation required adaptation to a new microenvironment in some ways similar to a subcutaneous metastatic site. The latency of months to years was consistent with our overall hypothesis that additional alterations were needed for progression to the next lesion type.

The GS model provides a model for evaluating genomic alterations associated with initiation and progression from nevi to melanomas. The strength of the GS model resides primarily in the modeling of early nevus and malignant transformation.

# Chapter 3: Melanocytic lesion development in a C57BL/6 model of cutaneous melanoma

***Summary***

Metastatic melanoma has a poor clinical outcome Patients with distant metastatic disease at the time of diagnosis have only 20% 5-year survival rate compared with >98% 5-year survival for patients with localized disease. In HGF mouse models, the presence of melanin pigment in cells can affect increase the amount of DNA damage. CDKN2A alterations often arise during melanoma progression to more aggressive forms. The BT model was designed with inducible melanocyte-specific Cdkn2a deletion, allowing us to model Cdkn2a loss following initial UV exposure. BT mice had a high frequency of melanocytic lesion development and nevi and VGP lesions. Additionally, 60% of BT mice had metastatic lesions, which is substantially higher than what has been noted in other HGF mouse models. The metastatic susceptibility in the BT mice could not be explained by genomic alterations in the tumor, so we performed whole genome sequencing on normal germline tissue from BT mice and a related strain without the high metastatic phenotype. Three BT variants were identified that affected gene expression in BT tumors and were significantly associated with survival in human melanoma. Through this project we were able to produce nevi, VGP and metastatic lesions for sequencing and to identify potential germline metastasis susceptibility genes in melanoma.

***Introduction***

Pigmentation can affect UV-induced DNA damage and melanoma development. Skin pigmentation in people strongly affects skin cancer risk. Pale skin and inability to tan are strong risk factors for both melanoma and non-melanoma skin cancer (Gandini, Sera et al. 2005) (cite). Melanin pigment, however, may also contribute to DNA damage. In human melanocytes, energy absorbed by melanin during UV exposure may be released later leading to additional cyclobutane pyrimidine dimer (CPD) dimer formation and accumulation of DNA damage in the hours following UV exposure (Premi, Wallisch et al. 2015). Additionally, studies in pigmented and albino HGF mice indicates that the presence of melanin pigment enhances UVA-associated oxidative damage and associated mutations without protecting against UVB-associated CPD dimers. This relationship between UVA-induced damage and melanin is supported by epidemiologic data and by *in vitro* studies with human melanocytes (Wenczl, Van der Schans et al. 1998, Hill and Hill 2000, Rouzaud, Kadekaro et al. 2005, Coelho and Hearing 2010).

CDKN2A alterations occur in the majority of human cutaneous melanomas. In human NAMs, CDKN2A alterations may be congenital (similar to the GS model) or acquired as part of progression (Shain, Yeh et al. 2015, Shain, Joseph et al. 2018). CDKN2A alterations, particularly p19/ARF, is associated with enhanced tumorigenicity in HGF mice (Recio, Noonan et al. 2002, Ha, Ichikawa et al. 2007). The BT model utilizes a tyrosinase driven Cre (Bosenberg, Muthusamy et al. 2006) for inducible melanocyte-specific loss of CDKN2A after UV exposure. This is the first HGF-mediated model with inducible CDKN2A alteration. In this study our aims

were to evaluate if adult CDKN2A alteration enhanced malignant transformation in melanocytic lesions. We did not anticipate alterations in the histologic appearance of the tumors.

## ***Methods***

### Mouse model

Mice in the C57BL/6 (BT) model are $HGF^{Tg/+}$; Tyr-$CreERTA2^{Tg/+}$; $CDKN2A^{Fl/+}$. Tyr-CreERTA2 mice were obtained from Marcus Bosenberg (Yale University) (Bosenberg, Muthusamy et al. 2006). HB mice are $HGF^{Tg/+}$; Tyr-$CreERTA2^{Tg/+}$; $CDKN2A^{Fl/+}$; $BRAF^{CA/+}$. $BRAF^{CA}$ mice were provided Martin McMahon (University of Utah) (Wang, Kobayashi et al. 2012). HB and BT mice were both F1 hybrids generated by breeding male $HGF^{Tg/+}$ mice with female Tyr-$CreERTA^{Tg/Tg}$; $CDKN2A^{fl/fl}$ mice (BT) or Tyr-$CreERTA^{Tg/Tg}$; $CDKN2A^{fl/fl}$; $BRAF^{CA/CA}$ mice (HB). HGF positive C57BL/6 mice have skin pigmentation and can be visually differentiated from wildtype littermates by their dark ears, paws and tails. Mice were treated with a single dose of UV at 3 days post-natal, as described in Chapter 2. Cre recombination is induced through topical application. 0.1 ml of a 25 mg/ml 4-hydroxy-tamoxifen in DMSO is applied to shaved dorsal skin for 3-5 consecutive days around one month of age (Vasioukhin, Degenstein et al. 1999). Both female and male mice were used in this study. Mice were monitored once weekly for lesion development and tumors were measured weekly starting after tamoxifen administration. Samples were collected at the time of euthanasia or as survival resections surgeries as described above in Chapter 2. All animal work was approved by the Animal Use Committees in NCI-Frederick and NCI-Bethesda.

### Transplantation

Tumor fragments were transplanted into C57BL/6 mice using the protocol described in Chapter 2. Transplanted tumor growth was measured twice weekly. Tumors were resected at >300 $mm^3$ and mice were then monitored for tumor regrowth or humane endpoints before euthanasia. Tumor samples at resection and euthanasia were collected for histology, genomics, re-transplantation or viably frozen.

### Histology and immunohistochemistry

Tissue processing was the same as described in Chapter 2. Heavily pigmented tumors were not tested with IHC. IHC was performed on poorly pigmented tumors to confirm melanocytic origin.

### BT melanoma cell line development

Melanoma cell line development was performed as described in Chapter 2.

### Whole genome sequencing

DNA was obtained from flash frozen spleen tissue from melanoma-bearing HB and BT mice. Spleen tissue was digested, and DNA was isolated according to the protocol for the Invitrogen PureLink Genomic DNA Kit. Library preparation and sequencing were performed by the CCR-Sequencing Facility at NCI-Frederick. Library preparation was done with the TruSeq DNA Sample Prep Kit (FC-121-1001, Illumina, San Diego, CA). 14 samples were pooled and sequenced on the HiSeq 4000. Samples were aligned to mm10. BT and HB splenic. Bioinformatics was performed by Maxwell Lee and Huaitian Liu (NCI). DNA sequences were compared to strain specific genomes from the Mouse Genomes Project (Keane, Goodstadt et al.

2011). The Sorting Intolerant from Tolerant (SIFT) algorithm was used to predict deleterious variants.

### RNA sequencing

Samples from 29 BT melanocytic lesions and 8 HB melanomas were used for RNA sequencing. Flash frozen samples were pulverized using a mortar and pestle with liquid nitrogen or using the cryoPREP Manual Dry Pulverizer (Covaris, Woburn, MA). Samples were mixed with tissue lysis reagent (Qiagen, Germantown, MD) and run through the Qiashredder (Qiagen, Germantown, MD) before following the manufacturer's instructions for the RNAeasy kit (Qiagen, Germantown, MD). Total RNA sequence library preparation and sequencing was done by the CCR Sequencing facility (Frederick, MD) using Illumina TruSeq kit (Illumina, San Diego, CA), and sequenced on Illumina HiSeq 4000. Library preparation was performed following New England Biolab's Total RNA Kit. RNA sequencing was aligned to mm10 genome build. Bioinformatics was performed by Maxwell Lee and Huaitian Liu.

### Statistics

Most statistics were performed using Prism 7 (GraphPad Software, La Jolla, CA). A two-sided Fisher's exact test was used to evaluate the distribution frequency and Odds ratio of metastasis in mice with different tumor size. Kaplan-Meier survival curves were used for evaluating survival and lesion-free survival. The Logrank test for trend was used to compare curves for serial rounds for transplantation. Column statistics were used to determine mean and median distribution. UCSC Xena Genome browser (https://xena.ucsc.edu) was used to analyze the relationship between

gene expression level and survival in the human databases and generate Kaplan-Meier curves from this data. The TCGA Cutaneous Melanoma (SKCM) and TCG Uveal Melanoma (UM) were selected for analysis.

***Results***

**Melanocytic lesion develop was similar to previous HGF models**

BT melanocytic lesion development was similar to historic HGF lesion development. A total of 43 BT mice were followed from birth through euthanasia. Median survival for BT mice was 254 (range 83-562) days (Fig 8A). The dark skin pigmentation precluded the identification of macular lesions in BT mice, so only raised nodules could be detected. Ninety percent (39/43) of BT mice developed measurable raised lesions. The first measurable lesion was identified at a median of 133 (range 65-244) days after birth and mice developed a median of 2 lesions (Fig 8B and 8C). Ten mice had numerous small raised lesions that made it difficult to distinguish or measure individual lesions and likely led to an artificial reduction in the number of measurable lesions in those mice. Of 90 measurable lesions, 10 (11%) regressed completely. Regression occurred only in small lesion. Lesion size varied widely with both small and large tumors. The median lesion size was 27.56 $mm^3$ (mean = 147.1 $mm^3$, range 0.5–1800 $mm^3$) (Fig 8D). Clinical ulceration of tumors was seen in 6 tumors. The frequency and speed of melanoma development was within the range of previous HGF mice.

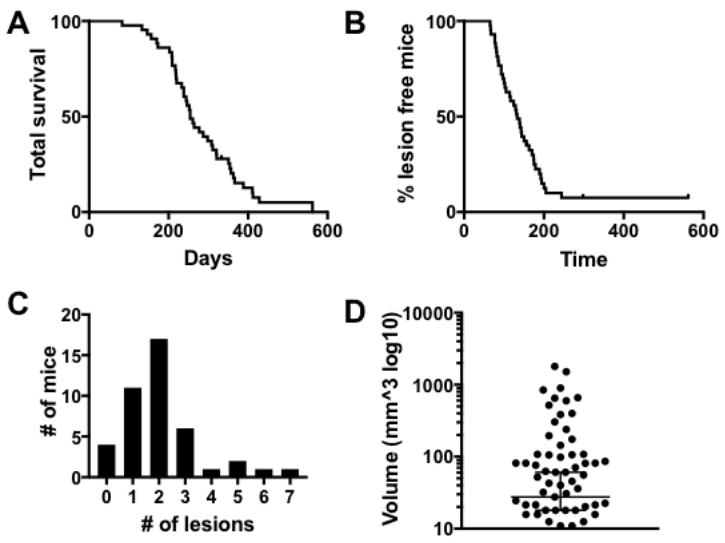


**Fig 8. BT mice frequently developed melanocytic lesions.** A) Median survival of BT mice was 254 days and B) median age at development of the first measurable lesion was 133 days. C) Measurable raised lesions were present in 90% of BT mice with a median of 2 lesions per mouse. D) Melanocytic lesions varied in size with a median volume of 27.56 mm^3 (range 0.5-1800mm^3). Lesion size was log transformed to see patterns. Median and 95% confidence interval lines shown.

### Melanomas in BT were highly metastatic

Surprisingly, metastasis differed significantly from past HGF models. Since metastatic frequency has been relatively stable or declining over time in C57BL/6 and FVB HGF mouse models (unpublished data), we had anticipated that the metastatic rate would be similar in the BT model. However, unlike historic C57BL/6 HGF models that had a 10-20% metastatic rate (Otsuka, Takayama et al. 1998) or GS mice with a 10% metastatic rate, 56% (22/39) lesion-bearing mice had metastatic lesions (Fig 9A). Metastatic tumors were grossly visible in 21 mice, and microscopically visible in 1 mouse (Fig 9B). Metastasis bearing lymph nodes were often markedly

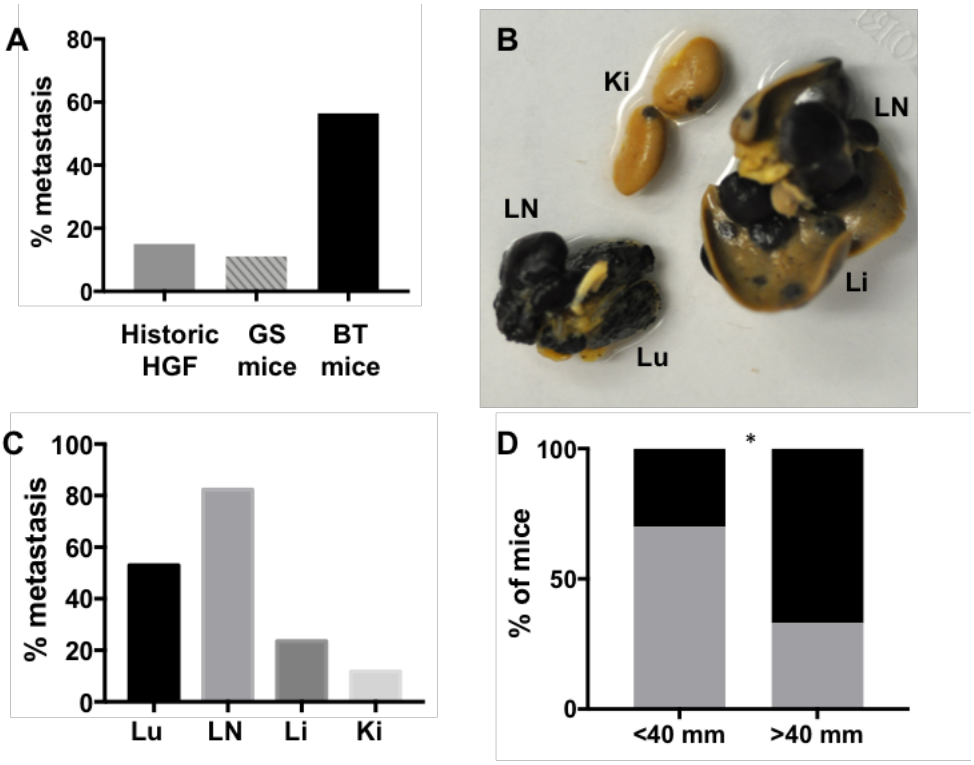


**Figure 9. Metastatic disease was widespread in BT mice.** A) Metastatic lesions were seen in the majority of tumor-bearing BT mice. This is 3-5x higher than the metastasis frequency that has historically been seen in HGF mice or in the GS model. B) An example of a primary BT mouse at necropsy with grossly visible, pigmented metastatic lesions in the lungs (Lu), mediastinal and mesenteric lymph nodes (LN), liver (Li) and Kidney (Ki). C) Lymph nodes and lung lesions were the most common site for metastatic disease. Liver and kidney lesions were present with lower frequency. D) Similar to human melanoma, the frequency of metastatic disease was higher in mice with larger tumors (>40mm$^3$) than mice with only small lesions ($p < 0.049$).

enlarged and pigmented (Fig 9B). Distant organ metastases were usually pigmented. Metastases were most commonly seen in lymph nodes and lung. Other metastatic sites including liver and kidney were seen less commonly (Fig 9B and 9C). Cutaneous and subcutaneous metastases were also identified by sequencing in 3 mice (see Chapter 4). For mice with cutaneous/subcutaneous metastases, the tumor that reached measurable size first in that pair was considered the primary tumor. Pigmentation in cutaneous/subcutaneous metastases was variable.

Since larger tumor size is linked to worse survival in melanoma (Breslow 1970, Clark, Elder et al. 1989, Balch 2009), we then looked at whether lesion size was a risk factor for metastasis in BT mice. The risk of metastasis was higher in mice with larger tumors. Mice with a tumor greater than 40mm$^3$ had a significantly higher frequency of metastatic lesions ($p = 0.049$, Odds ratio = 4.667). Mice with at least one tumor larger than 40 mm$^3$ were significantly more likely to have metastatic lesions than mice without tumors that large ($p = 0.049$) (Fig 9D). Metastatic lesions were present in 67% of mice with at least one lesion larger than 40 mm$^3$, compared with only 30% of mice with lesions smaller than 40 mm$^3$. However, metastatic lesions were associated with tumors as small as 12.5 mm$^3$.

**Melanocytic BT lesions showed a range of histologic appearances**

The nevi and melanomas that developed in the BT model were similar to those previously reported for HGF mice. The four nevi and 13 melanomas represented a variety of histologic appearances. One month after neonatal UV irradiation, BT mice had numerous well-differentiated small, pigmented, dendritic melanocytes along the dermal-epidermal junction and along the superficial hair follicle but not discrete raised areas (Fig 10A). Melanin-laden macrophages were rare in these early skin samples. Following Cdkn2a heterozygous deletion at one month, raised melanocytic lesions started to form. Nevi occurred primarily in the superficial dermis. Most nevi were symmetrical with heavily pigmented melanocytes in the superficial dermis. Unlike the GS melanomas, junctional and hair follicle melanocytes were uncommon. Superficial dermal lesions consisted heavily pigmented dendritic to spindle melanocytes and numerous melanin-laden macrophages (melanophages) (Fig 10B-D).

Dermal sclerosis with increased extracellular matrix was commonly seen. These lesions were similar to the “melanocytosis” lesions described in Florell et al (2007).

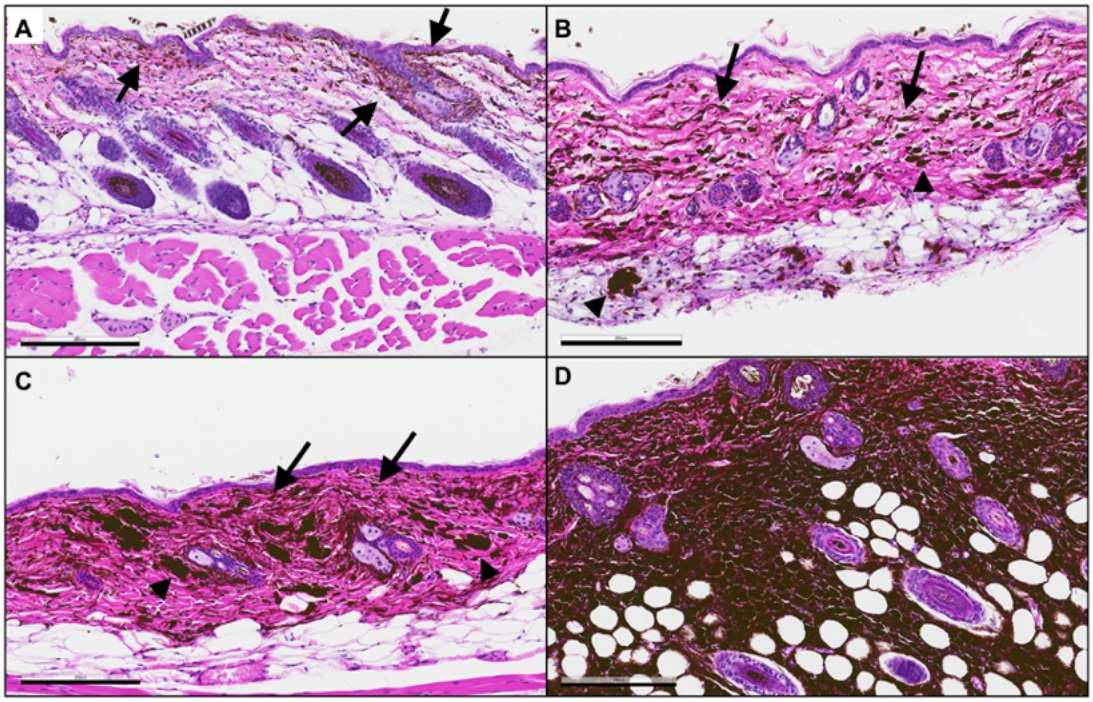


**Figure 10. Histologic appearance of BT nevi.** A) HGF skin and 1 month of age following neonatal UV but with no Cdkn2a alterations showing hyperplasia of melanocytes (arrows) long the junction and hair follicles. B) Nevus showing individual spindloid to dendritic melanocytes (arrows) and melanophages (arrow heads) in the dermis. C) Groups of spindle melanocytes (arrows) and melanophages (arrow heads) in the superficial dermis and along the junction. D) Larger nevus with pigmented melanocytes and numerous melanophages extending form the junction down to the deep dermis. Deeper areas consist primarily of melanophages. Size bar represents 200µm.

Larger nevus lesions were densely cellular with numerous melanophages and pigmented melanocytes. Mitotic figures and cellular atypia were rare or absent (Fig 10D). These lesions shared features with human epidermal blue nevi and HGF mouse tumors on a C57BL/6 x C3H background (Florell, Thomas et al. 2007).

Melanomas were also histologically variable and both junctional and dermal melanomas were identified. Unlike nevi, melanomas had asymmetrical margins,

deeper invasion, and evidence of cellular atypia. Junctional melanomas often had intraepithelial melanoma nests and spread laterally from the densest portion of the lesion along the junction or through the superficial dermis (Fig 11A). Melanocytes

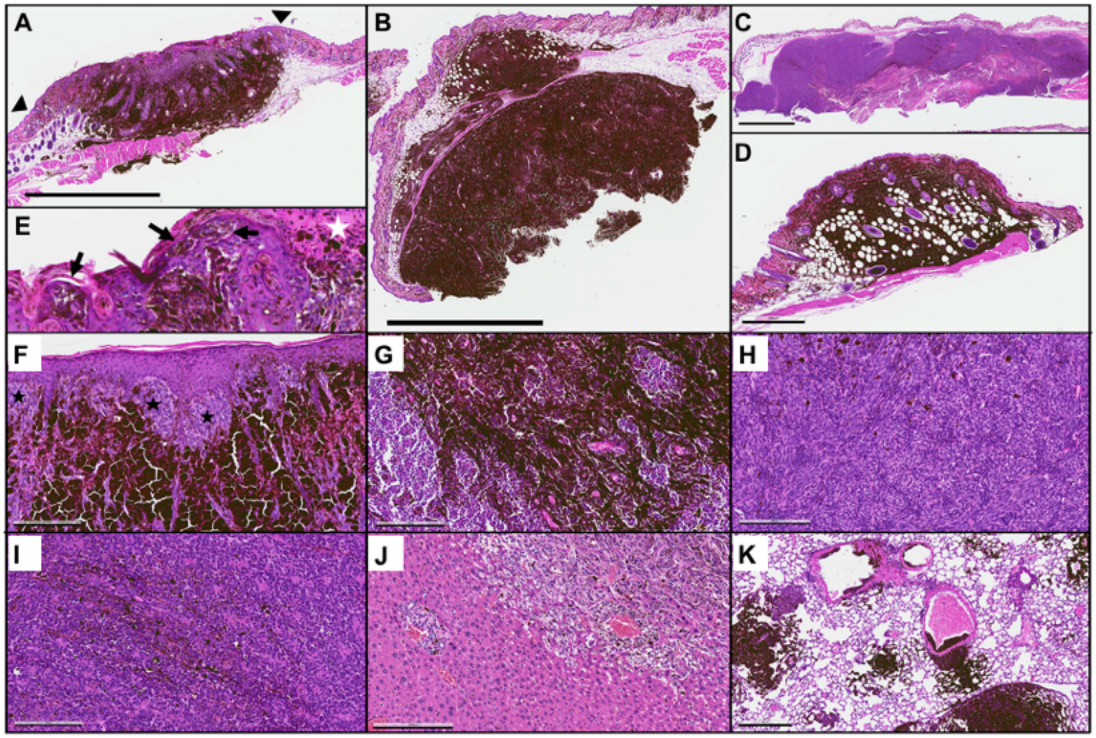


**Figure 11. Histologic appearance of BT melanomas.** A) Junctional melanomas had involvement of the dermal-epidermal junction with invasion into the dermis and subcutaneous tissue. Extension of melanoma cells laterally along the junction or in the superficial dermis was common (arrow heads). B). Several dermal lesions without junction or superficial dermal involvement were seen. One poorly pigmented dermal melanoma (C) was contiguous with a pigmented blue nevus-like remnant (D). E,F) Intraepithelial melanoma nests (E arrows) and junctional melanoma nests (F stars) were seen commonly in junctional melanomas. Ulceration (E white star) was seen primarily in junctional lesions, but some dermal tumors also had areas of ulceration.. Tumors often contained melanotic and poorly melanotic to amelanotic areas (C,F,G,H,I,J). Morphology of tumor varied from epitheloid (F) to spindloid, round cell and mixed morphologies (G, H). Gross and microscopic metastatic lesions were seen in a variety of locations including skin (I), liver (J) and lung (K). Size bars 300um (A), 1mm (B), 2mm (C), 500µm (D), 200µm (F-K).

within these laterally spreading areas were more differentiated and less cohesive than cells within the densest portion of the tumor. Junctional regions of tumors were often

highly pigmented, and some tumors contained high numbers of melanophages, similar to the nevi, particularly in more superficial areas of the tumor. Junctional melanomas often contained intra-epidermal or junctional melanoma nests (Fig 11 E, F). Four nodular melanomas arose from the dermis without a junctional tumor component (Fig 11B). In one tumor, a poorly pigmented dermal melanoma was connected with a junctional nevus remnant, although they were separated at the time of collection (Fig 11C, D). Epidermal ulceration was common (Fig 11E), particularly in junctional melanocytes, although dermal melanomas sometimes extended sufficiently into the dermis to cause ulceration. Morphology included epithelial, spindle and round cell morphologies, and many tumors included multiple morphologies (Fig 11G and H). Increased mitotic figures, atypical mitotic figures and increased cellular atypia cells also noted. Anisocytosis, anisokaryosis, and occasional giant atypical cells were observed. These were similar to the cells seen in the GS model. Many tumors had pigmented and nonpigmented areas. Similar to the GS model, vascular invasion and pseudo-vessel formation were commonly seen in deeper areas of the tumor. Metastatic lesions were morphologically similar to their matched primary tumors and were generally pigmented or partially pigmented (Fig 11I-K). Distant organ metastases were often associated with vessels and intravascular melanoma cells were commonly seen (Fig 11J and K).

### Tumor transplantation and tumor cell line development

Since BT tumors were primarily VGP lesions, tumors were expected to grow well following transplantation. However, it was unclear whether the metastatic propensity would be maintained following transplantation. Tumors from 5 mice were serially

transplanted into wildtype C57BL/6 mice. No tumors regressed after establishing tumors in transplant recipients and all reached resection size. Unlike in the GS model, the speed of tumor growth to resection size did not significantly change over rounds of serial transplantation (Fig 12B, C). Transplant recipients also had widely metastatic disease at the time of euthanasia (Fig 12A). Distribution and frequency of metastatic lesions in the transplant recipients were similar to the primary mouse. When metastatic lesions were transplanted, they did not show organ tropism. Transplantation of metastatic lesions from lymph node, liver, or lung resulted in widespread metastatic lesions in recipient mice. Transplanted lesion tissue was collected for histology, flash frozen, and viably frozen for further transplantation. Viably frozen tissue was stored in a transplantable tumor bank representing 11 BT mouse tumor groups for future *in vivo* studies. Tissue samples from 4 tumor groups were collected after 1-2 rounds of transplantation to create metastatic mouse melanoma cell lines for *in vitro* and *in vivo* mechanistic studies. One tumor line did not establish a self-perpetuating cell line after several attempts, but three new cell lines B7746HC, B8798HC, and B1508HC were successfully established. Maintenance of the metastatic propensity over multiple rounds of transplantation suggested that this was a tumor-intrinsic feature rather than due to tumor microenvironment.

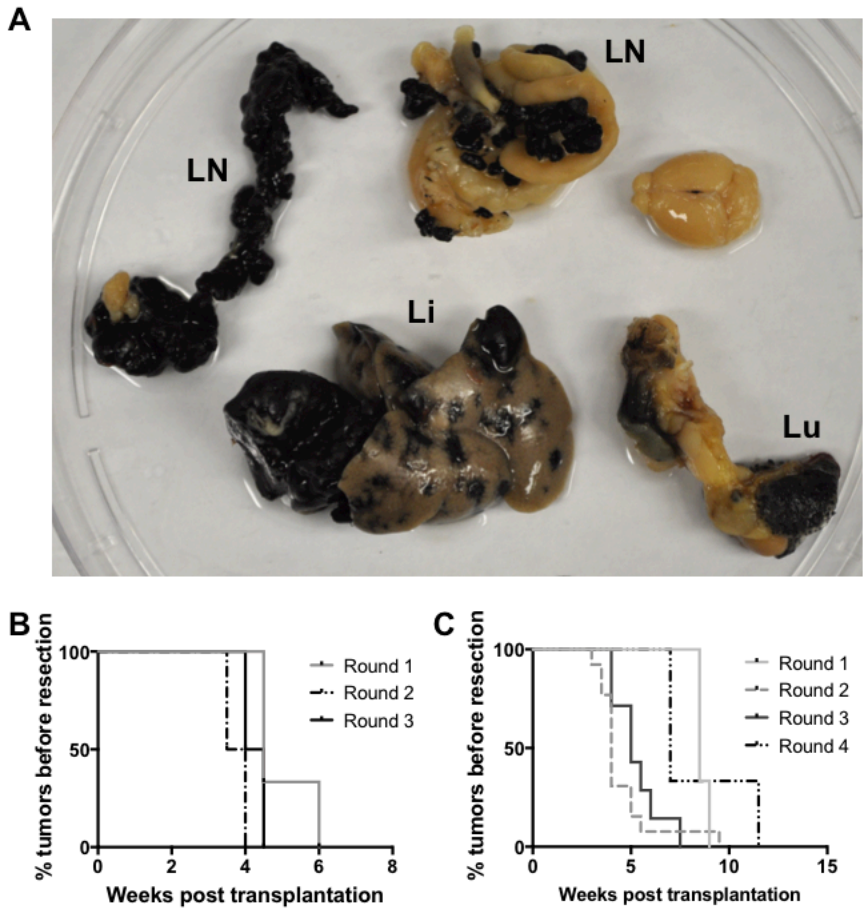


**Figure 12. BT tumors following transplantation were similar to primary tumors**. A) Metastatic lesions did not show organ tropism following transplantation. A transplanted lung metastasis gave rise to these metastatic lesions in lymph nodes (LN), lung (Lu), and liver (Li). Growth of tumor from transplantation to resection when size exceeded 300 mm^3 did not significantly with serial transplantation. B) There was no significant trend to growth acceleration after 4 rounds of transplantation in one tumor group ($p = 0.62$) or (C) after 3 rounds of transplantation in another tumor group ($p = 0.23$).

### Germline variants may be responsible for the metastatic propensity

The unexpectedly high tumor-intrinsic metastatic susceptibility in the BT model could have been caused by somatic mutations or by underlying germline variations unique to this HGF model. Although the metastatic phenotype was dramatic, somatic mutations in the BT model were similar to mutations in the GS, historic HGF, and

HB models (see Chapter 4). Therefore, the phenotype could not be explained by unique or consistent somatic gene or pathway alterations that distinguished the BT tumors. Therefore, we hypothesized that a germline variant within the BT mice was responsible for the dramatically increased metastasis. Germline polymorphisms are increasingly recognized as a contributing factor to metastatic susceptibility in cancer (Lifsted, Le Voyer et al. 1998, Crawford, Ziogas et al. 2006, Hsieh, Look et al. 2009, Markowitz, Nock et al. 2016). Although several studies have addressed variants involved in melanoma susceptibility, to our knowledge no studies to date have addressed germline variants involved in melanoma metastasis susceptibility. BT mice are related to another model, HB, also being used at that time in the lab. Mice in both models are F1 hybrids generated through breeding HGF males with either Tyr-CreERT2; CDKN2A$^{Fl/Fl}$ females (BT) or Tyr-CreERT2; CDKN2A$^{Fl/Fl}$; BRAFV600E$^{Ca/Ca}$ females (HB). Melanoma-bearing HB mice do not exhibit a high frequency of metastasis. Since both models were produced at the same time and used the same HGF mouse colony, HB mice were chosen as a low metastatic control for identifying metastasis-associated germline variants in the BT mice.

Since germline susceptibility loci may be located outside of coding regions, we performed whole genome sequencing on normal spleen DNA from 7 melanoma-bearing mice from each of the BT and HB models. C57BL/6 variants from mm10 and the Mouse Genomes project were removed. Additionally, variants present in only some individuals within a group or in both groups were filtered out of the dataset. A total of 30,239 germline variants were found between the BT and HB models. Many variations were in large blocks of variant DNA, suggesting recombination (Fig 13A).

The HB model had variant regions that were more similar to the FVB genome than to the C57BL/6 genome and this caused the BT and HB models to map to different areas of the mouse strain phylogenetic tree (Fig 13B). The $BRAF^{CA}$ mouse was originally created on a mixed strain background with contribution of C57BL/6, 129/Sv, and FVB and the results suggest some stretches of the FVB genome has been maintained despite backcrossing onto C57BL/6(Wang, Kobayashi et al. 2012). After removing HB variants, there were 3,042 variants unique to the BT model and not present in the C57BL/6 genome. The majority of variants were intergenic, and concentrated into dense areas of variation within a chromosome. Since the metastatic capacity of HGF-derived melanomas in most mouse strains was unknown, we decided not to remove germline variants from other strains from the Mouse Genome Project so that we did not erroneously remove variants that could contribute to metastasis formation.

To narrow the list of variants for future functional testing, we decided to focus on variants that could affect gene expression or function. Therefore, intergenic variants and synonymous coding variants were removed leaving only genes with variants in exome or UTR regions. Two genes did not have a human homolog, Vmn1r65 and AU018091, and they were removed from further analysis. This filtering limited the variant list to 8 nSNVs, 2 5' UTR variants, and 24 3' UTR variants affecting 21 genes (Appendix 1). NSNVs in *Mboat7* and *Ppp1r12c* were predicted to be detrimental alterations by SIFT, while the others were predicted to be tolerated. All 22 genes were retained on the list for further analysis. The genes identified in the germline variant screen are often poorly characterized, however multiple genes have

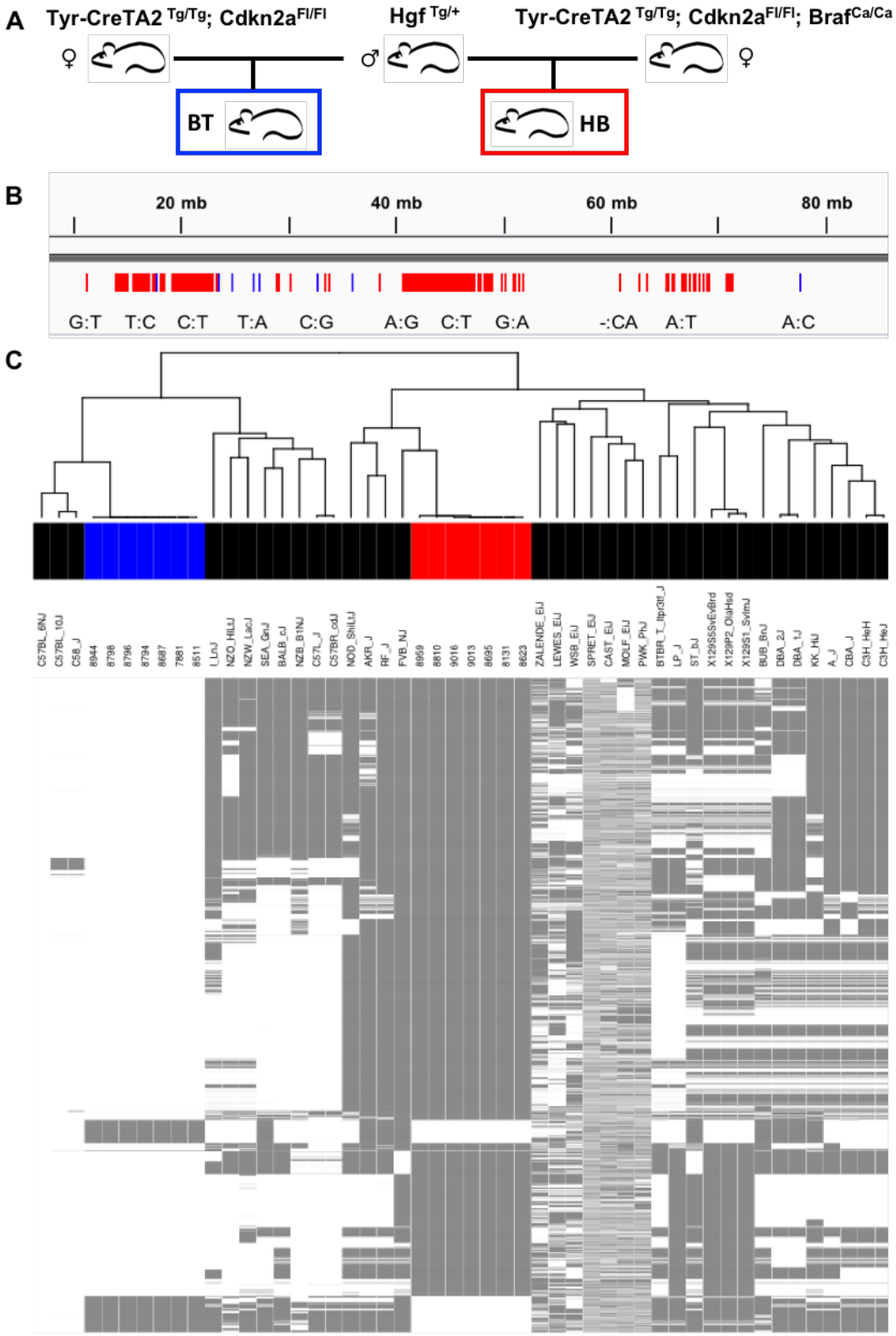
A
Tyr-CreTA2 Tg/Tg; Cdkn2aFl/Fl
Hgf Tg/+
Tyr-CreTA2 Tg/Tg; Cdkn2aFl/Fl; BrafCa/Ca
♀
♂
♀
BT
HB
B
20 mb
40 mb
60 mb
80 mb
G:T
T:C
C:T
T:A
C:G
A:G
C:T
G:A
-:CA
A:T
A:C
C
C57BL_6NJ
C57BL_10J
C58_J
8944
8798
8796
8794
8687
7881
8511
I_LnJ
NZO_HlLtJ
NZW_LacJ
SEA_GnJ
BALB_cJ
NZB_B1NJ
C57L_J
C57BR_cdJ
NOD_ShiLtJ
AKR_J
RF_J
FVB_NJ
8959
8810
9016
9013
8695
8131
8623
ZALENDE_EiJ
LEWES_EiJ
WSB_EiJ
SPRET_EiJ
CAST_EiJ
MOLF_EiJ
PWK_PhJ
BTBR_T_Itpr3tf_J
LP_J
ST_bJ
X129S5SvEvBrd
X129P2_OlaHsd
X129S1_SvImJ
BUB_BnJ
DBA_2J
DBA_1J
KK_HiJ
A_J
CBA_J
C3H_HeH
C3H_HeJ

**Figure 13. Numerous germline variants segregated the BT and HB models.** A) Breeding scheme showing relationship between the BT and HB models. Mice in both models are F1 hybrids of male HGF mice and female mice from separate colonies. B) Examples of variants in the BT (blue) and HB (red) models over an area of chromosome 1. Regions with numerous variants were often seen in the HB sequences, while BT variants were less frequent and less likely to be in concentrated areas. C) Variants that were not present in the reference C57BL/6 genome were compared to sequencing from different mouse strains. BT and HB variants mapped to different areas of the genome since some of the blocks of HB variants were most similar to the FVB/NJ consistent with the mixed strain background of the original Braf CA mouse. Variants present in BT mice were still most similar to C57BL/6 and closely related strains.

associations with cancer or cancer-related genes (Table 3). No connection between these genes and melanoma has been previously published.

To probe for potential functional alterations due to these germline variants, RNA expression was compared for these 22 genes in BT melanomas and HB melanomas. Nineteen of the genes had statistically significant differences in expression between BT and HB melanomas, and 13 had a > 2 log2 fold change between BT and HB tumors (Table 4). Allele specific RNA expression of the murine tumors did not reveal overrepresentation of the variant allele in the RNA sequencing for any of the BT nSNVs, suggesting that both alleles were expressed equally.

The TCGA Cutaneous Melanoma (SKCM) and TCG Uveal Melanoma (UM) databases were probed for significant relationships between gene expression and survival for the human primary tumors. Samples in the human melanoma sequencing databases were not collected to provide optimal survival information and primary tumor samples do not necessarily represent the tumor at the time of initial diagnosis. As a result, survival correlations from these studies must be interpreted with caveats.

**Table 3. Function and links to cancer in germline variant genes.**

| Gene | Proposed role | Refs |
|---|---|---|
| **Fiz1** | Interacts with FLT3<br>May be a transcriptional suppressor | (Wolf and Rohrschneider 1999, Mitton, Swain et al. 2003) |
| **Isoc2** | Overexpression inhibits p16/INK4A | (Huang, Shi et al. 2007) |
| **Mboat7** | Germline variant associated with HCC | (Donati, Dongiovanni et al. 2017) |
| **Myadm** | Regulates membrane functions and endothelial barrier integrity | (Aranda, Reglero-Real et al. 2011, Aranda, Reglero-Real et al. 2013) |
| **Ppp2r5a** | Regulates P53, β-Catenin and others | (Mao, Liu et al. 2018) |
| **Ncr1** | NK cell receptor influences tumor killing | (Glasner, Ghadially et al. 2012, Fend, Rusakiewicz et al. 2017) |
| **Ppp6r1** | Negative regulator of NFκB | (Ziembik, Bender et al. 2017) |
| **Ptprh** | Negative prognostic indicator in lung cancer | (Sato, Soejima et al. 2015) |
| **Tbl1xr1** | Linked to poor outcomes in a variety of cancers | (Liu, He et al. 2016, Liu, Xu et al. 2017, Ma and Yu 2017) |
| **Dnaaf3** | Role in cilia formation | |
| **Oscar** | Expressed in endothelial cells | (Goettsch, Rauner et al. 2011) |
| **Pank3** | Regulate CoA synthesis | (Sharma, Leonardi et al. 2015) |
| **Prpf31** | Splicing factor | (Vithana, Abu-Safieh et al. 2001) |
| **Shisa7** | Regulates synaptic function | (Schmitz, Klaassen et al. 2017) |
| **Tmem150b** | Autophagy regulator | (Mrschtik and Ryan 2016) |
| **Tmem190** | Lower expression in lung SCC | (Tian, Zhao et al. 2017) |
| **Lilra5** | Promotes innate immunity | (Mitchell, Rentero et al. 2008) |
| **Lilrb3** | Promote tumor-supportive inflammation | (Kang, Kim et al. 2016) |
| **Leng1** | Leukocyte receptor cluster member | |
| **Gp6** | Glycoprotein IV | |
| **Sbk3** | Protein tyrosine phosphatase | |

**Table 4. Expression of germline variants.**

| | BT vs HB tumors | | SKCM (primary) | UM (primary) |
|---|---|---|---|---|
| **Gene** | **L2fg** | **padj** | **p** | **p** |
| **Dnaaf3** | 2.76 | 6.81E-05 | NS | ND |
| **Fiz1** | 0.66 | 6.46E-09 | NS | NS |
| **Gp6** | 2.15 | 0.0966 | NS | 0.0078 (L) |
| **Isoc2b** | 8.37 | 7.50E-29 | NS | 0.00079 (H) |
| **Leng1** | -- | NS | NS | NS |
| **Lilra5** | 7.18 | 2.04E-12 | NS | 0.0069 (H) |
| **Lilrb3** | 8.67 | 2.45E-20 | NS | NS |
| **Mboat7** | 0.52 | 1.78E-05 | NS | NS |
| **Myadm** | 5.02 | 1.69E-29 | NS | NS |
| **Ncr1** | 6.41 | 3.25E-08 | NS | ND |
| **Oscar** | 2.58 | 0.00255 | NS | NS |
| **Pank3** | -0.67 | 7.68E-06 | NS | NS |
| **Ppp6r1** | 0.83 | 3.73E-09 | NS | ND |
| **Ppp1r12c** | 1.99 | 1.88E-40 | NS | NS |
| **Ptprh** | 2.99 | 0.000607 | 0.018 (L) | 0.00018 (H) |
| **Prpf31** | -2.37 | 8.32E-50 | NS | NS |
| **Sbk3** | 6.55 | 1.36E-09 | ND | ND |
| **Shisa7** | 4.05 | 9.22E-06 | NS | NS |
| **Tbl1xr1** | -- | -- | NS | NS |
| **Tmem150b** | 1.93 | 0.000339 | NS | 0.000019 (L) |
| **Tmem190** | 5.47 | 2.75E-09 | NS | NS |

However, these resources are currently the best available sources of genomic and survival data for non-BRAF, non-NRAS melanomas. Survival in mouse models and human patients is also not directly comparable because of differences in life span, treatment, euthanasia in mice, etc. Human melanoma survival, however, is linked to metastatic disease (Balch 2009). In this case, human total survival was used as a rough proxy for metastatic propensity since patients with metastatic disease have a

much lower survival rate. Since the majority of BT and HB tumors sequenced were primary tumors and only primary tumors were available in the UM database, the SKCM samples were filtered to include only primary samples for analysis, as well. The SKCM dataset contains 104 primary tumor samples and is dominated by tumors driven by BRAF, NRAS and NF1. The UM dataset contains 80 samples and is dominated by GNAQ and GNA11. Both were included to ensure that non-BRAF, non-NRAS mutant tumors were represented in the analysis. None of the primary cutaneous melanomas had a significant correlation between expression and survival that aligned with the difference in the BT mice. However, three genes, *Isoc2b/ISOC2*, *LILRA5,* and *PTPRH*, had a significant association between higher RNA expression and shorter survival in the UM dataset and had higher expression in the highly metastatic BT group than the HB group (Fig 14). These three genes were, therefore, the highest ranked within the list of 22 genes for functional validation and represent

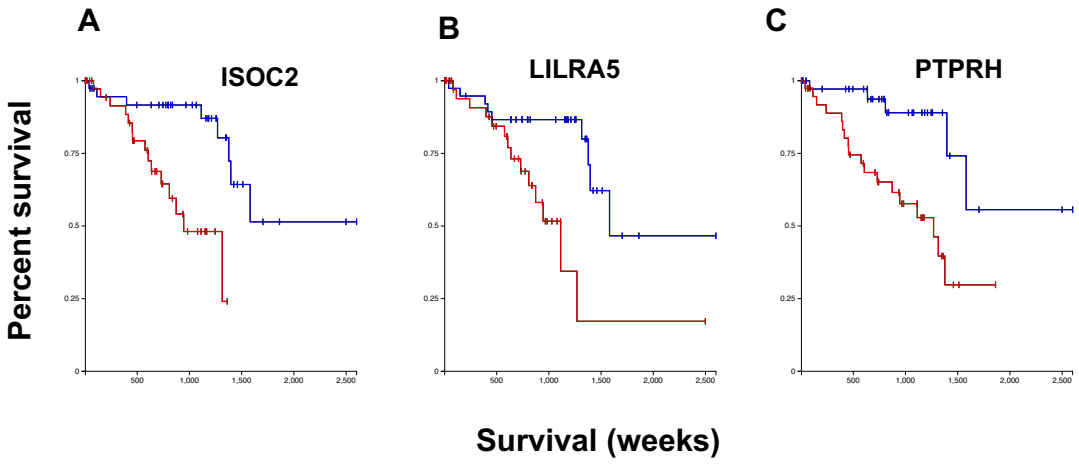


**Figure 14. Survival and gene expression in uveal melanoma.** A-C) Kaplan-Meier survival curves for ISOC2, LILRA5, and PTPRH showed significant associations between RNA expression survival in human uveal melanoma patients from the TCGA uveal melanoma database. RNA expression is stratified into higher than median (red) and lower than median (blue).

outstanding candidates for future functional validation of their ability to regulate metastatic potential.

## ***Conclusions***

Melanocytic nevus and cutaneous tumor development in the BT model was relatively similar to the GS mice and to that described previous in HGF models (Takayama, La Rochelle et al. 1996, Noonan, Otsuka et al. 2000, Recio, Noonan et al. 2002, De Fabo, Noonan et al. 2004, Florell, Thomas et al. 2007). Although the BT model developed tumors more quickly and developed more VGP and nodular tumors than the GS melanoma, speed of tumor development is similar to other models with congenital CDKN2A heterozygous loss (Recio, Noonan et al. 2002). A pitfall of this study is that the importance of the relative timing of UV and CDKN2A mutation could not be evaluated. Unfortunately, when UV is administered to adult mice without neonatal administration, HGF mice develop non-melanoma skin cancers (Noonan, Otsuka et al. 2000).

Melanoma research has been hampered by a dearth of metastatic melanoma cell lines and models that can be used in immunocompetent mice. The lack of these resources has hampered research into metastatic biology and preclinical testing of targeted therapy and immunotherapeutic agents in the metastatic setting. The metastatic transplantable tissue bank and low passage cell lines developed in this project help to fill those gaps. Preliminary studies will soon begin efficacy of immunotherapy as a neoadjuvant therapy before resection of the primary tumor and as adjuvant therapy following tumor resection to prevent local recurrence or

metastasis. We think these cell lines and transplantable tumors have the potential to be widely adopted in the melanoma research community.

The most striking difference between the mouse model compared to other HGF models is the marked metastatic phenotype. In other HGF models, metastasis has been an uncommon occurrence and are often small (Otsuka, Takayama et al. 1998, Florell, Thomas et al. 2007, McCorkle, Leonard et al. 2014, Leonard, Pamidimukkala et al. 2017). However, in the BT model, metastatic lesions are widespread and readily visible in a variety of organs. This unexpectedly metastatic model provided a platform to identify possible germline variants that could be associated with increased metastatic susceptibility. Although genome wide association studies and familial cohorts have identified germline variants associated with melanoma susceptibility, no studies have evaluated the effect of variants on germline susceptibility to metastasis (Monzon, Liu et al. 1998, Ciotti, Struewing et al. 2000, Chaudru, Laud et al. 2005, Harland, Taylor et al. 2005, Laud, Marian et al. 2006). Mouse models have been particularly useful in identifying germline metastasis susceptibility variants and metastasis-associated genes (Lifsted, Le Voyer et al. 1998, Crawford, Ziogas et al. 2006, Hsieh, Look et al. 2009). This project turned up a reasonable of 21 germline variants in exomic or UTR regions. Functional validation of a role for these genes in metastasis is being planned. The new highly metastatic BT cell lines, and less metastatic GS and HB cell lines developed in this project will be used to validate a role for these genes. It is possible that the metastatic susceptibility is not a single gene trait and may require multiple alterations to change metastatic potential. Additionally, the serial transplanted tumors used to create cell lines may

have evolved to no longer depend on germline variants that were needed for metastasis within the primary mouse. This study, however, is the first attempt to identify germline variants that enhance metastasis in melanoma.

In conclusion, the BT model provides a novel platform to investigate progression healthy individual to metastatic disease in non-BRAF, non-NRAS melanoma. The unexpectedly high metastatic frequency in this model facilitated the development of tools to help melanoma researchers investigate the biology and treatment of metastatic disease, but also to identify for the first-time germline variants affecting metastatic susceptibility in melanoma.

# Chapter 4: Genomic alterations in UV-induced murine melanocytic lesions


***Summary***

Progression of nevi to melanoma is an uncommon route to melanoma. Human nevi, like melanoma, frequently contain mutations in BRAF and NRAS. Targeted sequencing of human nevus remnants and associated melanomas has found accumulation of alterations in CDKN2A and SWI/SNF genes. We hypothesized that HGF mouse melanocytic lesions would similarly acquire additional mutations with progression from nevi to melanoma and to more aggressive forms of melanoma. Using lesions from the GS and BT models, we performed exome sequencing on nevi, RGP and VGP melanomas and transplanted and metastatic lesions. The mean number of nonsynonymous SNVs was lowest in the nevi and significantly high in tumors (BT model) and VGP melanomas (GS model). Known melanoma strong drivers, including Gnaq, Gna11 and Nf1 were found for approximately 40% of melanomas. Analysis of sequencing data also recurrently mutated genes potentially associated with nevus initiation. Pathway analysis also identified chromatin organization pathways in melanoma formation and progression to more aggressive forms. These study has generated new genes and pathways for investigation of their functional role in melanocytic lesions and the dataset provides information about melanocytic lesion progression in non-BRAF, non-NRAS melanocytic lesions.

***Introduction***

Sequencing of patient melanomas is increasingly available through easily accessible platforms like cBioportal.com. Although major drivers, including *BRAF, NRAS, NF1 and GNAQ/11* have been identified in most melanomas, these drivers are also present in most nevi. Therefore, they are sufficient for malignant transformation and progression. Some progression-associated genes have been identified or suggested, including *CDKN2A* deletion, and SWI/SNF alterations (Shain, Yeh et al. 2015, Shain, Joseph et al. 2018). Since melanoma is highly mutated, with an average of 10-12 nSNVs per megabase of DNA (Hodis, Watson et al. 2012, Lawrence, Stojanov et al. 2013), it is difficult to identify additional genes and pathways involved. Although NAMs comprise only approximately 30% of melanomas (Pampena, Kyrgidis et al. 2017), they provide a good model for evaluating progression-associated pathways since the timing and order of mutations can be identified. Several recent studies have evaluated the genomic changes in NAMs to better understand melanocytic lesion progression. Consistent with the general nevus populations, the majority of the nevus remnants had *BRAF* or *NRAS* (or rarely *KRAS*) mutations, or in other melanoma drivers including *NF1* and *KIT* (Shain, Yeh et al. 2015, Shain, Joseph et al. 2018). Progression to melanomas was associated with increased frequency of CDKN2A loss, other cell cycle gene alterations, and SWI/SNF alterations. Since very few triple wildtype NAMs have been examined, even less is known about progression in this group.

Exome sequencing of HGF models has not previously been published and little is known about drivers and significant pathways in this group, but BRAF and

NRAS mutations have not been identified by targeted sequencing (Gaffal, Landsberg et al. 2011). We hypothesize that each step during melanocytic lesion progression, including nevus initiation, malignant transformation, and progression of melanoma stages, will be associated with acquisition of additional genomic alterations. We further anticipate that analyzing these alterations will provide novel information about initiation and progression-associated genomic alterations in triple wildtype cutaneous melanoma. We will test these hypotheses using our novel GS and BT melanomas of melanocytic lesion progression

## ***Methods***

### DNA isolation and exome sequencing

Flash frozen tumor samples were isolated using the PureLink Genomic DNA kit (Invitrogen, Carlsbad, CA) following the manufacturer's protocol. Whole exome capture was performed by the CCR Genomics Technology Laboratory – ATRF (Frederick, MD) using the Agilent SureSelect Exome Capture Kit at the Genomics Technology Laboratory at the Frederick National Laboratory (Frederick, MD). Sequencing was performed on the Illumina HiSeq 4000 by the CCR Sequencing Facility (Frederick, MD). Samples were aligned to mouse genome build MM10. Bioinformatic analysis for exome data was performed by Maxwell Lee, Howard Yang and Huaitian Lee in the Laboratory of Cancer Biology and Genetics (CCR, Bethesda, MD). Mutect2 was used for variant calling, following by removing variants contained in normal spleen from colony mice or in the Mouse Genome Project version 5 and low-quality variants were filtered out. Genome annotation was performed using Annovar and VEP. SIFT analysis was performed to predict the effect of mutations.

**Identification of driver genes and mutations in human melanoma**

Drivers from any cancer were identified from the Cosmic Cancer Gene Census (https://cancer.sanger.ac.uk/census), and mutations in genes on that list were identified in the GS and BT samples. Recurrently mutated driver genes underwent enrichment analysis using the Panther Classification System (www.pantherdb,.org) using the Panther Overrepresentation Test (Released 20171205) with Fisher's Exact test with FRD multiple test correction for Panther Pathways was used.

Mutation frequency and prevalence in all melanoma and triple wildtype melanoma was determined by using www.cBioportal.org (Cerami, Gao et al. 2012, Gao, Aksoy et al. 2013). The melanoma studies used within cBioportal were "Uveal melanoma (TCGA, PanCancer Atlas)", "Paired-exome sequencing of acral melanoma (TGEN, Genome Res 2017)", "Melanoma (Broad/Dana Farber, Nature 2012)", "Skin Cutaneous Melanoma (Broad, Cell 2012)", "Skin Cutaneous Melanoma (TCGA, PanCancer Atlas)", "Skin Cutaneous Melanoma (Yale, Nat Genet 2012)", "Skin Cutaneous Melanoma (Broad, Cancer Discov 2014)", and "Desmoplastic Melanoma (Broad Institute, Nat Genet 2015)."

**Sanger sequencing**

DNA was amplified by PCR for Sanger sequencing to confirm Gnaq and Gna11 mutations. PCR was performed using the Q5 High Fidelity Master Mix (New England Biolabs) according to the manufacturer's protocol. Gnaq/11 primers were Gnaq exon 5 F GTGTACGGAAATGCATGGCA and 5R AGGCTCTTCACTCTGACAC, Gnaq exon 4F TCAGCTGCTGAGGAAATGGG, 4R TCTGTGACTCAGTTTTTGCTC and Gna11 exon 5F

TGTCTGACTCCACCAGGACT Gna11 5R GCCATCTGTACAAGGGGCTT. Samples were sequenced at the CCR sequencing core.

### RNA isolation

Flash frozen samples were pulverized using a mortar and pestle with liquid nitrogen or using the cryoPREP Manual Dry Pulverizer (Covaris, Woburn, MA). Samples were mixed with tissue lysis reagent (Qiagen, Germantown, MD) and run through the Qiashredder (Qiagen, Germantown, MD) before following the manufacturer's instructions for the RNAeasy kit (Qiagen, Germantown, MD). Total RNA sequence libraries preparation and sequencing was done by the CCR Sequencing facility (Frederick, MD) using Illumina TruSeq kit (Illumina, San Diego, CA), and sequenced on Illumina HiSeq 4000.

### Statistics

Most statistics were performed using Prism 7 for Mac (GraphPad, La Jolla, CA). Kruskal-Wallis test with multiple comparisons was used for comparing more than 2 groups. Adjusted p values are used in cases of multiple comparisons. A Kolmogorv-Smirnov test was used to evaluate unpaired analyses with only two groups. Wilcoxon matched-pairs signed rank test was used to evaluate data for paired primary and metastatic/transplantation samples. Proportional Venn diagrams were created using BioVenn (Hulsen, de Vlieg et al. 2008).

## ***Results***

### More aggressive melanocytic lesions had higher numbers of nonsynonymous single nucleotide variants

To test our hypothesis that progression would be associated with additional genomic alterations, we examined exome sequencing from 72 samples, including 42 GS lesions and 30 BT lesions. Sequenced samples included 15 cutaneous nevi and 43 melanomas, 6 distant metastatic lesions (5 lymph nodes and 1 lung lesions), and 7 transplanted samples. Twelve mice had two or more cutaneous lesions sequenced. Of these, six lesions were identified by sequencing as cutaneous metastases. Eleven of the mice also had multiple unique cutaneous lesions. Two of the transplanted lesions, one transplanted from a cutaneous and one from a lung metastasis, lacked a paired primary available for sequencing, so these transplanted lesions were used as the "initial" sample. Paired primary and transplanted lesions were available for the other transplanted lesions.

Single nucleotide variants (SNVs) were the most common type of somatic mutation in the GS and BT melanocytic lesions and SNVs were higher in more advanced lesions. The total number of mutations varied widely between lesions, with as few as 5 to as many as 433 nonsynonymous SNVs (nSNVs) (Fig 15A, top row). In GS mice, there were significantly higher mean numbers of nSNVs in VGP lesions (278.4) than in nevi (55.45) or RGP (105.5) ($p<0.0001$ and $p=0.0002$, respectively)

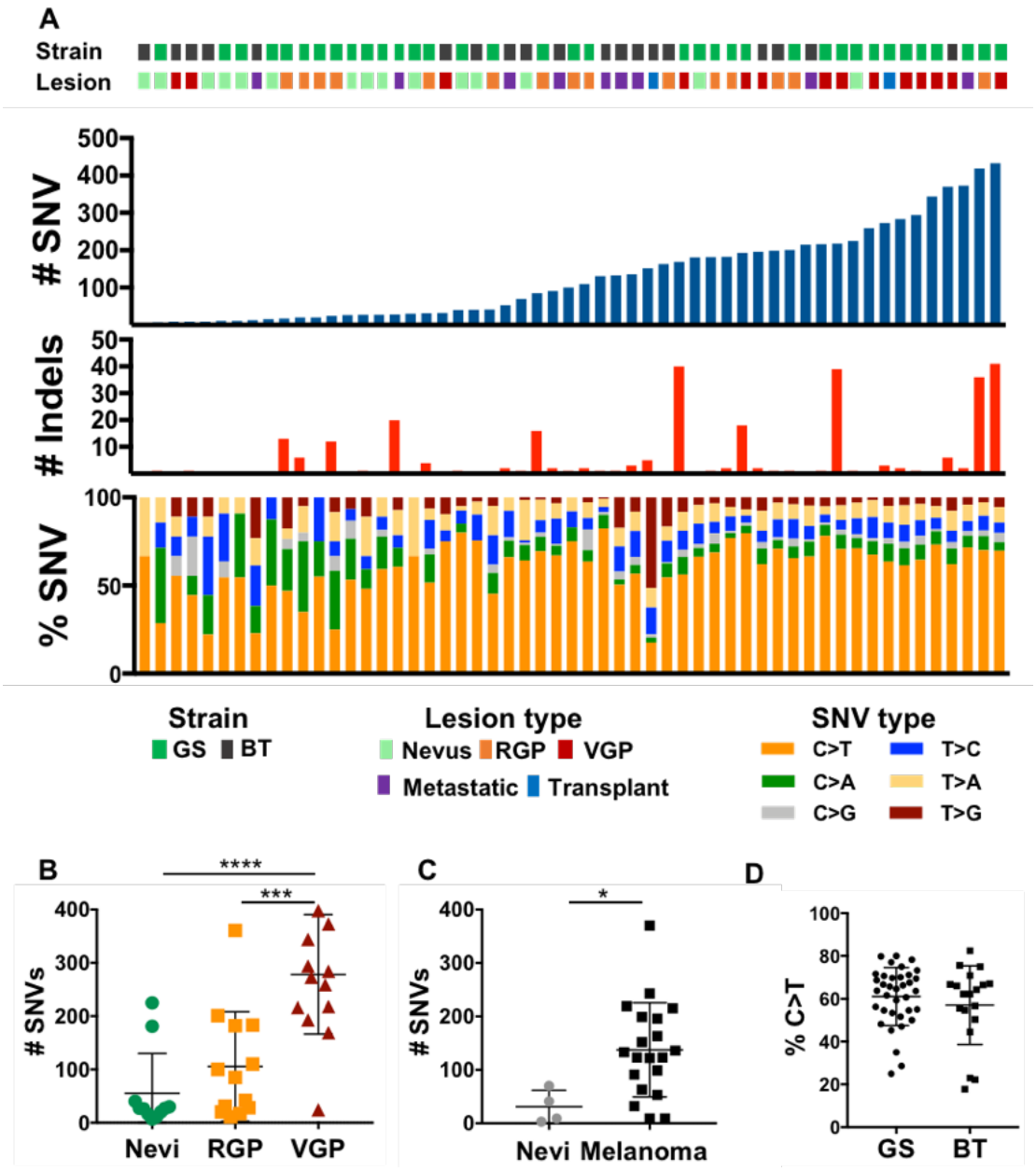


**Figure 15. Mutations in primary tumors consisted primarily of single nucleotide variants (SNVs).** A) Tumors are arranged by number of SNVs and identified by strain (top row) and lesion type (second row). The number of SNVs (top graph) and somatic indels (middle graph) are noted for each lesion. For SNVs, the proportion of SNVs represented by each type of mutation is represented in the bottom graph. C >T transitions are the most common type of mutation, especially with higher numbers of SNVs. B) There is no significant difference between C > T transitions between the GS and BT mice ($p = 0.82$). The number of SNVs is higher in VGP melanomas the GS (C) and BT (D) models.

(Fig 15B). Similarly, BT melanomas had higher significantly mean nSNVs than did nevi (137.5 vs 30.75, p = 0.024) (Fig 15C). There was no significant difference between nSNVs in nevi between the two models. Lesions contained lower numbers of INDELS (Fig 15A, middle row), which had poor correlation with the number of nSNVs in individual samples ($r^2 = 0.13$). NSNVs consist primarily of C >T transitions (Fig 15A, bottom row), consistent with UV exposure. There was no differenence in the frequency of C > T transitions between GS and BT lesions (Fig 14D).

**Potential nevus initiation genes**

Next to identify genes associated with nevus initiation, we looked at the subset of genes mutated in both nevi and tumors. Initiation-associated genes would be expected to be maintained in tumors following malignant transformation. Nevi had low numbers of mutations overall and major driver mutations were only identified in a single nevus with mutations in both *Nf1* and *Plcb4*. However, several genes were mutated in both nevi and tumors. Recurrent mutations were found in GS lesions in 6 genes: *Sycp1, Nme2, Rbm6, Ppp2r5a, Paip1* (Table 5). An additional gene, *Lrp1b,* was mutated at different sites clustered around the same region of the gene in GS and BT nevi and melanomas. Mutations in these genes were also seen in human melanomas in the cBioportal databases (Table 5) and occurred in tumors with and without BRAF or NRAS mutations. Each of these genes have previously been implicated in human cancer (Table 6), although none have been extensively studied and a role in melanocytic lesion development had not previously been suggested.

**Table 5. Recurrent mutations in GS nevi and melanoma**

| Gene | Mutation | Nevi | | Melanoma | | Human |
|---|---|---|---|---|---|---|
| **Sycp1** | D281E | **4** | 27% | **2** | 5% | 10% |
| **Nme2** | S122X | **3** | 20% | **5** | 12% | 0.5% |
| **Rbm6** | S301A | **5** | 33% | **2** | 5% | 4% |
| **Prrc2c** | V2513A | **4** | 27% | **2** | 5% | 9% |
| **Ppp2r5a** | V210I | **4** | 27% | **1** | 2% | 2.4% |
| **Paip1** | M379I | **2** | 13% | **4** | 10% | 2.7% |
| **Lrp1b** | various | **2** | 13% | **6** | 15% | 39% |

**Table 6. Links between recurrently mutated nevus genes and human cancer**

| Gene | Proposed role | Tumor types | Refs |
|---|---|---|---|
| **Sycp1** | Meiotic chromosome pairing | Medulloblastoma | (Oba-Shinjo, Caballero et al. 2008) |
| **Nme2** | Metastasis suppressor | Melanoma (mouse), Gastric cancer | (McCorkle, Leonard et al. 2014, Liu, Yang et al. 2015, Leonard, Pamidimukkala et al. 2017) |
| **Rbm6** | RBM6-RBM5 fusions | Breast cancer | (Wang, Ubriaco et al. 2007) |
| **Prrc2c** | Unknown function | Lymphoma, hepatocellular carcinoma | (Kim, Kim et al. 2012, Kaymaz, Oduor et al. 2017) |
| **Ppp2r5a** | Regulating cancer development | Various carcinomas | (Mao, Liu et al. 2018) |
| **Paip1** | Translational initiation | Breast, melanoma | (Greenwald, Friedman et al. 2012, Piao, Chen et al. 2018) |
| **Lrp1b** | Tumor suppressor | Ovarian, colon, and lung carcinomas | (Zilberberg, Yaniv et al. 2004, Cowin, George et al. 2012, Beer, Zenzmaier et al. 2016, Wang, Sun et al. 2017) |

### Gnaq/11 pathway mutations dominate in GS and BT melanomas

We then moved to identifying mutations associated with malignant transformation and progression from RGP to VGP or metastatic melanomas. In our search for strong drivers, we focused on genes mutated exclusively or primarily in tumors. Since these mutations should arise early in tumor development, they should be already have been noted at the earliest tumor stage. Mutations in melanoma-associated strong drivers were identified in approximately 51% (20/39) of GS/BT melanomas at the first stage sampled and only 6.7% (1/15) of nevi (Fig 16). Mutations in genes in the GNAQ/11 pathway, best known for their involvement in uveal melanoma, were the most

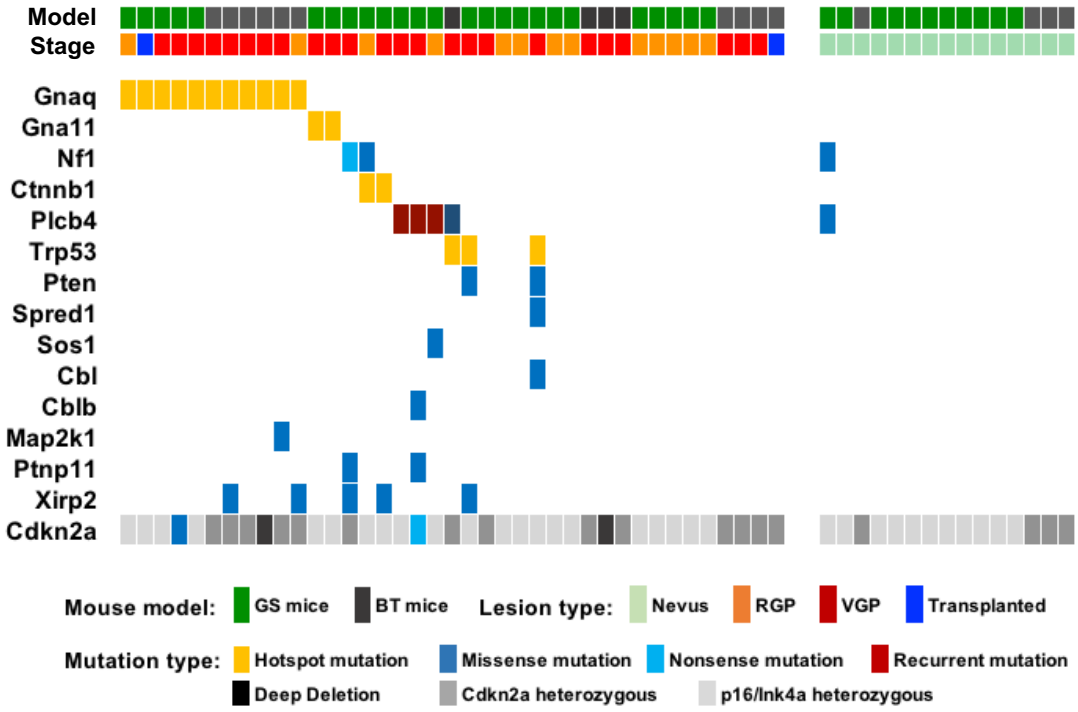


**Figure 16. Major driver mutations were identified in many GS and BT melanomas.** Hotspot mutations in known melanoma driver genes *Gnaq*, *Gna11*, *Ctnnb1* and *Trp53* as well as loss of function mutations in *Nf1* are noted. A novel, recurrent mutation is noted in the purported melanoma driver gene *Plcb4*. Mutations in driver genes from other cancer and RASopathy genes were also seen in tumors but not nevi. Additional alterations in *Cdkn2a* were uncommon.

common driver mutations. The single most common driver mutations were hotspot mutations in *Gnaq* at codons 209, 183, and 48 which were seen in 28% (11/39) of primary melanomas. An additional 5% of tumors had hotspot mutations in *Gna11* codon 209, which functions similarly to *Gnaq*. A recurrent novel mutation in *Plcb4* is seen in 3 (7%) of melanomas without a clear additional driver, and separate *Plcb4* mutations were seen in an additional melanoma and one nevus. PLCB4, a target of GNAQ/11, has recently been identified as a putative driver in human uveal melanoma. Outside of the Gnaq/11 pathway, previously identified melanoma major driver mutations included loss of function *Nf1* mutations (5%) and hotspot mutations *Ctnnb1* G48W (5%). Interestingly, *Gna11*, *Ctnnb1, and Nf1* mutations were seen exclusively in GS mice, while *Gnaq* mutations occurred in both GS and BT mice.

Activation of the MAPK pathway is a common early event in melanocytic nevus and tumor formation. In our murine models, HGF expression causes chronic activation of MET and low levels of MAPK signaling. We hypothesized that this constitutive signaling likely replaces the need for mutational activation of other MAPK genes. To test this, we looked for mutation of RASopathy genes, which are commonly seen weak drivers in triple wildtype nevi and melanoma (Krauthammer, Kong et al. 2015, Halaban and Krauthammer 2016, Shain, Joseph et al. 2018). RASpopathy mutations were uncommon in our melanomas and not identified in nevi. Mutations in *Spred1, Sos1, Cbl, Cblb, Map2k1, and Ptpn11* were found.

In addition to tumor major drivers in tumors, we wanted to look for genes associated with progression from less aggressive to more aggressive forms of melanoma. To identify “progression-associated” genes, we looked at both primary

melanomas and metastatic lesions. Progression-associated genes were present primarily or exclusively in VGP and metastatic tumors. *CDKN2A, PTEN,* and *TP53* have been identified as major progression associated genes in human melanoma cohorts (Hodis, Watson et al. 2012, Cancer Genome Atlas 2015, Rajkumar and Watson 2016) and were each identified in our murine melanomas. Over half of human cutaneous melanomas have *CDKN2A* loss of heterozygosity, deletion, or inactivation as part of melanocytic lesion progression (Hodis, Watson et al. 2012, Cancer Genome Atlas 2015, Shain, Yeh et al. 2015, Rajkumar and Watson 2016, Shain, Joseph et al. 2018), and *Cdkn2a* alterations were also seen in 6 murine melanomas. Somatic mutations in *Cdkn2a* were seen in 2 (4.8%) VGP melanomas. An additional 4 samples had deletion of the *Cdkn2a* locus. Deletion of the locus occurred in 2 primary samples and 2 samples following serial transplantation. Hotspot mutations in *Trp53* were seen in 3/39 tumors (7.6%) and *Pten* mutations were seen in 2 (4.8%) melanomas. Interestingly, *Pten* and *Trp53* mutations co-occurred in the tumors. A trend towards co-occurrence of mutations in this pair of genes has been identified in the cutaneous melanoma datasets in cBioportal, as well.

Despite the predominance of uveal melanoma-associated drivers GNAQ/11, the frequency of the major driver and progression associated genes is more similar to cutaneous melanoma than to uveal melanoma. The melanoma datasets available in cBioportal were used to determine the frequency of genomic alterations (including somatic mutations, amplifications and deletions) of these major driver and progression-associated genes in both cutaneous (784 samples) and uveal (80 samples) human melanoma. Overall, the frequency of mutations in these genes in our murine

melanomas was most similar to the frequency in human triple wildtype cutaneous melanoma (Table 7). Uveal melanomas, on the other hand, have a distinct pattern of mutation frequency and lack mutations in cutaneous progression-associated genes. This strongly suggests that the GS and BT models are most similar to other cutaneous triple wildtype melanomas.

**Table 7. Distribution of major driver and progression associated genes in GS/BT melanoma and human cutaneous and uveal melanoma.**

| Gene | GS/BT mouse Melanoma | Human Triple wildtype | Human All cutaneous | Human Uveal |
|---|---|---|---|---|
| **GNAQ** | 29% | 4% | 2.4% | 50% |
| **GNA11** | 7% | 4.9% | 3% | 48% |
| **PLCB4** | 12% | 13% | 21% | 2.5% |
| **NF1** | 5% | 1.3% | 16% | 1.3% |
| **CTNNB1** | 4.6% | 3% | 7% | 0% |
| **CDKN2A** | 14.6% | 6.5% | 27% | 0% |
| **TPR53/TP53** | 7% | 7% | 16% | 0% |
| **PTEN** | 4.8% | 5.7% | 14% | 0% |

### Identification of additional drivers in melanocytic lesions

To identify novel initiation and progression-associated genes, we widened our search beyond major genes associated with human melanoma. We used the Cosmic Cancer Gene Census database to assemble a list of driver genes in all tumor types and compare all of our samples (both primary and metastatic) to this list. This further search identified mutations in 223 additional driver genes. Similar mean numbers of

driver genes were identified in the GS model (6.19) and BT model (5) (p = 0.167). GS lesions had 170 mutations in driver genes, 82 of which were mutated in 2 or more GS samples. Like with total nSNVs, VGP tumors had significantly more mutations in driver genes than did RGP or nevi (p = 0.029 and 0.0016, respectively) (Fig 17A). The BT model had 93 mutated driver genes, 32 of which were mutated in more than one sample (Fig 17B). 41 driver genes were mutated in at least one lesion in each of the models. This group will be referred to as the "shared" mutation group for pathway analysis. More advanced lesions in the BT also trended towards higher numbers of driver genes (p = 0.17) (Fig 17B). There was a strong correlation between the total number of nSNVs and the number of mutations in driver genes ($R^2$ = 0.88) (Fig 17C).

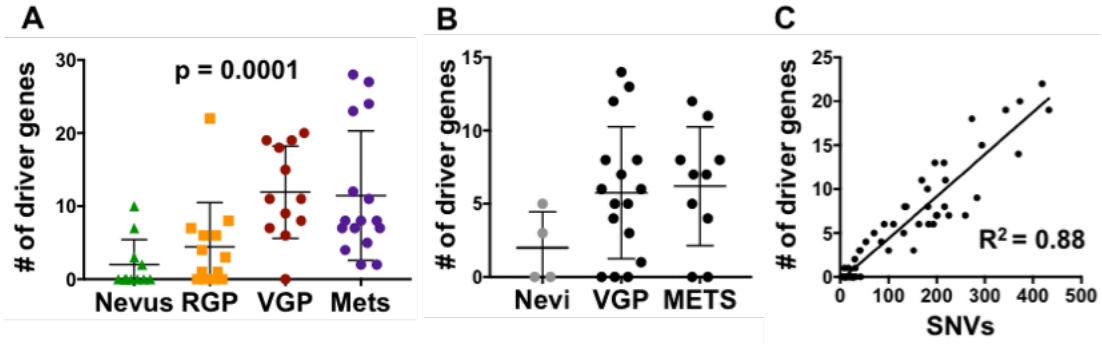


**Figure 17. Driver genes identified in melanocytic lesions.** A) VGP, Metastatic and transplanted tumors have significantly higher numbers of mutated driver genes than nevi. B) A similar trend exists in the BT lesions. C) There is a strong correlation between the total number of SNVs and the number of driver genes mutated in the sample.

This analysis did reveal some additional driver genes that are not commonly associated with cutaneous melanomas. Three tumors had mutations in *Dnmt3a*, including one mouse with a codon 878 mutation, equivalent to the human codon 882, which is a known driver in acute myeloid leukemia (Singh et al J Mol Diagnostics 2012; Xu et al PNAS 2014; Kumar et al Hematol Oncol Stem Cell Ther 2018; Lu et

al Cancer Cell 2016). One tumor had a mutation in *Egfr*, a driver associated with breast cancer as well as other tumors and has occasionally been implicated in AKT activation in melanoma (Ma and Niederkorn 1998, Schartl, Wilde et al. 2010, Amaro, Mirisola et al. 2013, Gross, Niemetz-Rahn et al. 2015). Interestingly, non-adjacent nonsynonymous mutations in *Xirp2* were found in 5 tumors. Four of these tumors gave rise to metastatic lesions. Although little is known about *Xirp2*, an actin-binding protein, it is significantly mutated in human cutaneous melanoma and other tumors and has been suggested as a potential driver gene (Hayward 2010, Fujimoto, Furuta et al. 2015, Li, Wu et al. 2016, McFadden, Politi et al. 2016). *Xirp2* mutations was seen only in VGP lesions and 3/5 melanomas with the mutation had metastatic lesions, suggesting that *Xirp2* may be associated with lesion and possible metastasis progression in our models.

**Identifying pathways involved in melanomas**

Signaling pathway alterations may also contribute to the initiation and progression of melanocytic lesions in our models. To find additional pathways involved in GS and BT melanoma development or progression, recurrently mutated driver genes from the analysis above were compared between the models. There were 82 genes with multiple mutations in the GS model, 32 in the BT model and 41 mutated in at least one gene from each model (Fig 18A). These recurrently mutated gene lists were entered into the Reactome database, a curated database focused on reaction pathways. The GS model had the highest number of significantly mutated pathways (95), compared with only 3 for the BT model and 15 for the shared group (Fig 18B). Three pathways were significantly overrepresented in all three gene lists: Chromatin

organization, chromatin modifying enzymes, and PKMTs methylate histone lysines.

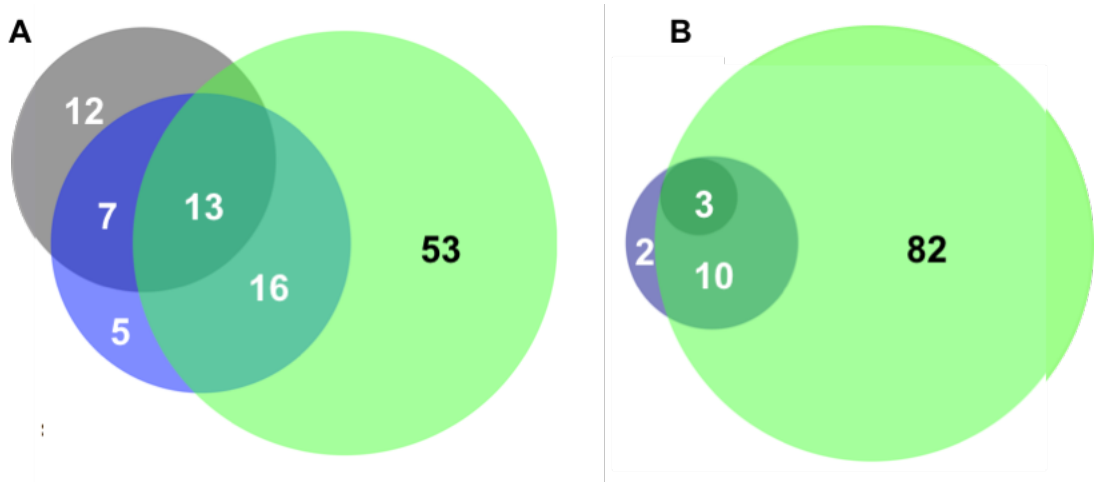


**Figure 18. Recurrently mutated driver genes and overrepresented reactome pathways**. A) Overlap of genes mutated in multiple samples. Genes were grouped as mutated in multiple GS tumors (green), multiple BT tumors (grey), or at least one tumor from both models (blue). While the majority of the blue group genes overlapped with the other groups, 5 genes were mutated in only a single GS tumor and a single BT tumor. B) Recurrently mutated gene lists were used to identify overrepresented reactome pathways. The green group has the highest number of unique overrepresented pathways, consistent with the higher number of unique pathways and the grey group had no unique overrepresented pathways. Three reactome pathways are overrepresented in all of the gene lists (dark green area).

These pathways are partially overlapping. Reactome pathways contain driver and non-driver genes, so to better evaluate overall mutation frequency of genes in these pathways, we looked at mutations in all genes within the pathway. Mutations were present in 29/39 (74%) of the tumors and 1/15 (6.7%) of nevi (Fig 19). Genes in these pathways were more likely to be mutated in RGP and metastatic lesions than in VGP melanomas. Additionally, metastatic and transplanted lesions have significantly more alterations in chromatin organization genes than their paired primary lesion ($p = 0.0039$). The group most likely to be mutated was the PKMTs methylate histone lysine group with 21/39 tumors having mutations in that group. The PKMTs group incorporates several histone methylation families and can be involved in both histone

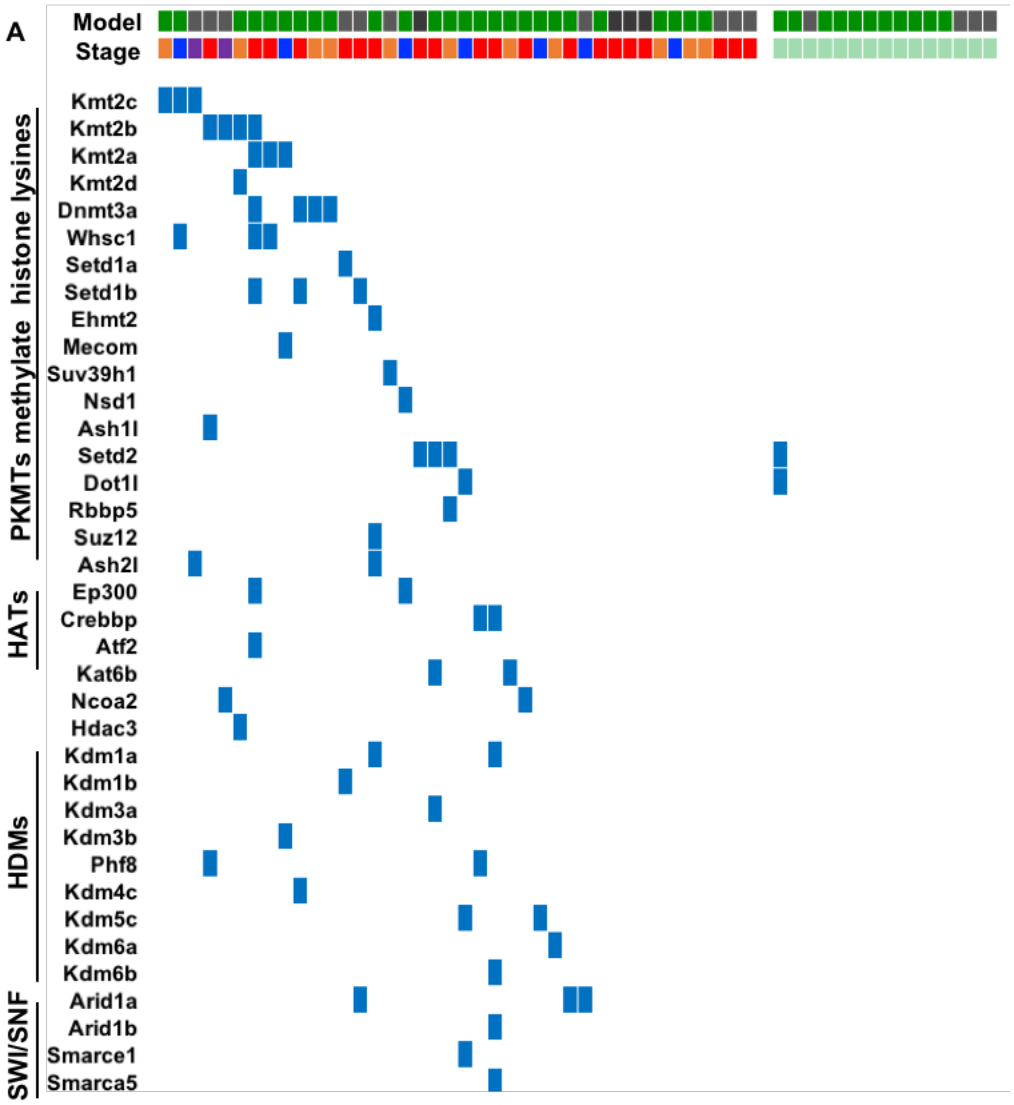


**Figure 19. Chromatin modifying genes were frequently mutated in melanomas.** The chromatin modifying pathway was heavily mutated in the GS and BT melanomas. The PKMTs group is particularly hard hit, but other chromatin organizational groups are also frequently mutated. Chromatin organization mutations were rare in nevi.

and non-histone methylation. A variety of genes in this family have been reported to play a role in cancer (Hamamoto, Saloura et al. 2015).

To test whether there were functional effects of mutations in these pathways, we evaluated RNA expression of pathway genes. Gene expression in these pathways

was widely altered. In the BT model, there was statistically significantly lower expression of a 77 chromatin organizing genes compared with tumors from the poorly metastatic HB model (Appendix 2); while only 15 chromatin remodeling genes were significantly increased in the BT model (Appendix 3). The pattern was similar in the GS model with 31 chromatin organization genes downregulated (Appendix 4) and 21 upregulated (Appendix 5) in VGP lesions. These data support a potential functional role for these pathways in melanoma progression.

### Progression of individual tumor groups is associated with accumulating mutations in driver genes

On a population basis, more aggressive lesion types have higher numbers of overall mutations and of driver mutations. To investigate whether this was true for individual lesions, we used tumors with samples of the same tumor at various stages of progression. Eleven tumor "groups" had a primary tumor and at least one metastasis or transplanted tumor. One group (7052) included a biopsy from an RGP lesion which then progressed to a VGP lesion and a cutaneous metastasis within the same mouse.

There was a statistically significant increase in the total number of driver mutations from the early to advanced melanomas in the paired samples (Fig 20A). There was also a trend toward a higher number of driver mutations ($p = 0.16$) (Fig 20B).

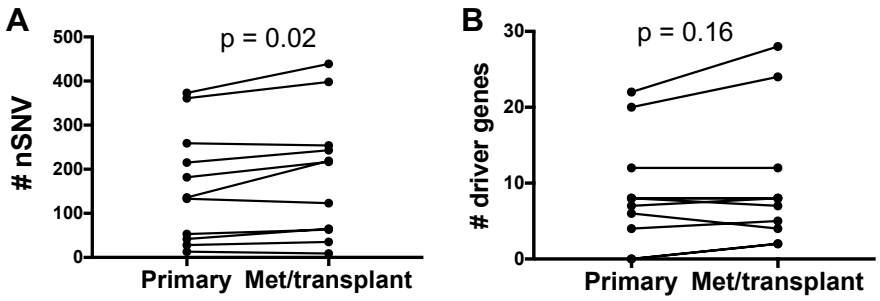


**Figure 20. Progression of individual lesions was associated with increased SNVs.** A) The number of nSNVs significantly increased in individual tumors with progression to metastasis or transplantation. B) There was a trend toward increased numbers of driver mutations with progression in all but 2 samples.

Analysis of tumor groups allowed us to more precisely identify the stage where mutations were acquired and the order of acquisition within individual lesions (Fig 21). Similar to stages within the cohort, individual groups acquired major drivers earlier in lesion development, followed by additional drivers and progression-associated gene mutations with progression to more aggressive stages. However, no mutations in driver genes were found in 2 groups in the first sample, but mutations in potential driver genes, *Apc, Kdm5c, Ptpn11,* and *Csf1r*, were acquired during transplanted tumor samples. Two genes, *Kdm5c* and *Ptpn11* have been associated with melanoma and *Apc* has been associated with other cancers. *KDM5C* is a lysine demethylase and members of the KDM5 family have been associated with stemness and proliferation in melanoma (Blair, Cao et al. 2011, Liu and Secombe 2015). A *Ptpn11* S502L mutation was found, which is a gain-of-function mutation involved in Noonan syndrome and acute myeloid leukemia (Tartaglia, Martinelli et al. 2006). SHP-2, the protein encoded by PTPN11 positively regulates both MAPK and PI3K pathway signaling and has recently been implicated in treatment resistance and in

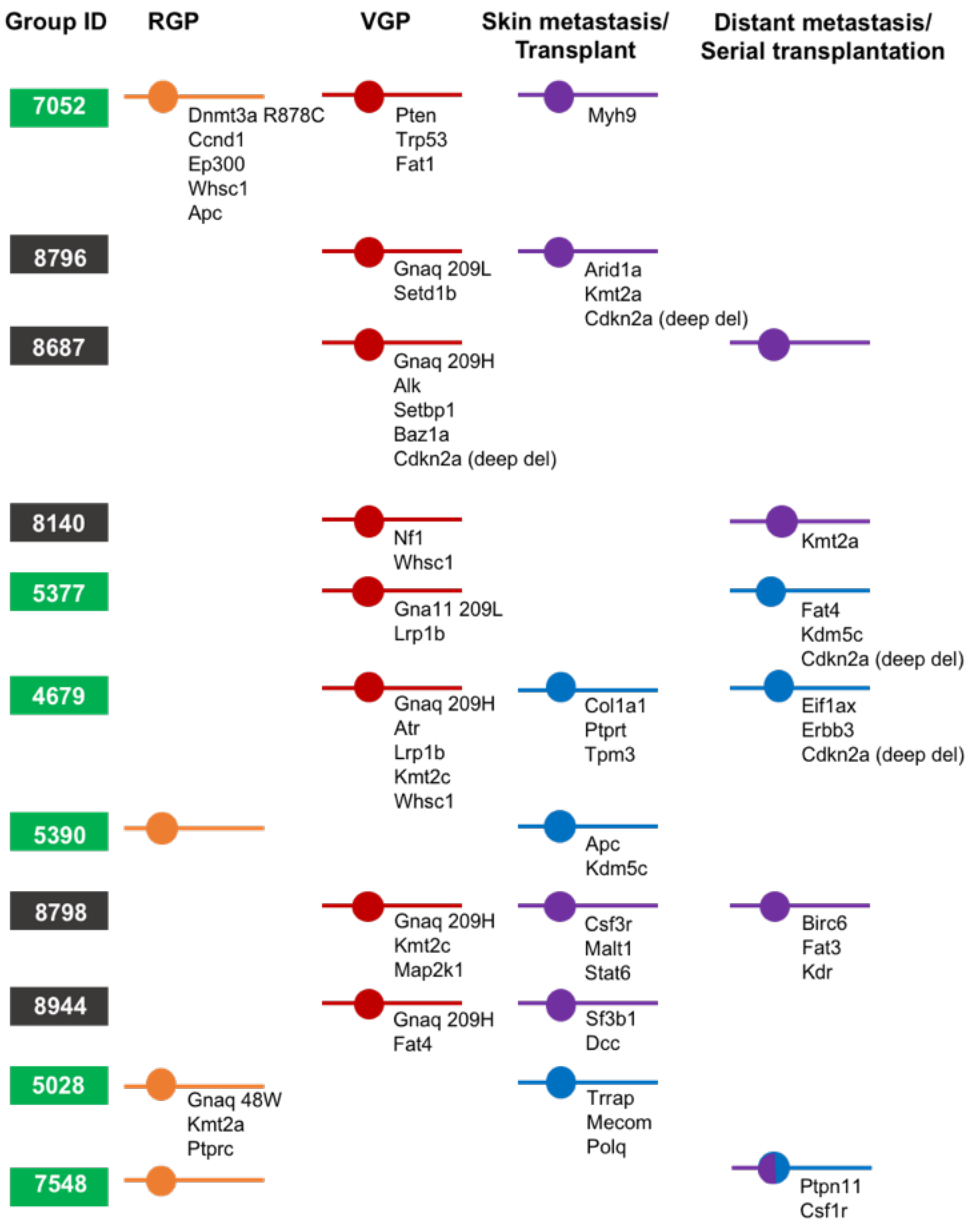


**Figure 21. Progression in individual tumor groups was associated with acquisition of additional mutations in driver genes**. Eleven tumor groups with sequencing of tumors at multiple stages were found, arising from 6 GS tumors (green) and 5 BT tumors (grey). Markers show lesion stage and selected mutated driver genes for individual lesions within the groups. Groups 5390 and 7548 had no mutated driver genes identified in the RGP stage but had driver mutations following transplantation. Group 8687 did not accumulate any additional driver mutations in any of the three lymph node metastases sequenced. Lesion marker color corresponds with stage: orange = RGP, red = VGP, blue = transplanted lesion. purple = metastatic lesion.

growth and survival of melanoma (Cheng, Chiu et al. 2013, Prahallad, Heynen et al. 2015, Zhang, Yu et al. 2016).

Individual tumor groups further supported a role for *Cdkn2a, Trp53, Pten,* and chromatin re-organization genes in progression. The number of mutated chromatin organization was significantly higher in more advanced lesions than in paired primaries. Further *Cdkn2a* alterations were in seen in only one group at the VGP stage and were acquired with metastasis or transplantation in the other groups. Similarly, *Trp53* and *Pten* mutations were absent from one group at the RGP stage but was acquired with progression to the VGP stage.

## ***Conclusions***

Within our models, melanocytic lesion initiation and progression occurs in a stepwise progression with acquisition of additional mutations at each stage. Mutations in major drivers, such as *Gnaq/11,* and *Nf1* were present in early melanomas, indicating a role in tumor initiation, while others progression-associated genes, including *Trp53, Pten,* and chromatin organization genes were present primarily in later stages.

Unlike most mouse models, HGF-mediated melanomas do not develop with a pre-existing strong driver and need neonatal UV exposure to produce melanomas. This makes it a powerful model for exploring the role of early UV exposure on melanoma development. Although the BRAF mutation, in particular, is associated with UV exposure skin (Bauer, Buttner et al. 2011), no *Braf* or *Nras* mutations spontaneously arose in the melanocytic lesions. Mutations in other MAPK-activating genes, including *Nf1* and RASopathy genes were also less common than in human cutaneous melanoma. This absence of *Braf and Nras* mutations may be due to the

chronic MET activation due to HGF which leads to mild MAPK activation. This mild activation may be sufficient to make BRAF or NRAS unnecessary for lesion development or may lead to excess MAPK signaling and senescence if melanocytes acquire a mutation in a strong MAPK activator.

Driver genes have been elusive in many human triple wildtype melanomas. A variety of drivers have been found at low frequencies in human triple wildtype tumors and no drivers have been identified in others. Similarly, a variety of driver genes were identified in the GS and BT melanomas. The most common mutations were hotspot mutations in *Gnaq/11* and the Gnaq/11 target *Plcb4*. Additionally, mutations in other melanoma drivers, including *Trp53, Pten, Ctnnb1*, RASopathy genes, and cancer drivers *Egfr, Erbb4, and Lrp1b* are noted. *LRP1B, ERBB4, and EGFR* mutations have occasionally been identified in human melanomas (Wiesner, He et al. 2014). *Lrp1b* may affect Wnt signaling and has recently been identified as a potential driver in ovarian cancer (Zilberberg, Yaniv et al. 2004, Cowin, George et al. 2012, Beer, Zenzmaier et al. 2016). *Xirp2* and the PKMTs histone lysines are also implicated in melanoma progression and potentially metastasis in this model.

The predominance of *Gnaq/11* pathway mutations was interesting. Although *GNAQ/11* mutations are the predominate driver in human uveal melanoma, they are less common in human cutaneous melanoma. Nearly 10% of triple wildtype cutaneous tumors contain mutations in these pathways and they are especially common in blue nevi and associated melanomas (Yilmaz, Gamsizkan et al. 2015, Patel, Kim et al. 2016). The role of GNAQ/11 in melanocyte development is unclear. Studies in mice have shown both progessive loss of dermal melanocytes and

melanogenesis, depending on the exact mutation and timing (Huang, Urtatiz et al. 2015, Moore, Ran et al. 2018). It is unclear why *Gnaq/11* mutations are overrepresented in the HGF model. Interestingly, mutations in this pathway have also been found in melanoma cells from HGF mice induced with neonatal DMBA instead of UV (provided by Thomas Tüting, University of Bonn). It is possible that HGF expression and subsequent mild MAPK activation may make the model more permissive of *Gnaq/11* mutant melanocytic lesions or decrease the frequency of lesions with strong MAPK signaling. Although HGF expression is important in uveal melanocytes and melanoma (Woodward, Elshaw et al. 2002, Woodman 2012), no clear association between HGF expression and GNAQ/11 mutation has been found in uveal melanoma (Chattopadhyay, Grimm et al. 2014). Additionally, in the TCGA Skin cutaneous melanoma group none of the 4 samples with hotspot *GNAQ/11* mutations have evidence of *HGF* or *MET* mRNA upregulation. We think that it is unlikely that HGF is contributing directly to the generation of GNAQ/11 mutations in our models.

Even after analysis, no identifiable driver was detected for most nevi or for approximately 33% of the melanomas. These samples tended to have low numbers of mutations detected overall. Since sequenced samples were mixed tumor and stroma, deeper sequencing or separation of melanocytes for sequencing, may be required to detect low frequency mutations. It is also possible that there are structural or epigenetic changes driving melanoma development in these tumors. Structural alterations and fusion genes are reported to be important in some triple wildtype melanomas (Rajkumar and Watson 2016). Structural changes estimated from the

RNA sequencing data did not reveal known driver-associated translocations and only rarely revealed amplifications or deletions linked with melanoma development (data not shown). This study was not designed to detect epigenetic alterations. Changes in methylation has been reported in melanoma and may be more important in triple wildtype melanomas lacking a clear strong driver (Fiziev, Akdemir et al. 2017). Exploration of methylation and other epigenetic markers in different stages of melanocytic lesions would be an interesting avenue for future research.

Both genomic alterations and expression changes suggest a role for chromatin organization genes in the development of GS and BT mice. A variety of chromatin modifiers have been implicated in melanoma development (Fang, Xia et al. 2013, Oike, Ogiwara et al. 2013, Lee, Sholl et al. 2015, Fiziev, Akdemir et al. 2017, Scahill, Digby et al. 2017). Scahill et al (2017) found that loss of *kdm2aa*, the zebrafish ortholog of *KDM2A,* was sufficient to induce melanoma in zebrafish without another driver. Interestingly, *Kdm5c* appears to be a clonal mutation in one transplanted tumor with no major driver, suggesting that it may be an initiating mutation in that case. The predominance of chromatin modifier genes in our GS and BT models provide further support for these genes in the development and progression of cutaneous melanocytic lesions.

Our murine models have provided a platform to analyze the role of genomic alterations in initiation and progression of non-BRAF, non-NRAS nevi and melanomas. Progression in these models was associated with accumulation of genomic alterations and driver genes in most of the samples and strong drivers were identified for many of the samples. However, some samples did not have clear

drivers, suggesting the need to assess epigenomic and genomic structural changes to better understand non-BRAF, non-NRAS melanocytic lesion development.

# Chapter 5: Conclusions and future directions

Modeling of melanocytic lesion development in HGF mice provides a way to observe development and progression of triple wildtype melanocytic lesions. Most mouse models use combinations of strong oncogenes to create melanomas. Although these models are very useful for evaluation of those oncogenes and for evaluation of targeted therapy, they are not appropriate for discovery of novel genes and pathways associated with melanomagenesis and progression. We hypothesized that stepwise progression of melanocytic lesions from nevi to melanoma would be associated with acquisition of additional mutations. The GS and BT models used in this project were designed to make tumorigenesis difficult to better reveal genes and pathways involved in melanocytic lesion and progression. Both rely on neonatal UV exposure for tumor development which should lead to heterogenous mutations. This design feature is reflected in the relatively low tumor incidence and the long latency to tumor development.

Consistent with our hypothesis, both GS and BT melanomas showed stepwise progression clinically and genomically. Progression of lesions was associated with an accumulation of nSNVs and with mutations in driver genes. Interestingly, despite the differences between the GS and BT models in mouse strain, CDKN2A status, and pigmentation, similar pathways, melanomas were very similar in driver genes and pathways associated with progression.

The GS and BT melanocytic lesions represented non-BRAF, non-NRAS melanomas, most of which did not have a mutation in a known strong driver for

melanoma. A variety of potential melanoma drivers were identified, including *Dnmt3a, Lrp1b,* and a novel recurrent mutation in *Plcb4*. Further exploration of the function of these genes in human melanocytes is planned. Previous investigation of melanoma drivers, including BRAF and NRAS, indicate that these mutations alone frequently cause senescence, suggesting that finding single genes capable of inducing melanoma may be difficult.

Our models also provided further support for the role of chromatin organization pathways, particularly the PKMTs histone lysine reactome in the development and progression of melanoma. The potential of this pathway to either initiate or cause progression in melanocytic lesions, particularly triple wildtype lesions, is another area for further investigation.

The most interesting aspect of this study may be the surprising metastatic susceptibility in the BT model. There have been no previous studies on germline variants and metastatic susceptibility in melanoma. Since this information is not represented in somatic mutation databases, this has the potential to identify novel metastasis genes as well as biomarkers to identify patients at increased risk of metastatic disease. Functional validations of genes identified in the germline variant analysis is currently being planned with cell lines derived from the highly metastatic tumors as well as poorly to moderately metastatic melanomas from the GS and HB models. Since metastasis can arise from patients with very small tumors, as occurred in some of the BT mice, and metastatic disease susceptibility markers could be very valuable in the treatment of patients with early melanomas.

Further projects have already developed from the genomic databases generated in this project. Our group was also awarded an internal NCI grant to collaborate with colleges in the Department of Cancer Epidemiology and Genetics to compare mutations in these models to human melanoma susceptibility loci identified from genome wide association studies (GWAS). Comparisons between these two data sets will be used to identify novel genes under GWAS peaks involved in melanoma development or progression. Over 100 mutated genes identified in this study fall under peaks identified in the human GWAS studies and functional validation of those genes is ongoing.

This project has also produced a variety of resources for the melanoma research community. There has been a dearth of metastatic melanoma models that can be transplanted into immunocompetent mice. This has hampered research into metastatic melanoma biology and into preclinical testing with small molecules and immunotherapies. In this project, we have generated transplantable tumor banks of both GS and BT melanomas and 6 low passage cell lines. These tumors are transplantable into syngeneic mice and have varying histologic, clinical and genomic characterizations. Several transplantable models developed in this project are already being used in preliminary testing to determine immunogenicity, and response to immunotherapy on primary and metastatic disease.

Substantial future work is still needed to understand the biology of melanocytic lesion development and progression; however, this project has produced resources and data that will be useful for investigations into melanoma biology, metastatic disease, and preclinical testing. This has the potential to identify

biomarkers to aid in melanoma diagnosis and predict metastatic disease, as well as identifying novel therapeutics and therapy combinations to help patients with melanoma.

# Appendices

**Appendix 1. Germline variants in highly metastatic BT mice**

| Gene | Type | Annovar |
|---|---|---|
| DNAAF3 | nSNV | NM_001033548:exon12:c.G1730C:p.W577S |
| FIZ1 | UTR3 | NM_001110329:c.*844T>C |
| GP6 | nSNV | NM_001163014:exon7:c.T766A:p.F256I |
| GP6 | nSNV | NM_001163014:exon4:c.T460C:p.S154P |
| ISOC2B | nSNV | M_026158:exon2:c.A119T:p.K40M |
| ISOC2B | UTR3 | NM_026158:c.*63A>G |
| LENG1 | UTR5 | NM_027203:c.-121A>G |
| LILRA5 | UTR3 | NM_001081239:c.*1132G>T |
| LILRB3 | UTR3 | NM_011095:c.*93G>T |
| MBOAT7 | nSNV † | NM_029934:exon7:c.C1015T:p.R339C |
| MBOAT7 | UTR3 | NM_029934:c.*147C>T |
| MBOAT7 | UTR5 | NM_029934:c.-731C>G |
| MYADM | UTR3 | NM_001093764:c.*398A>T |
| NCR1 | UTR3 | NM_010746:c.*402G>T |
| NCR1 | UTR3 | NM_010746:c.*403G>T |
| OSCAR | nSNV* | NM_175632:exon3:c.T187C:p.S63P |
| PANK3 | UTR3* | NM_145962:c.*4372T>C |
| PPP6R1 | UTR3 | NM_172894:c.*457G>C |
| PPP6R1 | nSNV | NM_172894:exon8:c.G925A:p.D309N |
| PPP1R12C | nSNV † | NM_029834:exon8:c.C1043T:p.S348F |
| PTPRH | UTR3 | NM_207270:c.*126C>T |
| PRPF31 | nSNV | NM_027328:exon3:c.T230C:p.V77A |
| PRPF31 | UTR3 | NM_027328:c.*975G>C |
| SBK3 | UTR3 | NM_001200041:c.*1450C>T |
| SBK3 | UTR3 | NM_001200041:c.*1382A>G |
| SHISA7 | UTR3 | NM_172737:c.*2238T>C |
| SHISA7 | UTR3 | NM_172737:c.*789G>T |
| SHISA7 | UTR3 | NM_172737:c.*5C>G |
| TBL1XR1 | UTR3 | NM_030732:c.*5459A>G |
| TMEM150B | UTR3* | NM_177887:c.*1145_*1142delACTT |
| TMEM150B | UTR3 | NM_177887:c.*1286A>G |
| TMEM150B | UTR3 | NM_177887:c.*1284A>G |
| TMEM150B | UTR3 | NM_177887:c.*1259T>C |
| TMEM150B | UTR3 | NM_177887:c.*410A>G |
| TMEM150B | UTR3 | NM_177887:c.-158A>T |

| | | |
|---|---|---|
| TMEM190 | UTR5 | NM_030028:c.-25G>A |

*Novel variants; † = predicted deleterious variants;

**Appendix 2. Chromatin organization genes with decreased expression in the BT model.**

| Gene ID | Log2 FC | FDR |
|---|---|---|
| SETD3 | -1.39 | 2.08E-41 |
| WHSC1L1 | -1.04 | 4.53E-13 |
| PRDM9 | -2.39 | 4.24E-16 |
| EHMT2 | -0.52 | 7.24E-06 |
| SUV39H1 | -0.97 | 7.31E-05 |
| SETDB1 | -2.07 | 4.47E-68 |
| WHSC1 | -1.54 | 2.00E-10 |
| NSD1 | -0.94 | 4.93E-12 |
| SMYD2 | -0.62 | 5.02E-10 |
| ASH1L | -1.95 | 2.66E-53 |
| SETD2 | -2.37 | 3.92E-77 |
| DOT1L | -0.92 | 4.19E-05 |
| SETD8 | -0.94 | 2.57E-05 |
| SUV420H1 | -1.38 | 2.80E-17 |
| KMT2A | -1.70 | 2.24E-15 |
| KMT2D | -2.22 | 3.46E-29 |
| KMT2C | -1.30 | 2.03E-09 |
| KMT2B | -1.91 | 8.28E-30 |
| SETD1A | -1.18 | 1.91E-20 |
| SETD1B | -1.23 | 4.80E-14 |
| RBBP5 | -2.32 | 3.20E-57 |
| ASH2 | -0.62 | 1.14E-15 |
| EED | -2.06 | 2.48E-45 |
| SUZ12 | -1.66 | 2.51E-20 |
| AEBP2 | -1.57 | 7.07E-26 |
| RBBP4 | -1.42 | 2.68E-17 |
| RBBP7 | -1.28 | 5.97E-14 |
| ASH2L | -0.62 | 1.14E-15 |
| EP300 | -2.25 | 9.82E-66 |
| CREBBP | -3.34 | 1.03E-137 |
| ATF2 | -2.03 | 8.23E-179 |
| KAT6A | -1.22 | 1.36E-24 |
| KAT6B | -3.27 | 6.18E-106 |
| KAT7 | -2.16 | 7.64E-93 |
| KAT7 | -2.16 | 7.64E-93 |
| NCOA1 | -1.22 | 2.47E-12 |
| NCOA2 | -1.36 | 1.87E-20 |

| | | |
|---|---|---|
| HDAC1 | -1.65 | 5.77E-18 |
| HDAC2 | -2.49 | 9.89E-78 |
| HDAC3 | -2.75 | 1.00E-305 |
| HDAC8 | -2.74 | 1.24E-49 |
| KDM1A | -2.16 | 1.13E-86 |
| KDM2A | -2.25 | 5.93E-46 |
| KDM2B | -1.54 | 7.88E-15 |
| KDM4A | -0.59 | 2.39E-06 |
| KDM3A | -1.39 | 4.70E-11 |
| KDM3B | -1.63 | 6.81E-25 |
| KDM7A | -1.88 | 1.17E-13 |
| ARID5B | -1.95 | 2.54E-21 |
| PHF8 | -0.81 | 8.70E-10 |
| KDM4B | -0.81 | 3.44E-05 |
| KDM4C | -0.79 | 2.15E-09 |
| KDM5A | -1.65 | 2.00E-32 |
| KDM5B | -0.72 | 8.08E-06 |
| KDM5C | -1.57 | 1.41E-24 |
| KDM6B | -1.29 | 4.83E-09 |
| KDM7A | -1.88 | 1.17E-13 |
| PRMT5 | -2.35 | 1.13E-68 |
| CDK4 | -1.30 | 6.06E-10 |
| RBBP7 | -1.28 | 5.97E-14 |
| DNMT3A | -1.03 | 2.36E-03 |
| PRMT1 | -2.95 | 6.01E-52 |
| CARM1 | -1.68 | 1.99E-40 |
| SMARCA4 | -1.90 | 2.93E-39 |
| ARID1A | -3.18 | 1.70E-66 |
| ARID1B | -1.07 | 3.69E-14 |
| SMARCB1 | -1.85 | 2.80E-35 |
| SMARCE1 | -3.23 | 1.78E-216 |
| SMARCC2 | -2.80 | 4.00E-196 |
| SMARCD3 | -2.86 | 2.67E-33 |
| SMARCD2 | -1.14 | 3.63E-07 |
| SMARCD1 | -1.73 | 1.71E-11 |
| SMARCA4 | -1.90 | 2.93E-39 |
| SMARCA2 | -2.49 | 1.07E-47 |
| ARID2 | -1.98 | 8.30E-48 |
| SMARCA5 | -2.09 | 3.03E-11 |

**Appendix 3. Chromatin organization genes with increased expression in the BT model**

| Gene ID | Log 2 FC | FDR |
|---|---|---|
| SETD7 | 4.17753388 | 1.14E-153 |
| SMYD3 | 0.80694084 | 3.25E-03 |
| SUV39H2 | 2.45705326 | 4.82E-21 |
| SETDB2 | 3.14855768 | 1.49E-32 |
| SETD6 | 0.34640836 | 9.49E-4 |
| Wdr5 | 3.11844385 | 1.56E-164 |
| HDAC10 | 3.37613111 | 9.38E-41 |
| KDM1B | 0.46537964 | 7.43E-03 |
| KDM8 | 4.09835531 | 2.47E-54 |
| MINA | 2.79594487 | 1.53E-31 |
| JMJD6 | 0.88952472 | 2.24E-06 |
| WDR77 | 0.44702384 | 4.6E-4 |
| COPRS | 6.91857398 | 7.96E-29 |
| PRMT3 | 1.41055681 | 1.12E-21 |
| PAD14 | 2.57920802 | 1.97E-3 |

**Appendix 4. Chromatin organization genes with decreased expression in the GS model**

| Gene ID | Log 2 FC | FDR |
|---|---|---|
| SETD7 | -0.9777224 | 2.19E-11 |
| WHSC1L1 | -0.4786916 | 0.036 |
| PRDM9 | -1.3073609 | 0.0044 |
| NSD1 | -0.3955061 | 0.051 |
| ASH1L | -0.5804547 | 0.0068 |
| SETD2 | -0.4165244 | 0.012 |
| SETD8 | -0.9038994 | 0.0067 |
| SUV420H1 | -0.9599479 | 3.89E-06 |
| kmt2a | -0.8352634 | 0.03 |
| kmt2d | -0.6856619 | 0.062 |
| kmt2c | -1.1403449 | 0.0023 |
| setd1b | -0.6149172 | 0.0079 |
| CREBBP | -0.7995539 | 4.74E-06 |
| KAT6A | -0.696301 | 2.27E-07 |
| KAT6B | -0.7539343 | 0.067 |

**Appendix 5. Chromatin organization genes with increased expression in the GS model**

| Gene ID | Log2 FC | FDR |
|---|---|---|
| SMYD3 | 1.07391359 | 0.05764164 |
| EHMT2 | 0.53622858 | 0.00171655 |
| SUV39H1 | 1.07182164 | 6.56E-05 |
| WHSC1 | 1.36574124 | 5.18E-06 |
| SMYD2 | 1.66280159 | 0.03732185 |
| SUZ12 | 0.35302313 | 0.04056548 |
| AEBP2 | 1.13484086 | 0.00994716 |
| RBBP4 | 0.47501147 | 0.05904054 |
| RBBP7 | 0.90778659 | 0.03547073 |
| ASH2L | 0.31770345 | 0.03457385 |
| KAT2 | 0.89780294 | 8.49E-05 |
| WDR77 | 0.39522072 | 0.01051057 |
| COPRS | 2.15100233 | 2.09E-05 |
| RBBP7 | 0.90778659 | 0.03547073 |
| DNMT3A | 1.00722356 | 0.01474862 |

# Bibliography


. "SEER Cancer Statistics Factsheets: Melanoma of the skin." Retrieved August 13, 2018, from http://seer.cancer.gov/statfacts/html/melan.html.

Aalborg, J., J. G. Morelli, S. T. Mokrohisky, N. L. Asdigian, T. E. Byers, R. P. Dellavalle, N. F. Box and L. A. Crane (2009). "Tanning and increased nevus development in very-light-skinned children without red hair." Arch Dermatol **145**(9): 989-996.

Aguissa-Toure, A. H. and G. Li (2012). "Genetic alterations of PTEN in human melanoma." Cell Mol Life Sci **69**(9): 1475-1491.

Amaro, A., V. Mirisola, G. Angelini, A. Musso, F. Tosetti, A. I. Esposito, P. Perri, F. Lanza, F. Nasciuti, C. Mosci, R. Puzone, S. Salvi, M. Truini, A. Poggi and U. Pfeffer (2013). "Evidence of epidermal growth factor receptor expression in uveal melanoma: inhibition of epidermal growth factor-mediated signalling by Gefitinib and Cetuximab triggered antibody-dependent cellular cytotoxicity." Eur J Cancer **49**(15): 3353-3365.

Aoki, H., Y. Yamada, A. Hara and T. Kunisada (2009). "Two distinct types of mouse melanocyte: differential signaling requirement for the maintenance of non-cutaneous and dermal versus epidermal melanocytes." Development **136**(15): 2511-2521.

Aranda, J. F., N. Reglero-Real, L. Kremer, B. Marcos-Ramiro, A. Ruiz-Saenz, M. Calvo, C. Enrich, I. Correas, J. Millan and M. A. Alonso (2011). "MYADM regulates Rac1 targeting to ordered membranes required for cell spreading and migration." Mol Biol Cell **22**(8): 1252-1262.

Aranda, J. F., N. Reglero-Real, B. Marcos-Ramiro, A. Ruiz-Saenz, L. Fernandez-Martin, M. Bernabe-Rubio, L. Kremer, A. J. Ridley, I. Correas, M. A. Alonso and J. Millan (2013). "MYADM controls endothelial barrier function through ERM-dependent regulation of ICAM-1 expression." Mol Biol Cell **24**(4): 483-494.

Balch, C. (2009). "Final Version of 2009 AJCC melanoma staging and classification." Journal of Clinical Oncology **27**.

Bald, T., T. Quast, J. Landsberg, M. Rogava, N. Glodde, D. Lopez-Ramos, J. Kohlmeyer, S. Riesenberg, D. van den Boorn-Konijnenberg, C. Homig-Holzel, R. Reuten, B. Schadow, H. Weighardt, D. Wenzel, I. Helfrich, D. Schadendorf, W. Bloch, M. E. Bianchi, C. Lugassy, R. L. Barnhill, M. Koch, B. K. Fleischmann, I. Forster, W. Kastenmuller, W. Kolanus, M. Holzel, E. Gaffal and T. Tuting (2014). "Ultraviolet-radiation-induced inflammation promotes angiotropism and metastasis in melanoma." Nature **507**(7490): 109-113.

Bao, Y., J. Prescott, C. Yuan, M. Zhang, P. Kraft, A. Babic, V. Morales-Oyarvide, Z. R. Qian, J. E. Buring, B. B. Cochrane, J. M. Gaziano, E. L. Giovannucci, J. E. Manson, K. Ng, S. Ogino, T. E. Rohan, H. D. Sesso, M. J. Stampfer, C. S. Fuchs, I. De Vivo, L. T. Amundadottir and B. M. Wolpin (2017). "Leucocyte telomere length, genetic variants at the TERT gene region and risk of pancreatic cancer." Gut **66**(6): 1116-1122.

Barnhill, R. L. (2014). Circumscribed pigmented lesions composed of basilar melanocytes. Pathology of melanocytic nevi and melanoma. R. L. Barnhill, M. Piepkorn and K. Busam. Berlin, Springer-Verlag.
Bauer, J., P. Buttner, R. Murali, I. Okamoto, N. A. Kolaitis, M. T. Landi, R. A. Scolyer and B. C. Bastian (2011). "BRAF mutations in cutaneous melanoma are independently associated with age, anatomic site of the primary tumor, and the degree of solar elastosis at the primary tumor site." Pigment Cell Melanoma Res **24**(2): 345-351.
Bauer, J., J. A. Curtin, D. Pinkel and B. C. Bastian (2007). "Congenital melanocytic nevi frequently harbor NRAS mutations but no BRAF mutations." J Invest Dermatol **127**(1): 179-182.
Beer, A. G., C. Zenzmaier, M. Schreinlechner, J. Haas, M. F. Dietrich, J. Herz and P. Marschang (2016). "Expression of a recombinant full-length LRP1B receptor in human non-small cell lung cancer cells confirms the postulated growth-suppressing function of this large LDL receptor family member." Oncotarget **7**(42): 68721-68733.
Bevona, C., W. Goggins, T. Quinn, J. Fullerton and H. Tsao (2003). "Cutaneous melanomas associated with nevi." Arch Dermatol **139**(12): 1620-1624; discussion 1624.
Birck, A., V. Ahrenkiel, J. Zeuthen, K. Hou-Jensen and P. Guldberg (2000). "Mutation and allelic loss of the PTEN/MMAC1 gene in primary and metastatic melanoma biopsies." J Invest Dermatol **114**(2): 277-280.
Blair, L. P., J. Cao, M. R. Zou, J. Sayegh and Q. Yan (2011). "Epigenetic Regulation by Lysine Demethylase 5 (KDM5) Enzymes in Cancer." Cancers (Basel) **3**(1): 1383-1404.
Bosenberg, M., V. Muthusamy, D. P. Curley, Z. Wang, C. Hobbs, B. Nelson, C. Nogueira, J. W. Horner, 2nd, R. Depinho and L. Chin (2006). "Characterization of melanocyte-specific inducible Cre recombinase transgenic mice." Genesis **44**(5): 262-267.
Bradford, P. T., A. M. Goldstein, M. L. McMaster and M. A. Tucker (2009). "Acral lentiginous melanoma: incidence and survival patterns in the United States, 1986-2005." Arch Dermatol **145**(4): 427-434.
Brash, D. E. (2015). "UV signature mutations." Photochem Photobiol **91**(1): 15-26.
Brash, D. E., J. A. Rudolph, J. A. Simon, A. Lin, G. J. McKenna, H. P. Baden, A. J. Halperin and J. Ponten (1991). "A role for sunlight in skin cancer: UV-induced p53 mutations in squamous cell carcinoma." Proc Natl Acad Sci U S A **88**(22): 10124-10128.
Brenner, M. and V. J. Hearing (2008). "The protective role of melanin against UV damage in human skin." Photochem Photobiol **84**(3): 539-549.
Breslow, A. (1970). "Thickness, cross-sectional areas and depth of invasion in the prognosis of cutaneous melanoma." Ann Surg **172**(5): 902-908.
Broome Powell, M., P. R. Gause, P. Hyman, J. Gregus, M. Lluria-Prevatt, R. Nagle and G. T. Bowden (1999). "Induction of melanoma in TPras transgenic mice." Carcinogenesis **20**(9): 1747-1753.
Byrne, S. N., N. Spinks and G. M. Halliday (2002). "Ultraviolet a irradiation of C57BL/6 mice suppresses systemic contact hypersensitivity or enhances secondary immunity depending on dose." J Invest Dermatol **119**(4): 858-864.

Cachia, A. R., J. O. Indsto, K. M. McLaren, G. J. Mann and M. J. Arends (2000). "CDKN2A mutation and deletion status in thin and thick primary melanoma." Clin Cancer Res **6**(9): 3511-3515.
Cancer Genome Atlas, N. (2015). "Genomic Classification of Cutaneous Melanoma." Cell **161**(7): 1681-1696.
Celebi, J. T., I. Shendrik, D. N. Silvers and M. Peacocke (2000). "Identification of PTEN mutations in metastatic melanoma specimens." J Med Genet **37**(9): 653-657.
Cerami, E., J. Gao, U. Dogrusoz, B. E. Gross, S. O. Sumer, B. A. Aksoy, A. Jacobsen, C. J. Byrne, M. L. Heuer, E. Larsson, Y. Antipin, B. Reva, A. P. Goldberg, C. Sander and N. Schultz (2012). "The cBio cancer genomics portal: an open platform for exploring multidimensional cancer genomics data." Cancer Discov **2**(5): 401-404.
Chan, J., E. S. Robinson, J. Atencio, Z. Wang, S. Kazianis, L. D. Coletta, R. S. Nairn and J. R. McCarrey (2001). "Characterization of the CDKN2A and ARF genes in UV-induced melanocytic hyperplasias and melanomas of an opossum (Monodelphis domestica)." Mol Carcinog **31**(1): 16-26.
Charbel, C., R. H. Fontaine, G. G. Malouf, A. Picard, N. Kadlub, N. El-Murr, A. How-Kit, X. Su, A. Coulomb-L'Hermine, J. Tost, S. Mourah, S. Aractingi and S. Guegan (2014). "NRAS mutation is the sole recurrent somatic mutation in large congenital melanocytic nevi." J Invest Dermatol **134**(4): 1067-1074.
Chattopadhyay, C., E. A. Grimm and S. E. Woodman (2014). "Simultaneous inhibition of the HGF/MET and Erk1/2 pathways affect uveal melanoma cell growth and migration." PLoS One **9**(2): e83957.
Chaudru, V., K. Laud, M. F. Avril, A. Miniere, A. Chompret, B. Bressac-de Paillerets and F. Demenais (2005). "Melanocortin-1 receptor (MC1R) gene variants and dysplastic nevi modify penetrance of CDKN2A mutations in French melanoma-prone pedigrees." Cancer Epidemiol Biomarkers Prev **14**(10): 2384-2390.
Cheng, Y. P., H. Y. Chiu, T. L. Hsiao, C. H. Hsiao, C. C. Lin and Y. H. Liao (2013). "Scalp melanoma in a woman with LEOPARD syndrome: possible implication of PTPN11 signaling in melanoma pathogenesis." J Am Acad Dermatol **69**(4): e186-187.
Chin, L., J. Pomerantz, D. Polsky, M. Jacobson, C. Cohen, C. Cordon-Cardo, J. W. Horner, 2nd and R. A. DePinho (1997). "Cooperative effects of INK4a and ras in melanoma susceptibility in vivo." Genes Dev **11**(21): 2822-2834.
Ciotti, P., J. P. Struewing, M. Mantelli, A. Chompret, M. F. Avril, P. L. Santi, M. A. Tucker, G. Bianchi-Scarra, B. Bressac-de Paillerets and A. M. Goldstein (2000). "A single genetic origin for the G101W CDKN2A mutation in 20 melanoma-prone families." Am J Hum Genet **67**(2): 311-319.
Clark, W. H., Jr., D. E. Elder, D. t. Guerry, L. E. Braitman, B. J. Trock, D. Schultz, M. Synnestvedt and A. C. Halpern (1989). "Model predicting survival in stage I melanoma based on tumor progression." J Natl Cancer Inst **81**(24): 1893-1904.
Clark, W. H., Jr., D. E. Elder, D. t. Guerry, M. N. Epstein, M. H. Greene and M. Van Horn (1984). "A study of tumor progression: the precursor lesions of superficial spreading and nodular melanoma." Hum Pathol **15**(12): 1147-1165.

Coelho, S. G. and V. J. Hearing (2010). "UVA tanning is involved in the increased incidence of skin cancers in fair-skinned young women." Pigment Cell Melanoma Res **23**(1): 57-63.
Cosgarea, I., S. Ugurel, A. Sucker, E. Livingstone, L. Zimmer, M. Ziemer, J. Utikal, P. Mohr, C. Pfeiffer, C. Pfohler, U. Hillen, S. Horn, D. Schadendorf, K. G. Griewank and A. Roesch (2017). "Targeted next generation sequencing of mucosal melanomas identifies frequent NF1 and RAS mutations." Oncotarget **8**(25): 40683-40692.
Cowin, P. A., J. George, S. Fereday, E. Loehrer, P. Van Loo, C. Cullinane, D. Etemadmoghadam, S. Ftouni, L. Galletta, M. S. Anglesio, J. Hendley, L. Bowes, K. E. Sheppard, E. L. Christie, R. B. Pearson, P. R. Harnett, V. Heinzelmann-Schwarz, M. Friedlander, O. McNally, M. Quinn, P. Campbell, A. deFazio, D. D. Bowtell and S. Australian Ovarian Cancer (2012). "LRP1B deletion in high-grade serous ovarian cancers is associated with acquired chemotherapy resistance to liposomal doxorubicin." Cancer Res **72**(16): 4060-4073.
Crane, L. A., S. T. Mokrohisky, R. P. Dellavalle, N. L. Asdigian, J. Aalborg, T. E. Byers, C. Zeng, A. E. Baron, J. M. Burch and J. G. Morelli (2009). "Melanocytic nevus development in Colorado children born in 1998: a longitudinal study." Arch Dermatol **145**(2): 148-156.
Crawford, N. P., A. Ziogas, D. J. Peel, J. Hess, H. Anton-Culver and K. W. Hunter (2006). "Germline polymorphisms in SIPA1 are associated with metastasis and other indicators of poor prognosis in breast cancer." Breast Cancer Res **8**(2): R16.
Crocetti, E. and P. Carli (2003). "Unexpected reduction of mortality rates from melanoma in males living in central Italy." Eur J Cancer **39**(6): 818-821.
Cubitt, J. J., A. A. Khan, E. Royston, M. Rughani, M. R. Middleton and P. G. Budny (2013). "Melanoma in buckinghamshire: data from the inception of the skin cancer multidisciplinary team." J Skin Cancer **2013**: 843282.
Cymerman, R. M., Y. Shao, K. Wang, Y. Zhang, E. C. Murzaku, L. A. Penn, I. Osman and D. Polsky (2016). "De Novo vs Nevus-Associated Melanomas: Differences in Associations With Prognostic Indicators and Survival." J Natl Cancer Inst **108**(10).
D'Orazio, J. A., T. Nobuhisa, R. Cui, M. Arya, M. Spry, K. Wakamatsu, V. Igras, T. Kunisada, S. R. Granter, E. K. Nishimura, S. Ito and D. E. Fisher (2006). "Topical drug rescue strategy and skin protection based on the role of Mc1r in UV-induced tanning." Nature **443**(7109): 340-344.
Day, C. P., J. Carter, Z. Weaver Ohler, C. Bonomi, R. El Meskini, P. Martin, C. Graff-Cherry, L. Feigenbaum, T. Tuting, T. Van Dyke, M. Hollingshead and G. Merlino (2014). ""Glowing head" mice: a genetic tool enabling reliable preclinical image-based evaluation of cancers in immunocompetent allografts." PLoS One **9**(11): e109956.
Day, C. P., R. Marchalik, G. Merlino and H. Michael (2017). "Mouse models of UV-induced melanoma: genetics, pathology, and clinical relevance." Lab Invest **97**(6): 698-705.
De Fabo, E. C., F. P. Noonan, T. Fears and G. Merlino (2004). "Ultraviolet B but not ultraviolet A radiation initiates melanoma." Cancer Res **64**(18): 6372-6376.

Demierre, M. F., C. Chung, D. R. Miller and A. C. Geller (2005). "Early detection of thick melanomas in the United States: beware of the nodular subtype." Arch Dermatol **141**(6): 745-750.
Dennis, L. K., M. J. Vanbeek, L. E. Beane Freeman, B. J. Smith, D. V. Dawson and J. A. Coughlin (2008). "Sunburns and risk of cutaneous melanoma: does age matter? A comprehensive meta-analysis." Ann Epidemiol **18**(8): 614-627.
Donati, B., P. Dongiovanni, S. Romeo, M. Meroni, M. McCain, L. Miele, S. Petta, S. Maier, C. Rosso, L. De Luca, E. Vanni, S. Grimaudo, R. Romagnoli, F. Colli, F. Ferri, R. M. Mancina, P. Iruzubieta, A. Craxi, A. L. Fracanzani, A. Grieco, S. G. Corradini, A. Aghemo, M. Colombo, G. Soardo, E. Bugianesi, H. Reeves, Q. M. Anstee, S. Fargion and L. Valenti (2017). "MBOAT7 rs641738 variant and hepatocellular carcinoma in non-cirrhotic individuals." Sci Rep **7**(1): 4492.
Dong, J., R. G. Phelps, R. Qiao, S. Yao, O. Benard, Z. Ronai and S. A. Aaronson (2003). "BRAF oncogenic mutations correlate with progression rather than initiation of human melanoma." Cancer Res **63**(14): 3883-3885.
Douki, T., A. Reynaud-Angelin, J. Cadet and E. Sage (2003). "Bipyrimidine photoproducts rather than oxidative lesions are the main type of DNA damage involved in the genotoxic effect of solar UVA radiation." Biochemistry **42**(30): 9221-9226.
Eichmuller, S., C. van der Veen, I. Moll, B. Hermes, U. Hofmann, S. Muller-Rover and R. Paus (1998). "Clusters of perifollicular macrophages in normal murine skin: physiological degeneration of selected hair follicles by programmed organ deletion." J Histochem Cytochem **46**(3): 361-370.
Ekedahl, H., M. Lauss, H. Olsson, K. G. Griewank, D. Schadendorf, C. Ingvar and G. Jonsson (2016). "High TERT promoter mutation frequency in non-acral cutaneous metastatic melanoma." Pigment Cell Melanoma Res **29**(5): 598-600.
El Ghissassi, F., R. Baan, K. Straif, Y. Grosse, B. Secretan, V. Bouvard, L. Benbrahim-Tallaa, N. Guha, C. Freeman, L. Galichet, V. Cogliano and W. H. O. I. A. f. R. o. C. M. W. Group (2009). "A review of human carcinogens--part D: radiation." Lancet Oncol **10**(8): 751-752.
Epstein, J. H., W. L. Epstein and T. Nakai (1967). "Production of melanomas from DMBA-induced "blue nevi" in hairless mice with ultraviolet light." J Natl Cancer Inst **38**(1): 19-30.
Fang, M., F. Xia, M. Mahalingam, C. M. Virbasius, N. Wajapeyee and M. R. Green (2013). "MEN1 is a melanoma tumor suppressor that preserves genomic integrity by stimulating transcription of genes that promote homologous recombination-directed DNA repair." Mol Cell Biol **33**(13): 2635-2647.
Fend, L., S. Rusakiewicz, J. Adam, B. Bastien, A. Caignard, M. Messaoudene, C. Iribarren, I. Cremer, A. Marabelle, C. Borg, M. Semeraro, L. Barraud, J. M. Limacher, A. Eggermont, G. Kroemer and L. Zitvogel (2017). "Prognostic impact of the expression of NCR1 and NCR3 NK cell receptors and PD-L1 on advanced non-small cell lung cancer." Oncoimmunology **6**(1): e1163456.
Field, M. G., C. L. Decatur, S. Kurtenbach, G. Gezgin, P. A. van der Velden, M. J. Jager, K. N. Kozak and J. W. Harbour (2016). "PRAME as an Independent Biomarker for Metastasis in Uveal Melanoma." Clin Cancer Res **22**(5): 1234-1242.

Fiziev, P., K. C. Akdemir, J. P. Miller, E. Z. Keung, N. S. Samant, S. Sharma, C. A. Natale, C. J. Terranova, M. Maitituoheti, S. B. Amin, E. Martinez-Ledesma, M. Dhamdhere, J. B. Axelrad, A. Shah, C. S. Cheng, H. Mahadeshwar, S. Seth, M. C. Barton, A. Protopopov, K. Y. Tsai, M. A. Davies, B. A. Garcia, I. Amit, L. Chin, J. Ernst and K. Rai (2017). "Systematic Epigenomic Analysis Reveals Chromatin States Associated with Melanoma Progression." Cell Rep **19**(4): 875-889.
Florell, S. R., J. Thomas and D. Grossman (2007). "Predominant formation of heavily pigmented dermal melanocytomas resembling 'animal-type' melanomas in hepatocyte growth factor (C57BL/6 x C3H)F1 mice following neonatal UV irradiation." J Cutan Pathol **34**(9): 667-674.
Fredriksson, N. J., K. Elliott, S. Filges, J. Van den Eynden, A. Stahlberg and E. Larsson (2017). "Recurrent promoter mutations in melanoma are defined by an extended context-specific mutational signature." PLoS Genet **13**(5): e1006773.
Friedman, R. J., D. S. Rigel, A. W. Kopf, L. Lieblich, R. Lew, M. N. Harris, D. F. Roses, S. L. Gumport, A. Ragaz, E. Waldo, J. Levine, M. Levenstein, R. Koenig, R. S. Bart and H. Trau (1983). "Favorable prognosis for malignant melanomas associated with acquired melanocytic nevi." Arch Dermatol **119**(6): 455-462.
Fujimoto, A., M. Furuta, Y. Shiraishi, K. Gotoh, Y. Kawakami, K. Arihiro, T. Nakamura, M. Ueno, S. Ariizumi, H. H. Nguyen, D. Shigemizu, T. Abe, K. A. Boroevich, K. Nakano, A. Sasaki, R. Kitada, K. Maejima, Y. Yamamoto, H. Tanaka, T. Shibuya, T. Shibata, H. Ojima, K. Shimada, S. Hayami, Y. Shigekawa, H. Aikata, H. Ohdan, S. Marubashi, T. Yamada, M. Kubo, S. Hirano, O. Ishikawa, M. Yamamoto, H. Yamaue, K. Chayama, S. Miyano, T. Tsunoda and H. Nakagawa (2015). "Whole-genome mutational landscape of liver cancers displaying biliary phenotype reveals hepatitis impact and molecular diversity." Nat Commun **6**: 6120.
Furney, S. J., S. Turajlic, G. Stamp, J. M. Thomas, A. Hayes, D. Strauss, M. Gavrielides, W. Xing, M. Gore, J. Larkin and R. Marais (2014). "The mutational burden of acral melanoma revealed by whole-genome sequencing and comparative analysis." Pigment Cell Melanoma Res **27**(5): 835-838.
Gaffal, E., J. Landsberg, T. Bald, A. Sporleder, J. Kohlmeyer and T. Tuting (2011). "Neonatal UVB exposure accelerates melanoma growth and enhances distant metastases in Hgf-Cdk4(R24C) C57BL/6 mice." Int J Cancer **129**(2): 285-294.
Gaggioli, C., M. Deckert, G. Robert, P. Abbe, M. Batoz, M. U. Ehrengruber, J. P. Ortonne, R. Ballotti and S. Tartare-Deckert (2005). "HGF induces fibronectin matrix synthesis in melanoma cells through MAP kinase-dependent signaling pathway and induction of Egr-1." Oncogene **24**(8): 1423-1433.
Gandini, S., F. Sera, M. S. Cattaruzza, P. Pasquini, O. Picconi, P. Boyle and C. F. Melchi (2005). "Meta-analysis of risk factors for cutaneous melanoma: II. Sun exposure." Eur J Cancer **41**(1): 45-60.
Gao, J., B. A. Aksoy, U. Dogrusoz, G. Dresdner, B. Gross, S. O. Sumer, Y. Sun, A. Jacobsen, R. Sinha, E. Larsson, E. Cerami, C. Sander and N. Schultz (2013). "Integrative analysis of complex cancer genomics and clinical profiles using the cBioPortal." Sci Signal **6**(269): pl1.
Garbe, C. and U. Leiter (2009). "Melanoma epidemiology and trends." Clin Dermatol **27**(1): 3-9.

Garbe, C., G. R. McLeod and P. G. Buettner (2000). "Time trends of cutaneous melanoma in Queensland, Australia and Central Europe." Cancer **89**(6): 1269-1278.
Gessi, M., J. van de Nes, K. Griewank, V. Barresi, M. E. Buckland, J. Kirfel, R. Caltabiano, J. Hammes, L. Lauriola, T. Pietsch and A. Waha (2014). "Absence of TERT promoter mutations in primary melanocytic tumours of the central nervous system." Neuropathol Appl Neurobiol **40**(6): 794-797.
Ghiasvand, R., E. Weiderpass, A. C. Green, E. Lund and M. B. Veierod (2016). "Sunscreen Use and Subsequent Melanoma Risk: A Population-Based Cohort Study." J Clin Oncol **34**(33): 3976-3983.
Glasner, A., H. Ghadially, C. Gur, N. Stanietsky, P. Tsukerman, J. Enk and O. Mandelboim (2012). "Recognition and prevention of tumor metastasis by the NK receptor NKp46/NCR1." J Immunol **188**(6): 2509-2515.
Goel, V. K., A. J. Lazar, C. L. Warneke, M. S. Redston and F. G. Haluska (2006). "Examination of mutations in BRAF, NRAS, and PTEN in primary cutaneous melanoma." J Invest Dermatol **126**(1): 154-160.
Goettsch, C., M. Rauner, K. Sinningen, S. Helas, N. Al-Fakhri, K. Nemeth, C. Hamann, S. Kopprasch, E. Aikawa, S. R. Bornstein, M. Schoppet and L. C. Hofbauer (2011). "The osteoclast-associated receptor (OSCAR) is a novel receptor regulated by oxidized low-density lipoprotein in human endothelial cells." Endocrinology **152**(12): 4915-4926.
Golan, T., A. R. Messer, A. Amitai-Lange, Z. Melamed, R. Ohana, R. E. Bell, O. Kapitansky, G. Lerman, S. Greenberger, M. Khaled, N. Amar, J. Albrengues, C. Gaggioli, P. Gonen, Y. Tabach, D. Sprinzak, R. Shalom-Feuerstein and C. Levy (2015). "Interactions of Melanoma Cells with Distal Keratinocytes Trigger Metastasis via Notch Signaling Inhibition of MITF." Mol Cell **59**(4): 664-676.
Goldstein, A. M. and M. A. Tucker (2013). "Dysplastic nevi and melanoma." Cancer Epidemiol Biomarkers Prev **22**(4): 528-532.
Greenwald, H. S., E. B. Friedman and I. Osman (2012). "Superficial spreading and nodular melanoma are distinct biological entities: a challenge to the linear progression model." Melanoma Res **22**(1): 1-8.
Griewank, K. G., R. Murali, B. Schilling, S. Scholz, A. Sucker, M. Song, D. Susskind, F. Grabellus, L. Zimmer, U. Hillen, K. P. Steuhl, D. Schadendorf, H. Westekemper and M. Zeschnigk (2013). "TERT promoter mutations in ocular melanoma distinguish between conjunctival and uveal tumours." Br J Cancer **109**(2): 497-501.
Gross, A., A. Niemetz-Rahn, A. Nonnenmacher, J. Tucholski, U. Keilholz and A. Fusi (2015). "Expression and activity of EGFR in human cutaneous melanoma cell lines and influence of vemurafenib on the EGFR pathway." Target Oncol **10**(1): 77-84.
Guldberg, P., P. thor Straten, A. Birck, V. Ahrenkiel, A. F. Kirkin and J. Zeuthen (1997). "Disruption of the MMAC1/PTEN gene by deletion or mutation is a frequent event in malignant melanoma." Cancer Res **57**(17): 3660-3663.
Gupta, M. P., A. M. Lane, M. M. DeAngelis, K. Mayne, M. Crabtree, E. S. Gragoudas and I. K. Kim (2015). "Clinical Characteristics of Uveal Melanoma in Patients With Germline BAP1 Mutations." JAMA Ophthalmol **133**(8): 881-887.

Ha, L., T. Ichikawa, M. Anver, R. Dickins, S. Lowe, N. E. Sharpless, P. Krimpenfort, R. A. Depinho, D. C. Bennett, E. V. Sviderskaya and G. Merlino (2007). "ARF functions as a melanoma tumor suppressor by inducing p53-independent senescence." Proc Natl Acad Sci U S A **104**(26): 10968-10973.
Haass, N. K. and M. Herlyn (2005). "Normal human melanocyte homeostasis as a paradigm for understanding melanoma." J Investig Dermatol Symp Proc **10**(2): 153-163.
Hacker, E., H. K. Muller, N. Irwin, B. Gabrielli, D. Lincoln, S. Pavey, M. B. Powell, M. Malumbres, M. Barbacid, N. Hayward and G. Walker (2006). "Spontaneous and UV radiation-induced multiple metastatic melanomas in Cdk4R24C/R24C/TPras mice." Cancer Res **66**(6): 2946-2952.
Halaban, R. and M. Krauthammer (2016). "RASopathy Gene Mutations in Melanoma." J Invest Dermatol **136**(9): 1755-1759.
Halaban, R., J. S. Rubin, Y. Funasaka, M. Cobb, T. Boulton, D. Faletto, E. Rosen, A. Chan, K. Yoko, W. White and et al. (1992). "Met and hepatocyte growth factor/scatter factor signal transduction in normal melanocytes and melanoma cells." Oncogene **7**(11): 2195-2206.
Hamamoto, R., V. Saloura and Y. Nakamura (2015). "Critical roles of non-histone protein lysine methylation in human tumorigenesis." Nat Rev Cancer **15**(2): 110-124.
Harbour, J. W., M. D. Onken, E. D. Roberson, S. Duan, L. Cao, L. A. Worley, M. L. Council, K. A. Matatall, C. Helms and A. M. Bowcock (2010). "Frequent mutation of BAP1 in metastasizing uveal melanomas." Science **330**(6009): 1410-1413.
Harbour, J. W., E. D. Roberson, H. Anbunathan, M. D. Onken, L. A. Worley and A. M. Bowcock (2013). "Recurrent mutations at codon 625 of the splicing factor SF3B1 in uveal melanoma." Nat Genet **45**(2): 133-135.
Harland, M., C. F. Taylor, S. Bass, M. Churchman, J. A. Randerson-Moor, E. A. Holland, G. J. Mann, D. T. Bishop and J. A. Newton Bishop (2005). "Intronic sequence variants of the CDKN2A gene in melanoma pedigrees." Genes Chromosomes Cancer **43**(2): 128-136.
Hartmann, G., T. Prospero, V. Brinkmann, C. Ozcelik, G. Winter, J. Hepple, S. Batley, F. Bladt, M. Sachs, C. Birchmeier, W. Birchmeier and E. Gherardi (1998). "Engineered mutants of HGF/SF with reduced binding to heparan sulphate proteoglycans, decreased clearance and enhanced activity in vivo." Curr Biol **8**(3): 125-134.
Hayward, N. K. (2010). "Mutation spectrum of the first melanoma genome points finger firmly at ultraviolet light as the primary carcinogen." Pigment Cell Melanoma Res **23**(2): 153-154.
Hayward, N. K., J. S. Wilmott, N. Waddell, P. A. Johansson, M. A. Field, K. Nones, A. M. Patch, H. Kakavand, L. B. Alexandrov, H. Burke, V. Jakrot, S. Kazakoff, O. Holmes, C. Leonard, R. Sabarinathan, L. Mularoni, S. Wood, Q. Xu, N. Waddell, V. Tembe, G. M. Pupo, R. De Paoli-Iseppi, R. E. Vilain, P. Shang, L. M. S. Lau, R. A. Dagg, S. J. Schramm, A. Pritchard, K. Dutton-Regester, F. Newell, A. Fitzgerald, C. A. Shang, S. M. Grimmond, H. A. Pickett, J. Y. Yang, J. R. Stretch, A. Behren, R. F. Kefford, P. Hersey, G. V. Long, J. Cebon, M. Shackleton, A. J. Spillane, R. P. M. Saw, N. Lopez-Bigas, J. V. Pearson, J. F. Thompson, R. A. Scolyer and G. J. Mann

(2017). "Whole-genome landscapes of major melanoma subtypes." Nature **545**(7653): 175-180.
Helsing, P., D. A. Nymoen, S. Ariansen, S. J. Steine, L. Maehle, S. Aamdal, F. Langmark, M. Loeb, L. A. Akslen, A. Molven and P. A. Andresen (2008). "Population-based prevalence of CDKN2A and CDK4 mutations in patients with multiple primary melanomas." Genes Chromosomes Cancer **47**(2): 175-184.
Hennessy, A., C. Oh, B. Diffey, K. Wakamatsu, S. Ito and J. Rees (2005). "Eumelanin and pheomelanin concentrations in human epidermis before and after UVB irradiation." Pigment Cell Res **18**(3): 220-223.
Herrling, T., K. Jung and J. Fuchs (2006). "Measurements of UV-generated free radicals/reactive oxygen species (ROS) in skin." Spectrochim Acta A Mol Biomol Spectrosc **63**(4): 840-845.
Hill, H. Z. and G. J. Hill (2000). "UVA, pheomelanin and the carcinogenesis of melanoma." Pigment Cell Res **13 Suppl 8**: 140-144.
Hintzsche, J. D., N. T. Gorden, C. M. Amato, J. Kim, K. E. Wuensch, S. E. Robinson, A. J. Applegate, K. L. Couts, T. M. Medina, K. R. Wells, J. A. Wisell, M. D. McCarter, N. F. Box, Y. G. Shellman, R. C. Gonzalez, K. D. Lewis, J. J. Tentler, A. C. Tan and W. A. Robinson (2017). "Whole-exome sequencing identifies recurrent SF3B1 R625 mutation and comutation of NF1 and KIT in mucosal melanoma." Melanoma Res **27**(3): 189-199.
Hirobe, T. (1984). "Histochemical survey of the distribution of the epidermal melanoblasts and melanocytes in the mouse during fetal and postnatal periods." Anat Rec **208**(4): 589-594.
Hodi, F. S., S. J. O'Day, D. F. McDermott, R. W. Weber, J. A. Sosman, J. B. Haanen, R. Gonzalez, C. Robert, D. Schadendorf, J. C. Hassel, W. Akerley, A. J. van den Eertwegh, J. Lutzky, P. Lorigan, J. M. Vaubel, G. P. Linette, D. Hogg, C. H. Ottensmeier, C. Lebbe, C. Peschel, I. Quirt, J. I. Clark, J. D. Wolchok, J. S. Weber, J. Tian, M. J. Yellin, G. M. Nichol, A. Hoos and W. J. Urba (2010). "Improved survival with ipilimumab in patients with metastatic melanoma." N Engl J Med **363**(8): 711-723.
Hodis, E., I. R. Watson, G. V. Kryukov, S. T. Arold, M. Imielinski, J. P. Theurillat, E. Nickerson, D. Auclair, L. R. Li, C. Place, D. DiCara, A. H. Ramos, M. S. Lawrence, K. Cibulskis, A. Sivachenko, D. Voet, G. Saksena, N. Stransky, R. C. Onofrio, W. Winckler, K. Ardlie, N. Wagle, J. Wargo, K. Chong, D. L. Morton, K. Stemke-Hale, G. Chen, M. Noble, M. Meyerson, J. E. Ladbury, M. A. Davies, J. E. Gershenwald, S. N. Wagner, D. S. B. Hoon, D. Schadendorf, E. S. Lander, S. B. Gabriel, G. Getz, L. A. Garraway and L. Chin (2012). "A Landscape of Driver Mutations in Melanoma." Cell **150**(2): 251-263.
Horn, S., A. Figl, P. S. Rachakonda, C. Fischer, A. Sucker, A. Gast, S. Kadel, I. Moll, E. Nagore, K. Hemminki, D. Schadendorf and R. Kumar (2013). "TERT promoter mutations in familial and sporadic melanoma." Science **339**(6122): 959-961.
Hsieh, S. M., M. P. Look, A. M. Sieuwerts, J. A. Foekens and K. W. Hunter (2009). "Distinct inherited metastasis susceptibility exists for different breast cancer subtypes: a prognosis study." Breast Cancer Res **11**(5): R75.

Hsueh, E. C., R. K. Gupta, R. Yee, Z. C. Leopoldo, K. Qi and D. L. Morton (2000). "Does endogenous immune response determine the outcome of surgical therapy for metastatic melanoma?" Ann Surg Oncol **7**(3): 232-238.
Huang, F. W., E. Hodis, M. J. Xu, G. V. Kryukov, L. Chin and L. A. Garraway (2013). "Highly recurrent TERT promoter mutations in human melanoma." Science **339**(6122): 957-959.
Huang, J. L., O. Urtatiz and C. D. Van Raamsdonk (2015). "Oncogenic G Protein GNAQ Induces Uveal Melanoma and Intravasation in Mice." Cancer Res **75**(16): 3384-3397.
Huang, X., Z. Shi, W. Wang, J. Bai, Z. Chen, J. Xu, D. Zhang and S. Fu (2007). "Identification and characterization of a novel protein ISOC2 that interacts with p16INK4a." Biochem Biophys Res Commun **361**(2): 287-293.
Hulsen, T., J. de Vlieg and W. Alkema (2008). "BioVenn - a web application for the comparison and visualization of biological lists using area-proportional Venn diagrams." BMC Genomics **9**: 488.
Husain, Z., M. A. Pathak, T. Flotte and M. M. Wick (1991). "Role of ultraviolet radiation in the induction of melanocytic tumors in hairless mice following 7,12-dimethylbenz(a)anthracene application and ultraviolet irradiation." Cancer Res **51**(18): 4964-4970.
Imokawa, G. (2004). "Autocrine and paracrine regulation of melanocytes in human skin and in pigmentary disorders." Pigment Cell Res **17**(2): 96-110.
Jiang, W., H. N. Ananthaswamy, H. K. Muller and M. L. Kripke (1999). "p53 protects against skin cancer induction by UV-B radiation." Oncogene **18**(29): 4247-4253.
Kaddu, S., J. Smolle, P. Zenahlik, R. Hofmann-Wellenhof and H. Kerl (2002). "Melanoma with benign melanocytic naevus components: reappraisal of clinicopathological features and prognosis." Melanoma Res **12**(3): 271-278.
Kaidbey, K. H., P. P. Agin, R. M. Sayre and A. M. Kligman (1979). "Photoprotection by melanin--a comparison of black and Caucasian skin." J Am Acad Dermatol **1**(3): 249-260.
Kalirai, H., A. Dodson, S. Faqir, B. E. Damato and S. E. Coupland (2014). "Lack of BAP1 protein expression in uveal melanoma is associated with increased metastatic risk and has utility in routine prognostic testing." Br J Cancer **111**(7): 1373-1380.
Kang, X., J. Kim, M. Deng, S. John, H. Chen, G. Wu, H. Phan and C. C. Zhang (2016). "Inhibitory leukocyte immunoglobulin-like receptors: Immune checkpoint proteins and tumor sustaining factors." Cell Cycle **15**(1): 25-40.
Kannan, K., N. E. Sharpless, J. Xu, R. C. O'Hagan, M. Bosenberg and L. Chin (2003). "Components of the Rb pathway are critical targets of UV mutagenesis in a murine melanoma model." Proc Natl Acad Sci U S A **100**(3): 1221-1225.
Karimkhani, C., A. C. Green, T. Nijsten, M. A. Weinstock, R. P. Dellavalle, M. Naghavi and C. Fitzmaurice (2017). "The global burden of melanoma: results from the Global Burden of Disease Study 2015." Br J Dermatol **177**(1): 134-140.
Karram, S., M. Novy, M. Saroufim, A. Loya, S. Taraif, M. A. Houreih, B. Rauscher, R. H. Habib, C. Oberkanins and I. Khalifeh (2013). "Predictors of BRAF mutation in melanocytic nevi: analysis across regions with different UV radiation exposure." Am J Dermatopathol **35**(4): 412-418.

Kaymaz, Y., C. I. Oduor, H. Yu, J. A. Otieno, J. M. Ong'echa, A. M. Moormann and J. A. Bailey (2017). "Comprehensive Transcriptome and Mutational Profiling of Endemic Burkitt Lymphoma Reveals EBV Type-Specific Differences." Mol Cancer Res **15**(5): 563-576.
Keane, T. M., L. Goodstadt, P. Danecek, M. A. White, K. Wong, B. Yalcin, A. Heger, A. Agam, G. Slater, M. Goodson, N. A. Furlotte, E. Eskin, C. Nellaker, H. Whitley, J. Cleak, D. Janowitz, P. Hernandez-Pliego, A. Edwards, T. G. Belgard, P. L. Oliver, R. E. McIntyre, A. Bhomra, J. Nicod, X. Gan, W. Yuan, L. van der Weyden, C. A. Steward, S. Bala, J. Stalker, R. Mott, R. Durbin, I. J. Jackson, A. Czechanski, J. A. Guerra-Assuncao, L. R. Donahue, L. G. Reinholdt, B. A. Payseur, C. P. Ponting, E. Birney, J. Flint and D. J. Adams (2011). "Mouse genomic variation and its effect on phenotypes and gene regulation." Nature **477**(7364): 289-294.
Kelsall, S. R. and B. Mintz (1998). "Metastatic cutaneous melanoma promoted by ultraviolet radiation in mice with transgene-initiated low melanoma susceptibility." Cancer Res **58**(18): 4061-4065.
Kim, H. E., D. G. Kim, K. J. Lee, J. G. Son, M. Y. Song, Y. M. Park, J. J. Kim, S. W. Cho, S. G. Chi, H. S. Cheong, H. D. Shin, S. W. Lee and J. K. Lee (2012). "Frequent amplification of CENPF, GMNN and CDK13 genes in hepatocellular carcinomas." PLoS One **7**(8): e43223.
Kinsler, V. A., A. C. Thomas, M. Ishida, N. W. Bulstrode, S. Loughlin, S. Hing, J. Chalker, K. McKenzie, S. Abu-Amero, O. Slater, E. Chanudet, R. Palmer, D. Morrogh, P. Stanier, E. Healy, N. J. Sebire and G. E. Moore (2013). "Multiple congenital melanocytic nevi and neurocutaneous melanosis are caused by postzygotic mutations in codon 61 of NRAS." J Invest Dermatol **133**(9): 2229-2236.
Kligman, L. H., F. J. Akin and A. M. Kligman (1985). "The contributions of UVA and UVB to connective tissue damage in hairless mice." J Invest Dermatol **84**(4): 272-276.
Klug, H. L., J. A. Tooze, C. Graff-Cherry, M. R. Anver, F. P. Noonan, T. R. Fears, M. A. Tucker, E. C. De Fabo and G. Merlino (2010). "Sunscreen prevention of melanoma in man and mouse." Pigment Cell Melanoma Res **23**(6): 835-837.
Kobayashi, N., A. Nakagawa, T. Muramatsu, Y. Yamashina, T. Shirai, M. W. Hashimoto, Y. Ishigaki, T. Ohnishi and T. Mori (1998). "Supranuclear melanin caps reduce ultraviolet induced DNA photoproducts in human epidermis." J Invest Dermatol **110**(5): 806-810.
Koopmans, A. E., K. Ober, H. J. Dubbink, D. Paridaens, N. C. Naus, S. Belunek, B. Krist, E. Post, E. C. Zwarthoff, A. de Klein, R. M. Verdijk and G. Rotterdam Ocular Melanoma Study (2014). "Prevalence and implications of TERT promoter mutation in uveal and conjunctival melanoma and in benign and premalignant conjunctival melanocytic lesions." Invest Ophthalmol Vis Sci **55**(9): 6024-6030.
Koopmans, A. E., R. M. Verdijk, R. W. Brouwer, T. P. van den Bosch, M. M. van den Berg, J. Vaarwater, C. E. Kockx, D. Paridaens, N. C. Naus, M. Nellist, I. W. F. van, E. Kilic and A. de Klein (2014). "Clinical significance of immunohistochemistry for detection of BAP1 mutations in uveal melanoma." Mod Pathol **27**(10): 1321-1330.

Kos, L., A. Aronzon, H. Takayama, F. Maina, C. Ponzetto, G. Merlino and W. Pavan (1999). "Hepatocyte growth factor/scatter factor-MET signaling in neural crest-derived melanocyte development." Pigment Cell Res **12**(1): 13-21.
Krauthammer, M., Y. Kong, A. Bacchiocchi, P. Evans, N. Pornputtapong, C. Wu, J. P. McCusker, S. Ma, E. Cheng, R. Straub, M. Serin, M. Bosenberg, S. Ariyan, D. Narayan, M. Sznol, H. M. Kluger, S. Mane, J. Schlessinger, R. P. Lifton and R. Halaban (2015). "Exome sequencing identifies recurrent mutations in NF1 and RASopathy genes in sun-exposed melanomas." Nat Genet **47**(9): 996-1002.
Kulichova, D., J. Danova, C. Kunte, T. Ruzicka and A. M. Celko (2014). "Risk factors for malignant melanoma and preventive methods." Cutis **94**(5): 241-248.
Kumar, R., S. Angelini, E. Snellman and K. Hemminki (2004). "BRAF mutations are common somatic events in melanocytic nevi." J Invest Dermatol **122**(2): 342-348.
Labat-Robert, J., A. Fourtanier, B. Boyer-Lafargue and L. Robert (2000). "Age dependent increase of elastase type protease activity in mouse skin. Effect of UV-irradiation." J Photochem Photobiol B **57**(2-3): 113-118.
Laud, K., C. Marian, M. F. Avril, M. Barrois, A. Chompret, A. M. Goldstein, M. A. Tucker, P. A. Clark, G. Peters, V. Chaudru, F. Demenais, A. Spatz, M. W. Smith, G. M. Lenoir, B. Bressac-de Paillerets and G. French Hereditary Melanoma Study (2006). "Comprehensive analysis of CDKN2A (p16INK4A/p14ARF) and CDKN2B genes in 53 melanoma index cases considered to be at heightened risk of melanoma." J Med Genet **43**(1): 39-47.
Lawrence, M. S., P. Stojanov, P. Polak, G. V. Kryukov, K. Cibulskis, A. Sivachenko, S. L. Carter, C. Stewart, C. H. Mermel, S. A. Roberts, A. Kiezun, P. S. Hammerman, A. McKenna, Y. Drier, L. H. Zou, A. H. Ramos, T. J. Pugh, N. Stransky, E. Helman, J. Kim, C. Sougnez, L. Ambrogio, E. Nickerson, E. Shefler, M. L. Cortes, D. Auclair, G. Saksena, D. Voet, M. Noble, D. DiCara, P. Lin, L. Lichtenstein, D. I. Heiman, T. Fennell, M. Imielinski, B. Hernandez, E. Hodis, S. Baca, A. M. Dulak, J. Lohr, D. A. Landau, C. J. Wu, J. Melendez-Zajgla, A. Hidalgo-Miranda, A. Koren, S. A. McCarroll, J. Mora, R. S. Lee, B. Crompton, R. Onofrio, M. Parkin, W. Winckler, K. Ardlie, S. B. Gabriel, C. W. M. Roberts, J. A. Biegel, K. Stegmaier, A. J. Bass, L. A. Garraway, M. Meyerson, T. R. Golub, D. A. Gordenin, S. Sunyaev, E. S. Lander and G. Getz (2013). "Mutational heterogeneity in cancer and the search for new cancer-associated genes." Nature **499**(7457): 214-218.
Lee, J. J., L. M. Sholl, N. I. Lindeman, S. R. Granter, A. C. Laga, P. Shivdasani, G. Chin, J. J. Luke, P. A. Ott, F. S. Hodi, M. C. Mihm, Jr., J. Y. Lin, A. E. Werchniak, H. A. Haynes, N. Bailey, R. Liu, G. F. Murphy and C. G. Lian (2015). "Targeted next-generation sequencing reveals high frequency of mutations in epigenetic regulators across treatment-naive patient melanomas." Clin Epigenetics **7**: 59.
Lee, L., S. Sharma, B. Morgan, P. Allegrini, C. Schnell, J. Brueggen, R. Cozens, M. Horsfield, C. Guenther, W. P. Steward, J. Drevs, D. Lebwohl, J. Wood and P. M. McSheehy (2006). "Biomarkers for assessment of pharmacologic activity for a vascular endothelial growth factor (VEGF) receptor inhibitor, PTK787/ZK 222584 (PTK/ZK): translation of biological activity in a mouse melanoma metastasis model to phase I studies in patients with advanced colorectal cancer with liver metastases." Cancer Chemother Pharmacol **57**(6): 761-771.

Leonard, M. K., N. Pamidimukkala, G. S. Puts, D. E. Snyder, A. T. Slominski and D. M. Kaetzel (2017). "The HGF/SF Mouse Model of UV-Induced Melanoma as an In Vivo Sensor for Metastasis-Regulating Gene." Int J Mol Sci **18**(8).
Leyvraz, S., V. Spataro, J. Bauer, S. Pampallona, R. Salmon, T. Dorval, R. Meuli, M. Gillet, F. Lejeune and L. Zografos (1997). "Treatment of ocular melanoma metastatic to the liver by hepatic arterial chemotherapy." J Clin Oncol **15**(7): 2589-2595.
Li, G., K. Satyamoorthy and M. Herlyn (2001). "N-cadherin-mediated intercellular interactions promote survival and migration of melanoma cells." Cancer Res **61**(9): 3819-3825.
Li, G., K. Satyamoorthy, F. Meier, C. Berking, T. Bogenrieder and M. Herlyn (2003). "Function and regulation of melanoma-stromal fibroblast interactions: when seeds meet soil." Oncogene **22**(20): 3162-3171.
Li, X., W. K. Wu, R. Xing, S. H. Wong, Y. Liu, X. Fang, Y. Zhang, M. Wang, J. Wang, L. Li, Y. Zhou, S. Tang, S. Peng, K. Qiu, L. Chen, K. Chen, H. Yang, W. Zhang, M. T. Chan, Y. Lu, J. J. Sung and J. Yu (2016). "Distinct Subtypes of Gastric Cancer Defined by Molecular Characterization Include Novel Mutational Signatures with Prognostic Capability." Cancer Res **76**(7): 1724-1732.
Liang, Q., Y. Chen, K. Yu, C. Chen, S. Zhang, A. Wang, W. Wang, H. Wu, X. Liu, B. Wang, L. Wang, Z. Hu, W. Wang, T. Ren, S. Zhang, Q. Liu, C. H. Yun and J. Liu (2017). "Discovery of N-(3-(5-((3-acrylamido-4-(morpholine-4-carbonyl)phenyl)amino)-1-methyl-6-oxo-1,6- dihydropyridin-3-yl)-2-methylphenyl)-4-(tert-butyl)benzamide (CHMFL-BTK-01) as a highly selective irreversible Bruton's tyrosine kinase (BTK) inhibitor." Eur J Med Chem **131**: 107-125.
Lifsted, T., T. Le Voyer, M. Williams, W. Muller, A. Klein-Szanto, K. H. Buetow and K. W. Hunter (1998). "Identification of inbred mouse strains harboring genetic modifiers of mammary tumor age of onset and metastatic progression." Int J Cancer **77**(4): 640-644.
Lin, W. M., S. Luo, A. Muzikansky, A. Z. Lobo, K. K. Tanabe, A. J. Sober, A. B. Cosimi, H. Tsao and L. M. Duncan (2015). "Outcome of patients with de novo versus nevus-associated melanoma." J Am Acad Dermatol **72**(1): 54-58.
Liu, F., Y. He, Q. Cao, N. Liu and W. Zhang (2016). "TBL1XR1 Is Highly Expressed in Gastric Cancer and Predicts Poor Prognosis." Dis Markers **2016**: 2436518.
Liu, H., Y. Xu, Q. Zhang, K. Li, D. Wang, S. Li, S. Ning, H. Yang, W. Shi, Z. Liu and Y. Chen (2017). "Correlations between TBL1XR1 and recurrence of colorectal cancer." Sci Rep **7**: 44275.
Liu, X. and J. Secombe (2015). "The Histone Demethylase KDM5 Activates Gene Expression by Recognizing Chromatin Context through Its PHD Reader Motif." Cell Rep **13**(10): 2219-2231.
Liu, Y., V. R. Kempf, J. B. Nofsinger, E. E. Weinert, M. Rudnicki, K. Wakamatsu, S. Ito and J. D. Simon (2003). "Comparison of the structural and physical properties of human hair eumelanin following enzymatic or acid/base extraction." Pigment Cell Res **16**(4): 355-365.
Liu, Y. F., A. Yang, W. Liu, C. Wang, M. Wang, L. Zhang, D. Wang, J. F. Dong and M. Li (2015). "NME2 reduces proliferation, migration and invasion of gastric cancer cells to limit metastasis." PLoS One **10**(2): e0115968.

Loser, K. and S. Beissert (2009). "Regulation of cutaneous immunity by the environment: an important role for UV irradiation and vitamin D." Int Immunopharmacol **9**(5): 587-589.
Luo, C., J. Sheng, M. G. Hu, F. G. Haluska, R. Cui, Z. Xu, P. N. Tsichlis, G. F. Hu and P. W. Hinds (2013). "Loss of ARF sensitizes transgenic BRAFV600E mice to UV-induced melanoma via suppression of XPC." Cancer Res **73**(14): 4337-4348.
Ma, D. and J. Y. Niederkorn (1998). "Role of epidermal growth factor receptor in the metastasis of intraocular melanomas." Invest Ophthalmol Vis Sci **39**(7): 1067-1075.
Ma, M. and N. Yu (2017). "Over-Expression of TBL1XR1 Indicates Poor Prognosis of Serous Epithelial Ovarian Cancer." Tohoku J Exp Med **241**(3): 239-247.
MacKie, R. M., J. English, T. C. Aitchison, C. P. Fitzsimons and P. Wilson (1985). "The number and distribution of benign pigmented moles (melanocytic naevi) in a healthy British population." Br J Dermatol **113**(2): 167-174.
Madigan, L. M. and H. W. Lim (2016). "Tanning beds: Impact on health, and recent regulations." Clin Dermatol **34**(5): 640-648.
Mantelli, M., M. Barile, P. Ciotti, P. Ghiorzo, F. Lantieri, L. Pastorino, C. Catricala, G. D. Torre, U. Folco, P. Grammatico, L. Padovani, B. Pasini, D. Rovini, P. Queirolo, M. L. Rainero, P. L. Santi, R. M. Sertoli, A. M. Goldstein, G. Bianchi-Scarra, D. Societa Italiana and D. Gruppo Italiano Studi Epidemiologici in (2002). "High prevalence of the G101W germline mutation in the CDKN2A (P16(ink4a)) gene in 62 Italian malignant melanoma families." Am J Med Genet **107**(3): 214-221.
Mao, Z., C. Liu, X. Lin, B. Sun and C. Su (2018). "PPP2R5A: A multirole protein phosphatase subunit in regulating cancer development." Cancer Lett **414**: 222-229.
Markowitz, S. D., N. L. Nock, S. L. Schmit, Z. K. Stadler, V. Joseph, L. Zhang, J. E. Willis, P. Scacheri, M. Veigl, M. D. Adams, L. Raskin, J. F. Sullivan, K. Stratton, J. Shia, N. Ellis, H. S. Rennert, C. Manschreck, L. Li, K. Offit, R. C. Elston, G. Rennert and S. B. Gruber (2016). "A Germline Variant on Chromosome 4q31.1 Associates with Susceptibility to Developing Colon Cancer Metastasis." PLoS One **11**(1): e0146435.
McCorkle, J. R., M. K. Leonard, S. D. Kraner, E. M. Blalock, D. Ma, S. G. Zimmer and D. M. Kaetzel (2014). "The metastasis suppressor NME1 regulates expression of genes linked to metastasis and patient outcome in melanoma and breast carcinoma." Cancer Genomics Proteomics **11**(4): 175-194.
McFadden, D. G., K. Politi, A. Bhutkar, F. K. Chen, X. Song, M. Pirun, P. M. Santiago, C. Kim-Kiselak, J. T. Platt, E. Lee, E. Hodges, A. P. Rosebrock, R. T. Bronson, N. D. Socci, G. J. Hannon, T. Jacks and H. Varmus (2016). "Mutational landscape of EGFR-, MYC-, and Kras-driven genetically engineered mouse models of lung adenocarcinoma." Proc Natl Acad Sci U S A **113**(42): E6409-E6417.
Meinhardt, M., R. Krebs, A. Anders, U. Heinrich and H. Tronnier (2008). "Wavelength-dependent penetration depths of ultraviolet radiation in human skin." J Biomed Opt **13**(4): 044030.
Miao, Y., R. Wang, H. Ju, G. Ren, W. Guo and J. Lyu (2015). "TERT promoter mutation is absent in oral mucosal melanoma." Oral Oncol **51**(8): e65-66.
Mikhail, M., E. Velazquez, R. Shapiro, R. Berman, A. Pavlick, L. Sorhaindo, J. Spira, C. Mir, K. S. Panageas, D. Polsky and I. Osman (2005). "PTEN expression in

melanoma: relationship with patient survival, Bcl-2 expression, and proliferation." Clin Cancer Res **11**(14): 5153-5157.
Mitchell, A., C. Rentero, Y. Endoh, K. Hsu, K. Gaus, C. Geczy, H. P. McNeil, L. Borges and N. Tedla (2008). "LILRA5 is expressed by synovial tissue macrophages in rheumatoid arthritis, selectively induces pro-inflammatory cytokines and IL-10 and is regulated by TNF-alpha, IL-10 and IFN-gamma." Eur J Immunol **38**(12): 3459-3473.
Mitra, D., X. Luo, A. Morgan, J. Wang, M. P. Hoang, J. Lo, C. R. Guerrero, J. K. Lennerz, M. C. Mihm, J. A. Wargo, K. C. Robinson, S. P. Devi, J. C. Vanover, J. A. D'Orazio, M. McMahon, M. W. Bosenberg, K. M. Haigis, D. A. Haber, Y. Wang and D. E. Fisher (2012). "An ultraviolet-radiation-independent pathway to melanoma carcinogenesis in the red hair/fair skin background." Nature **491**(7424): 449-453.
Mitton, K. P., P. K. Swain, H. Khanna, M. Dowd, I. J. Apel and A. Swaroop (2003). "Interaction of retinal bZIP transcription factor NRL with Flt3-interacting zinc-finger protein Fiz1: possible role of Fiz1 as a transcriptional repressor." Hum Mol Genet **12**(4): 365-373.
Montagna, W. and K. Carlisle (1991). "The architecture of black and white facial skin." J Am Acad Dermatol **24**(6 Pt 1): 929-937.
Monzon, J., L. Liu, H. Brill, A. M. Goldstein, M. A. Tucker, L. From, J. McLaughlin, D. Hogg and N. J. Lassam (1998). "CDKN2A mutations in multiple primary melanomas." N Engl J Med **338**(13): 879-887.
Moon, K. R., Y. D. Choi, J. M. Kim, S. Jin, M. H. Shin, H. J. Shim, J. B. Lee and S. J. Yun (2018). "Genetic Alterations in Primary Acral Melanoma and Acral Melanocytic Nevus in Korea: Common Mutated Genes Show Distinct Cytomorphological Features." J Invest Dermatol **138**(4): 933-945.
Moore, A. R., E. Ceraudo, J. J. Sher, Y. X. Guan, A. N. Shoushtari, M. T. Chang, J. Q. Zhang, E. G. Walczak, M. A. Kazmi, B. S. Taylor, T. Huber, P. Chi, T. P. Sakmar and Y. Chen (2016). "Recurrent activating mutations of G-protein-coupled receptor CYSLTR2 in uveal melanoma." Nature Genetics **48**(6): 675-+.
Moore, A. R., L. Ran, Y. Guan, J. J. Sher, T. D. Hitchman, J. Q. Zhang, C. Hwang, E. G. Walzak, A. N. Shoushtari, S. Monette, R. Murali, T. Wiesner, K. G. Griewank, P. Chi and Y. Chen (2018). "GNA11 Q209L Mouse Model Reveals RasGRP3 as an Essential Signaling Node in Uveal Melanoma." Cell Rep **22**(9): 2455-2468.
Mrschtik, M. and K. M. Ryan (2016). "Another DRAM involved in autophagy and cell death." Autophagy **12**(3): 603-605.
Murali, R., T. Wiesner and R. A. Scolyer (2013). "Tumours associated with BAP1 mutations." Pathology **45**(2): 116-126.
Nairn, R. S., S. Kazianis, L. Della Coletta, D. Trono, A. P. Butler, R. B. Walter and D. C. Morizot (2001). "Genetic analysis of susceptibility to spontaneous and UV-induced carcinogenesis in Xiphophorus hybrid fish." Mar Biotechnol (NY) **3**(Supplement 1): S24-36.
Nakayama, A., M. T. Nguyen, C. C. Chen, K. Opdecamp, C. A. Hodgkinson and H. Arnheiter (1998). "Mutations in microphthalmia, the mouse homolog of the human deafness gene MITF, affect neuroepithelial and neural crest-derived melanocytes differently." Mech Dev **70**(1-2): 155-166.

Natarajan, V. T., P. Ganju, A. Ramkumar, R. Grover and R. S. Gokhale (2014). "Multifaceted pathways protect human skin from UV radiation." Nat Chem Biol **10**(7): 542-551.
Newton-Bishop, J. A., Y. M. Chang, M. M. Iles, J. C. Taylor, B. Bakker, M. Chan, S. Leake, B. Karpavicius, S. Haynes, E. Fitzgibbon, F. Elliott, P. A. Kanetsky, M. Harland, J. H. Barrett and D. T. Bishop (2010). "Melanocytic nevi, nevus genes, and melanoma risk in a large case-control study in the United Kingdom." Cancer Epidemiol Biomarkers Prev **19**(8): 2043-2054.
Nissan, M. H., C. A. Pratilas, A. M. Jones, R. Ramirez, H. Won, C. Liu, S. Tiwari, L. Kong, A. J. Hanrahan, Z. Yao, T. Merghoub, A. Ribas, P. B. Chapman, R. Yaeger, B. S. Taylor, N. Schultz, M. F. Berger, N. Rosen and D. B. Solit (2014). "Loss of NF1 in cutaneous melanoma is associated with RAS activation and MEK dependence." Cancer Res **74**(8): 2340-2350.
Njauw, C. N., I. Kim, A. Piris, M. Gabree, M. Taylor, A. M. Lane, M. M. DeAngelis, E. Gragoudas, L. M. Duncan and H. Tsao (2012). "Germline BAP1 inactivation is preferentially associated with metastatic ocular melanoma and cutaneous-ocular melanoma families." PLoS One **7**(4): e35295.
Noonan, F. P., J. Dudek, G. Merlino and E. C. De Fabo (2003). "Animal models of melanoma: an HGF/SF transgenic mouse model may facilitate experimental access to UV initiating events." Pigment Cell Res **16**(1): 16-25.
Noonan, F. P., T. Otsuka, S. Bang, M. R. Anver and G. Merlino (2000). "Accelerated ultraviolet radiation-induced carcinogenesis in hepatocyte growth factor/scatter factor transgenic mice." Cancer Res **60**(14): 3738-3743.
Noonan, F. P., J. A. Recio, H. Takayama, P. Duray, M. R. Anver, W. L. Rush, E. C. De Fabo and G. Merlino (2001). "Neonatal sunburn and melanoma in mice." Nature **413**(6853): 271-272.
Noonan, F. P., M. R. Zaidi, A. Wolnicka-Glubisz, M. R. Anver, J. Bahn, A. Wielgus, J. Cadet, T. Douki, S. Mouret, M. A. Tucker, A. Popratiloff, G. Merlino and E. C. De Fabo (2012). "Melanoma induction by ultraviolet A but not ultraviolet B radiation requires melanin pigment." Nat Commun **3**: 884.
Oba-Shinjo, S. M., O. L. Caballero, A. A. Jungbluth, S. Rosemberg, L. J. Old, A. J. Simpson and S. K. Marie (2008). "Cancer-testis (CT) antigen expression in medulloblastoma." Cancer Immun **8**: 7.
Oike, T., H. Ogiwara, T. Nakano, J. Yokota and T. Kohno (2013). "Inactivating mutations in SWI/SNF chromatin remodeling genes in human cancer." Jpn J Clin Oncol **43**(9): 849-855.
Oliveria, S. A., M. Saraiya, A. C. Geller, M. K. Heneghan and C. Jorgensen (2006). "Sun exposure and risk of melanoma." Arch Dis Child **91**(2): 131-138.
Otsuka, T., H. Takayama, R. Sharp, G. Celli, W. J. LaRochelle, D. P. Bottaro, N. Ellmore, W. Vieira, J. W. Owens, M. Anver and G. Merlino (1998). "c-Met autocrine activation induces development of malignant melanoma and acquisition of the metastatic phenotype." Cancer Research **58**(22): 5157-5167.
Pampena, R., A. Kyrgidis, A. Lallas, E. Moscarella, G. Argenziano and C. Longo (2017). "A meta-analysis of nevus-associated melanoma: Prevalence and practical implications." J Am Acad Dermatol **77**(5): 938-945.e934.

Pampena, R., G. Pellacani and C. Longo (2018). "Nevus-Associated Melanoma: Patient Phenotype and Potential Biological Implications." J Invest Dermatol **138**(8): 1696-1698.
Pandeya, N., M. Kvaskoff, C. M. Olsen, A. C. Green, S. Perry, C. Baxter, M. B. Davis, R. Mortimore, L. Westacott, D. Wood, J. Triscott, R. Williamson and D. C. Whiteman (2018). "Factors Related to Nevus-Associated Cutaneous Melanoma: A Case-Case Study." J Invest Dermatol **138**(8): 1816-1824.
Papp, T., H. Pemsel, R. Zimmermann, R. Bastrop, D. G. Weiss and D. Schiffmann (1999). "Mutational analysis of the N-ras, p53, p16INK4a, CDK4, and MC1R genes in human congenital melanocytic naevi." J Med Genet **36**(8): 610-614.
Pasparakis, M., I. Haase and F. O. Nestle (2014). "Mechanisms regulating skin immunity and inflammation." Nat Rev Immunol **14**(5): 289-301.
Patel, S. P., D. W. Kim, C. L. Lacey and P. Hwu (2016). "GNA11 Mutation in a Patient With Cutaneous Origin Melanoma: A Case Report." Medicine (Baltimore) **95**(4): e2336.
Pathak, M. A. (1991). "Ultraviolet radiation and the development of non-melanoma and melanoma skin cancer: clinical and experimental evidence." Skin Pharmacol **4 Suppl 1**: 85-94.
Pearse, A. D., S. A. Gaskell and R. Marks (1987). "Epidermal changes in human skin following irradiation with either UVB or UVA." J Invest Dermatol **88**(1): 83-87.
Perkins, A. and R. L. Duffy (2015). "Atypical moles: diagnosis and management." Am Fam Physician **91**(11): 762-767.
Piao, J., L. Chen, T. Jin, M. Xu, C. Quan and Z. Lin (2018). "Paip1 affects breast cancer cell growth and represents a novel prognostic biomarker." Hum Pathol **73**: 33-40.
Plummer, E. R., M. R. Middleton, C. Jones, A. Olsen, I. Hickson, P. McHugh, G. P. Margison, G. McGown, M. Thorncroft, A. J. Watson, A. V. Boddy, A. H. Calvert, A. L. Harris, D. R. Newell and N. J. Curtin (2005). "Temozolomide pharmacodynamics in patients with metastatic melanoma: dna damage and activity of repair enzymes O6-alkylguanine alkyltransferase and poly(ADP-ribose) polymerase-1." Clin Cancer Res **11**(9): 3402-3409.
Pollock, P. M., U. L. Harper, K. S. Hansen, L. M. Yudt, M. Stark, C. M. Robbins, T. Y. Moses, G. Hostetter, U. Wagner, J. Kakareka, G. Salem, T. Pohida, P. Heenan, P. Duray, O. Kallioniemi, N. K. Hayward, J. M. Trent and P. S. Meltzer (2003). "High frequency of BRAF mutations in nevi." Nat Genet **33**(1): 19-20.
Populo, H., P. Boaventura, J. Vinagre, R. Batista, A. Mendes, R. Caldas, J. Pardal, F. Azevedo, M. Honavar, I. Guimaraes, J. Manuel Lopes, M. Sobrinho-Simoes and P. Soares (2014). "TERT promoter mutations in skin cancer: the effects of sun exposure and X-irradiation." J Invest Dermatol **134**(8): 2251-2257.
Poynter, J. N., J. T. Elder, D. R. Fullen, R. P. Nair, M. S. Soengas, T. M. Johnson, B. Redman, N. E. Thomas and S. B. Gruber (2006). "BRAF and NRAS mutations in melanoma and melanocytic nevi." Melanoma Res **16**(4): 267-273.
Prahallad, A., G. J. Heynen, G. Germano, S. M. Willems, B. Evers, L. Vecchione, V. Gambino, C. Lieftink, R. L. Beijersbergen, F. Di Nicolantonio, A. Bardelli and R. Bernards (2015). "PTPN11 Is a Central Node in Intrinsic and Acquired Resistance to Targeted Cancer Drugs." Cell Rep **12**(12): 1978-1985.

Premi, S., S. Wallisch, C. M. Mano, A. B. Weiner, A. Bacchiocchi, K. Wakamatsu, E. J. Bechara, R. Halaban, T. Douki and D. E. Brash (2015). "Photochemistry. Chemiexcitation of melanin derivatives induces DNA photoproducts long after UV exposure." Science **347**(6224): 842-847.
Puntervoll, H. E., X. R. Yang, H. H. Vetti, I. M. Bachmann, M. F. Avril, M. Benfodda, C. Catricala, S. Dalle, A. B. Duval-Modeste, P. Ghiorzo, P. Grammatico, M. Harland, N. K. Hayward, H. H. Hu, T. Jouary, T. Martin-Denavit, A. Ozola, J. M. Palmer, L. Pastorino, D. Pjanova, N. Soufir, S. J. Steine, A. J. Stratigos, L. Thomas, J. Tinat, H. Tsao, R. Veinalde, M. A. Tucker, B. Bressac-de Paillerets, J. A. Newton-Bishop, A. M. Goldstein, L. A. Akslen and A. Molven (2013). "Melanoma prone families with CDK4 germline mutation: phenotypic profile and associations with MC1R variants." J Med Genet **50**(4): 264-270.
Purdue, M. P., L. From, B. K. Armstrong, A. Kricker, R. P. Gallagher, J. R. McLaughlin, N. S. Klar, L. D. Marrett, E. Genes and G. Melanoma Study (2005). "Etiologic and other factors predicting nevus-associated cutaneous malignant melanoma." Cancer Epidemiol Biomarkers Prev **14**(8): 2015-2022.
Rajkumar, S. and I. R. Watson (2016). "Molecular characterisation of cutaneous melanoma: creating a framework for targeted and immune therapies." Br J Cancer **115**(2): 145-155.
Recio, J. A., F. P. Noonan, H. Takayama, M. R. Anver, P. Duray, W. L. Rush, G. Lindner, E. C. De Fabo, R. A. DePinho and G. Merlino (2002). "Ink4a/arf deficiency promotes ultraviolet radiation-induced melanomagenesis." Cancer Res **62**(22): 6724-6730.
Reddy, K. K., M. J. Farber, J. Bhawan, R. G. Geronemus and G. S. Rogers (2013). "Atypical (Dysplastic) Nevi Outcomes of Surgical Excision and Association With Melanoma." Jama Dermatology **149**(8): 928-934.
Reifenberger, J., M. Wolter, J. Bostrom, R. Buschges, K. W. Schulte, M. Megahed, T. Ruzicka and G. Reifenberger (2000). "Allelic losses on chromosome arm 10q and mutation of the PTEN (MMAC1) tumour suppressor gene in primary and metastatic malignant melanomas." Virchows Arch **436**(5): 487-493.
Rhodes, A. R. and J. W. Melski (1982). "Small congenital nevocellular nevi and the risk of cutaneous melanoma." J Pediatr **100**(2): 219-224.
Rivers, J. K., R. MacLennan, J. W. Kelly, A. E. Lewis, B. J. Tate, S. Harrison and W. H. McCarthy (1995). "The eastern Australian childhood nevus study: prevalence of atypical nevi, congenital nevus-like nevi, and other pigmented lesions." J Am Acad Dermatol **32**(6): 957-963.
Robinson, E. S., J. L. VandeBerg, G. B. Hubbard and T. P. Dooley (1994). "Malignant melanoma in ultraviolet irradiated laboratory opossums: initiation in suckling young, metastasis in adults, and xenograft behavior in nude mice." Cancer Res **54**(22): 5986-5991.
Roh, M. R., P. Eliades, S. Gupta and H. Tsao (2015). "Genetics of melanocytic nevi." Pigment Cell Melanoma Res **28**(6): 661-672.
Romerdahl, C. A., C. Donawho, I. J. Fidler and M. L. Kripke (1988). "Effect of ultraviolet-B radiation on the in vivo growth of murine melanoma cells." Cancer Res **48**(14): 4007-4010.

Rouzaud, F., A. L. Kadekaro, Z. A. Abdel-Malek and V. J. Hearing (2005). "MC1R and the response of melanocytes to ultraviolet radiation." Mutat Res **571**(1-2): 133-152.
Sato, T., K. Soejima, E. Arai, J. Hamamoto, H. Yasuda, D. Arai, K. Ishioka, K. Ohgino, K. Naoki, T. Kohno, K. Tsuta, S. Watanabe, Y. Kanai and T. Betsuyaku (2015). "Prognostic implication of PTPRH hypomethylation in non-small cell lung cancer." Oncol Rep **34**(3): 1137-1145.
Scahill, C. M., Z. Digby, I. M. Sealy, S. Wojciechowska, R. J. White, J. E. Collins, D. L. Stemple, T. Bartke, M. E. Mathers, E. E. Patton and E. M. Busch-Nentwich (2017). "Loss of the chromatin modifier Kdm2aa causes BrafV600E-independent spontaneous melanoma in zebrafish." PLoS Genet **13**(8): e1006959.
Schafer, T., J. Merkl, E. Klemm, H. E. Wichmann, J. Ring and K. S. Group (2006). "The epidemiology of nevi and signs of skin aging in the adult general population: Results of the KORA-survey 2000." J Invest Dermatol **126**(7): 1490-1496.
Schartl, M., B. Wilde, J. A. Laisney, Y. Taniguchi, S. Takeda and S. Meierjohann (2010). "A mutated EGFR is sufficient to induce malignant melanoma with genetic background-dependent histopathologies." J Invest Dermatol **130**(1): 249-258.
Schmitz, L. J. M., R. V. Klaassen, M. Ruiperez-Alonso, A. E. Zamri, J. Stroeder, P. Rao-Ruiz, J. C. Lodder, R. J. van der Loo, H. D. Mansvelder, A. B. Smit and S. Spijker (2017). "The AMPA receptor-associated protein Shisa7 regulates hippocampal synaptic function and contextual memory." Elife **6**.
Seynnaeve, B., S. Lee, S. Borah, Y. Park, A. Pappo, J. M. Kirkwood and A. Bahrami (2017). "Genetic and Epigenetic Alterations of TERT Are Associated with Inferior Outcome in Adolescent and Young Adult Patients with Melanoma." Sci Rep **7**: 45704.
Shah, J., A. M. Feintisch and M. S. Granick (2016). "Congenital Melanocytic Nevi." Eplasty **16**: ic4.
Shain, A. H. and B. C. Bastian (2016). "From melanocytes to melanomas." Nat Rev Cancer **16**(6): 345-358.
Shain, A. H., N. M. Joseph, R. Yu, J. Benhamida, S. Liu, T. Prow, B. Ruben, J. North, L. Pincus, I. Yeh, R. Judson and B. C. Bastian (2018). "Genomic and Transcriptomic Analysis Reveals Incremental Disruption of Key Signaling Pathways during Melanoma Evolution." Cancer Cell **34**(1): 45-55 e44.
Shain, A. H., I. Yeh, I. Kovalyshyn, A. Sriharan, E. Talevich, A. Gagnon, R. Dummer, J. North, L. Pincus, B. Ruben, W. Rickaby, C. D'Arrigo, A. Robson and B. C. Bastian (2015). "The Genetic Evolution of Melanoma from Precursor Lesions." New England Journal of Medicine **373**(20): 1926-1936.
Sharma, L. K., R. Leonardi, W. Lin, V. A. Boyd, A. Goktug, A. A. Shelat, T. Chen, S. Jackowski and C. O. Rock (2015). "A high-throughput screen reveals new small-molecule activators and inhibitors of pantothenate kinases." J Med Chem **58**(3): 1563-1568.
Sheng, X., Y. Kong, Y. Li, Q. Zhang, L. Si, C. Cui, Z. Chi, B. Tang, L. Mao, B. Lian, X. Wang, X. Yan, S. Li, J. Dai and J. Guo (2016). "GNAQ and GNA11 mutations occur in 9.5% of mucosal melanoma and are associated with poor prognosis." Eur J Cancer **65**: 156-163.

Shitara, D., G. Tell-Marti, C. Badenas, M. M. Enokihara, L. Alos, A. B. Larque, N. Michalany, J. A. Puig-Butille, C. Carrera, J. Malvehy, S. Puig and E. Bagatin (2015). "Mutational status of naevus-associated melanomas." Br J Dermatol **173**(3): 671-680.
Silva, J. H., B. C. Sa, A. L. Avila, G. Landman and J. P. Duprat Neto (2011). "Atypical mole syndrome and dysplastic nevi: identification of populations at risk for developing melanoma - review article." Clinics (Sao Paulo) **66**(3): 493-499.
Spritz, R. A. and V. J. Hearing, Jr. (1994). "Genetic disorders of pigmentation." Adv Hum Genet **22**: 1-45.
Stahl, P. L., H. Stranneheim, A. Asplund, L. Berglund, F. Ponten and J. Lundeberg (2011). "Sun-induced nonsynonymous p53 mutations are extensively accumulated and tolerated in normal appearing human skin." J Invest Dermatol **131**(2): 504-508.
Straussman, R., T. Morikawa, K. Shee, M. Barzily-Rokni, Z. R. Qian, J. Du, A. Davis, M. M. Mongare, J. Gould, D. T. Frederick, Z. A. Cooper, P. B. Chapman, D. B. Solit, A. Ribas, R. S. Lo, K. T. Flaherty, S. Ogino, J. A. Wargo and T. R. Golub (2012). "Tumour micro-environment elicits innate resistance to RAF inhibitors through HGF secretion." Nature **487**(7408): 500-504.
Takayama, H., W. J. La Rochelle, M. Anver, D. E. Bockman and G. Merlino (1996). "Scatter factor/hepatocyte growth factor as a regulator of skeletal muscle and neural crest development." Proc Natl Acad Sci U S A **93**(12): 5866-5871.
Tartaglia, M., S. Martinelli, L. Stella, G. Bocchinfuso, E. Flex, V. Cordeddu, G. Zampino, I. Burgt, A. Palleschi, T. C. Petrucci, M. Sorcini, C. Schoch, R. Foa, P. D. Emanuel and B. D. Gelb (2006). "Diversity and functional consequences of germline and somatic PTPN11 mutations in human disease." Am J Hum Genet **78**(2): 279-290.
Tassabehji, M., V. E. Newton and A. P. Read (1994). "Waardenburg syndrome type 2 caused by mutations in the human microphthalmia (MITF) gene." Nat Genet **8**(3): 251-255.
Thody, A. J., E. M. Higgins, K. Wakamatsu, S. Ito, S. A. Burchill and J. M. Marks (1991). "Pheomelanin as well as eumelanin is present in human epidermis." J Invest Dermatol **97**(2): 340-344.
Thomas, J., T. Liu, M. A. Cotter, S. R. Florell, K. Robinette, A. N. Hanks and D. Grossman (2007). "Melanocyte expression of survivin promotes development and metastasis of UV-induced melanoma in HGF-transgenic mice." Cancer Res **67**(11): 5172-5178.
Tian, F., J. Zhao, X. Fan and Z. Kang (2017). "Weighted gene co-expression network analysis in identification of metastasis-related genes of lung squamous cell carcinoma based on the Cancer Genome Atlas database." J Thorac Dis **9**(1): 42-53.
Troxel, D. B. (2003). "Pitfalls in the diagnosis of malignant melanoma - Findings of a risk management panel study." American Journal of Surgical Pathology **27**(9): 1278-1283.
Tsao, H., C. Bevona, W. Goggins and T. Quinn (2003). "The transformation rate of moles (melanocytic nevi) into cutaneous melanoma - A population-based estimate." Archives of Dermatology **139**(3): 282-288.
Tsao, H., X. Zhang, K. Fowlkes and F. G. Haluska (2000). "Relative reciprocity of NRAS and PTEN/MMAC1 alterations in cutaneous melanoma cell lines." Cancer Res **60**(7): 1800-1804.

Tschandl, P., A. Berghoff, M. Preusser, S. Burgstaller-Muhlbacher, H. Pehamberger, I. Okamoto and H. Kittler (2013). "NRAS and BRAF mutations in melanoma-associated nevi and uninvolved nevi." Journal Der Deutschen Dermatologischen Gesellschaft **11**: 41-41.
Tyrrell, R. M. (1973). "Induction of pyrimidine dimers in bacterial DNA by 365 nm radiation." Photochem Photobiol **17**(1): 69-73.
Tyrrell, R. M., R. D. Ley and R. B. Webb (1974). "Induction of single-strand breaks (alkali-labile bonds) in bacterial and phage DNA by near UV (365 nm) radiation." Photochem Photobiol **20**(5): 395-398.
Uribe, P., Wistuba, II and S. Gonzalez (2003). "BRAF mutation: a frequent event in benign, atypical, and malignant melanocytic lesions of the skin." Am J Dermatopathol **25**(5): 365-370.
Valiukeviciene, S., I. Miseviciene and H. Gollnick (2005). "The prevalence of common acquired melanocytic nevi and the relationship with skin type characteristics and sun exposure among children in Lithuania." Arch Dermatol **141**(5): 579-586.
van der Spek-Keijser, L. M., H. J. van der Rhee, G. Toth, R. Van Westering, J. A. Bruijn and J. W. Coebergh (1997). "Site, histological type, and thickness of primary cutaneous malignant melanoma in western Netherlands since 1980." Br J Dermatol **136**(4): 565-571.
Van Raamsdonk, C. D., V. Bezrookove, G. Green, J. Bauer, L. Gaugler, J. M. O'Brien, E. M. Simpson, G. S. Barsh and B. C. Bastian (2009). "Frequent somatic mutations of GNAQ in uveal melanoma and blue naevi." Nature **457**(7229): 599-602.
Van Raamsdonk, C. D., K. G. Griewank, M. B. Crosby, M. C. Garrido, S. Vemula, T. Wiesner, A. C. Obenauf, W. Wackernagel, G. Green, N. Bouvier, M. M. Sozen, G. Baimukanova, R. Roy, A. Heguy, I. Dolgalev, R. Khanin, K. Busam, M. R. Speicher, J. O'Brien and B. C. Bastian (2010). "Mutations in GNA11 in Uveal Melanoma." New England Journal of Medicine **363**(23): 2191-2199.
Vasioukhin, V., L. Degenstein, B. Wise and E. Fuchs (1999). "The magical touch: genome targeting in epidermal stem cells induced by tamoxifen application to mouse skin." Proc Natl Acad Sci U S A **96**(15): 8551-8556.
Vazquez Vde, L., A. L. Vicente, A. Carloni, G. Berardinelli, P. Soares, C. Scapulatempo, O. Martinho and R. M. Reis (2016). "Molecular profiling, including TERT promoter mutations, of acral lentiginous melanomas." Melanoma Res **26**(2): 93-99.
Villanueva, J., A. Vultur and M. Herlyn (2011). "Resistance to BRAF inhibitors: unraveling mechanisms and future treatment options." Cancer Res **71**(23): 7137-7140.
Viros, A., B. Sanchez-Laorden, M. Pedersen, S. J. Furney, J. Rae, K. Hogan, S. Ejiama, M. R. Girotti, M. Cook, N. Dhomen and R. Marais (2014). "Ultraviolet radiation accelerates BRAF-driven melanomagenesis by targeting TP53." Nature **511**(7510): 478-482.
Vithana, E. N., L. Abu-Safieh, M. J. Allen, A. Carey, M. Papaioannou, C. Chakarova, M. Al-Maghtheh, N. D. Ebenezer, C. Willis, A. T. Moore, A. C. Bird, D. M. Hunt and S. S. Bhattacharya (2001). "A human homolog of yeast pre-mRNA splicing gene, PRP31, underlies autosomal dominant retinitis pigmentosa on chromosome 19q13.4 (RP11)." Mol Cell **8**(2): 375-381.

Wang, H., R. B. Presland and M. Piepkorn (2005). "A search for CDKN2A/p16INK4a mutations in melanocytic nevi from patients with melanoma and spouse controls by use of laser-captured microdissection." Arch Dermatol **141**(2): 177-180.
Wang, J., T. Kobayashi, N. Floc'h, C. W. Kinkade, A. Aytes, D. Dankort, C. Lefebvre, A. Mitrofanova, R. D. Cardiff, M. McMahon, A. Califano, M. M. Shen and C. Abate-Shen (2012). "B-Raf activation cooperates with PTEN loss to drive c-Myc expression in advanced prostate cancer." Cancer Res **72**(18): 4765-4776.
Wang, J. X., M. Fukunaga-Kalabis and M. Herlyn (2016). "Crosstalk in skin: melanocytes, keratinocytes, stem cells, and melanoma." J Cell Commun Signal **10**(3): 191-196.
Wang, K., G. Ubriaco and L. C. Sutherland (2007). "RBM6-RBM5 transcription-induced chimeras are differentially expressed in tumours." BMC Genomics **8**: 348.
Wang, S. Q., R. Setlow, M. Berwick, D. Polsky, A. A. Marghoob, A. W. Kopf and R. S. Bart (2001). "Ultraviolet A and melanoma: a review." J Am Acad Dermatol **44**(5): 837-846.
Wang, Z., P. Sun, C. Gao, J. Chen, J. Li, Z. Chen, M. Xu, J. Shao, Y. Zhang and J. Xie (2017). "Down-regulation of LRP1B in colon cancer promoted the growth and migration of cancer cells." Exp Cell Res **357**(1): 1-8.
Wenczl, E., G. P. Van der Schans, L. Roza, R. M. Kolb, A. J. Timmerman, N. P. Smit, S. Pavel and A. A. Schothorst (1998). "(Pheo)melanin photosensitizes UVA-induced DNA damage in cultured human melanocytes." J Invest Dermatol **111**(4): 678-682.
Whiteman, D. C., C. A. Whiteman and A. C. Green (2001). "Childhood sun exposure as a risk factor for melanoma: a systematic review of epidemiologic studies." Cancer Causes Control **12**(1): 69-82.
Wicks, N. L., J. W. Chan, J. A. Najera, J. M. Ciriello and E. Oancea (2011). "UVA phototransduction drives early melanin synthesis in human melanocytes." Curr Biol **21**(22): 1906-1911.
Wiesner, T., J. He, R. Yelensky, R. Esteve-Puig, T. Botton, I. Yeh, D. Lipson, G. Otto, K. Brennan, R. Murali, M. Garrido, V. A. Miller, J. S. Ross, M. F. Berger, A. Sparatta, G. Palmedo, L. Cerroni, K. J. Busam, H. Kutzner, M. T. Cronin, P. J. Stephens and B. C. Bastian (2014). "Kinase fusions are frequent in Spitz tumours and spitzoid melanomas." Nat Commun **5**: 3116.
Wiesner, T., M. Kiuru, S. N. Scott, M. Arcila, A. C. Halpern, T. Hollmann, M. F. Berger and K. J. Busam (2015). "NF1 Mutations Are Common in Desmoplastic Melanoma." Am J Surg Pathol **39**(10): 1357-1362.
Wolchok, J. D., V. Chiarion-Sileni, R. Gonzalez, P. Rutkowski, J. J. Grob, C. L. Cowey, C. D. Lao, J. Wagstaff, D. Schadendorf, P. F. Ferrucci, M. Smylie, R. Dummer, A. Hill, D. Hogg, J. Haanen, M. S. Carlino, O. Bechter, M. Maio, I. Marquez-Rodas, M. Guidoboni, G. McArthur, C. Lebbe, P. A. Ascierto, G. V. Long, J. Cebon, J. Sosman, M. A. Postow, M. K. Callahan, D. Walker, L. Rollin, R. Bhore, F. S. Hodi and J. Larkin (2017). "Overall Survival with Combined Nivolumab and Ipilimumab in Advanced Melanoma." N Engl J Med **377**(14): 1345-1356.
Wolf, I. and L. R. Rohrschneider (1999). "Fiz1, a novel zinc finger protein interacting with the receptor tyrosine kinase Flt3." J Biol Chem **274**(30): 21478-21484.

Wolf, P., C. K. Donawho and M. L. Kripke (1994). "Effect of sunscreens on UV radiation-induced enhancement of melanoma growth in mice." J Natl Cancer Inst **86**(2): 99-105.
Woodman, S. E. (2012). "Metastatic uveal melanoma: biology and emerging treatments." Cancer J **18**(2): 148-152.
Woodward, J. K., S. R. Elshaw, A. K. Murray, C. E. Nichols, N. Cross, D. Laws, I. G. Rennie and K. Sisley (2002). "Stimulation and inhibition of uveal melanoma invasion by HGF, GRO, IL-1alpha and TGF-beta." Invest Ophthalmol Vis Sci **43**(10): 3144-3152.
Yamaguchi, Y. and V. J. Hearing (2009). "Physiological factors that regulate skin pigmentation." Biofactors **35**(2): 193-199.
Yang, X. M. and M. Park (1995). "Expression of the hepatocyte growth factor/scatter factor receptor tyrosine kinase is localized to epithelia in the adult mouse." Lab Invest **73**(4): 483-491.
Yazdi, A. S., G. Palmedo, M. J. Flaig, U. Puchta, A. Reckwerth, A. Rutten, T. Mentzel, H. Hugel, M. Hantschke, M. H. Schmid-Wendtner, H. Kutzner and C. A. Sander (2003). "Mutations of the BRAF gene in benign and malignant melanocytic lesions." J Invest Dermatol **121**(5): 1160-1162.
Yeh, I., A. von Deimling and B. C. Bastian (2013). "Clonal BRAF mutations in melanocytic nevi and initiating role of BRAF in melanocytic neoplasia." J Natl Cancer Inst **105**(12): 917-919.
Yilmaz, I., M. Gamsizkan, Z. Kucukodaci, U. Berber, D. Demirel, A. Haholu and G. Narli (2015). "BRAF, KIT, NRAS, GNAQ and GNA11 mutation analysis in cutaneous melanomas in Turkish population." Indian J Pathol Microbiol **58**(3): 279-284.
Zaidi, M. R., S. Davis, F. P. Noonan, C. Graff-Cherry, T. S. Hawley, R. L. Walker, L. Feigenbaum, E. Fuchs, L. Lyakh, H. A. Young, T. J. Hornyak, H. Arnheiter, G. Trinchieri, P. S. Meltzer, E. C. De Fabo and G. Merlino (2011). "Interferon-gamma links ultraviolet radiation to melanomagenesis in mice." Nature **469**(7331): 548-553.
Zaidi, M. R., T. J. Hornyak and G. Merlino (2011). "A genetically engineered mouse model with inducible GFP expression in melanocytes." Pigment Cell & Melanoma Research **24**(2): 393-394.
Zaidi, M. R., T. J. Hornyak and G. Merlino (2011). "A genetically engineered mouse model with inducible GFP expression in melanocytes." Pigment Cell Melanoma Res **24**(2): 393-394.
Zeng, H., A. Jorapur, A. H. Shain, U. E. Lang, R. Torres, Y. Zhang, A. S. McNeal, T. Botton, J. Lin, M. Donne, I. N. Bastian, R. Yu, J. P. North, L. Pincus, B. S. Ruben, N. M. Joseph, I. Yeh, B. C. Bastian and R. L. Judson (2018). "Bi-allelic Loss of CDKN2A Initiates Melanoma Invasion via BRN2 Activation." Cancer Cell **34**(1): 56-68 e59.
Zerp, S. F., A. van Elsas, L. T. Peltenburg and P. I. Schrier (1999). "p53 mutations in human cutaneous melanoma correlate with sun exposure but are not always involved in melanomagenesis." Br J Cancer **79**(5-6): 921-926.
Zhang, R. Y., Z. H. Yu, L. Zeng, S. Zhang, Y. Bai, J. Miao, L. Chen, J. Xie and Z. Y. Zhang (2016). "SHP2 phosphatase as a novel therapeutic target for melanoma treatment." Oncotarget **7**(45): 73817-73829.

Zhang, W., M. Dai, A. Fridberger, A. Hassan, J. Degagne, L. Neng, F. Zhang, W. He, T. Ren, D. Trune, M. Auer and X. Shi (2012). "Perivascular-resident macrophage-like melanocytes in the inner ear are essential for the integrity of the intrastrial fluid-blood barrier." Proc Natl Acad Sci U S A **109**(26): 10388-10393.
Zhou, X. P., O. Gimm, H. Hampel, T. Niemann, M. J. Walker and C. Eng (2000). "Epigenetic PTEN silencing in malignant melanomas without PTEN mutation." Am J Pathol **157**(4): 1123-1128.
Ziembik, M. A., T. P. Bender, J. M. Larner and D. L. Brautigan (2017). "Functions of protein phosphatase-6 in NF-kappaB signaling and in lymphocytes." Biochem Soc Trans **45**(3): 693-701.
Zilberberg, A., A. Yaniv and A. Gazit (2004). "The low density lipoprotein receptor-1, LRP1, interacts with the human frizzled-1 (HFz1) and down-regulates the canonical Wnt signaling pathway." J Biol Chem **279**(17): 17535-17542.